

A NEW ROUTE TO THE SYNTHESIS OF NANOCOMPOSITES
BY USING AN UNSATURATED POLYESTER MATRIX

A THESIS SUBMITTED TO
THE GRADUATE SCHOOL OF NATURAL AND APPLIED SCIENCES
OF
MIDDLE EAST TECHNICAL UNIVERSITY

BY

PELİN TOPRAK

IN PARTIAL FULFILLMENT OF THE REQUIREMENTS
FOR
THE DEGREE OF MASTER OF SCIENCE
IN
CHEMICAL ENGINEERING

SEPTEMBER 2004

Approval of the Graduate School of Natural and Applied Sciences

Prof. Dr. Canan Özgen
Director

I certify that this thesis satisfies all the requirements as a thesis for the degree of Master of Science.

Prof. Dr. Timur Doğu
Head of Department

This is to certify that we have read this thesis and that in our opinion it is fully adequate, in scope and quality, as a thesis and for the degree of Master of Science.

Prof. Dr. Ülkü Yilmazer
Supervisor

Examining Committee Members

Prof. Dr. Leyla Aras	(METU,CHEM)	_____
Prof. Dr. Ülkü Yilmazer	(METU,CHE)	_____
Dr. Cevdet Öztin	(METU,CHE)	_____
Assoc. Prof. Dr. Göknur Bayram	(METU,CHE)	_____
Prof. Dr. Erdal Bayramlı	(METU,CHEM)	_____

I hereby declare that all information in this document has been obtained and presented in accordance with academic rules and ethical conduct. I also declare that, as required by these rules and conduct, I have fully cited and referenced all material and results that are not original to this work.

Name, Last name : Pelin Toprak

Signature

ABSTRACT

A NEW ROUTE TO THE SYNTHESIS OF NANOCOMPOSITES BY USING AN UNSATURATED POLYESTER MATRIX

Toprak, Pelin

M.S., Department of Chemical Engineering

Supervisor: Prof. Dr. Ülkü YILMAZER

September 2004, 96 pages

This study was conducted to investigate the effects of organoclay type and concentration on the nanocomposites synthesized by "In-Situ Polymerization" and "Prepolymerization" methods. In-Situ Polymerization Method was in fact a new route which consisted of dispersing the monomers; propylene glycol, maleic anhydride and o-phthalic anhydride into the galleries of montmorillonite followed by subsequent polymerization. The Prepolymerization Method involved the addition of montmorillonite to the previously synthesized unsaturated polyester. As the first step, all the compositions were prepared by Cloisite 30B, and then for comparison of clay type, nanocomposites containing 3 wt.% of Cloisite 15A and Cloisite 25A were also synthesized.

The efficiency of the two methods were compared with regards to their structural, thermal and mechanical properties. According to the results of XRD analysis, in both methods, maximum intercalation was observed when Cloisite 30B was used. An exfoliated structure was obtained in the Prepolymerization Method at 3 wt. % Cloisite 30B content. In all clay types, the increase in the d-spacings of the organoclays was higher when the Prepolymerization Method was applied.

With Cloisite 30B, maximum improvement in the impact strength was obtained at 3 wt. % organoclay loading and the In-Situ Method yielded better results leading to a 77% increase in the impact strength at this organoclay loading. Among the organoclay types, Cloisite 15A was found to give rise to maximum increase in the impact strength.

With the Prepolymerization Method higher improvement in flexural strength and flexural modulus was obtained owing to the lower styrene content in the crosslinking medium. The elongation at break values followed a decreasing trend with increasing clay content but did not show any significant difference when the clay types were compared.

Keywords: unsaturated polyester, nanocomposites, organoclay, in-situ polymerization, prepolymerization.

ÖZ

DOYMAMIŞ POLİESTER KULLANARAK NANOKOMPOZİT SENTEZİNDE YENİ BİR YÖNTEM

Toprak, Pelin

Yüksek Lisans, Kimya Mühendisliği

Tez Yöneticisi: Prof. Dr. Ülkü Yılmaz

Eylül 2004, 96 sayfa

Bu çalışma, yerinde polimerleştirme ve ön polimerleştirme metoduyla sentezlenen nanokompozitler üzerinde kil tipi ve miktarının etkisini incelemek amacıyla yürütülmüştür. Yerinde polimerleştirme esas olarak monomerlerin; propilen glikol, maleik anhidrid ve o-ftalik anhidridin kil tabakaları arasında dağılımını takiben polimerleştirilmesini içermektedir. Ön polimerleştirme metodu ise kilin önceden sentezlenmiş poliestere eklenmesini içermektedir. İlk basamak olarak, bütün kompozisyonlar Cloisite 30B ile hazırlanmıştır; daha sonra, kil tiplerini karşılaştırmak için ağırlıkça %3 Cloisite 15A ve Cloisite 25A içeren nanokompozitler ayrıca sentezlenmiştir.

İki metodun verimliliği yapısal, ısı ve mekanik özellikler açısından incelenmiştir. XRD analizi sonuçlarına göre, her iki metotta da maksimum açılma Cloisite 30B kullanıldığında gözlenmiştir. Ön polimerleştirme metodunda ağırlıkça %3 Cloisite 30B kullanıldığında tamamen dağılmış bir yapı elde edilmiştir. Tüm kil tiplerinde, kil tabakaları arasındaki boşluk ön polimerleştirme metodu uygulandığında daha fazla artış göstermiştir.

Cloisite 30B ile darbe dayanımında en fazla gelişme ağırlıkça %3 organik kil içeriğinde gözlenmiştir ve bu kil miktarında yerinde polimerleştirme metodunda daha iyi sonuçlar elde edilerek darbe dayanımında %77 artış sağlanmıştır. Kil tipleri arasında, Cloisite 15A darbe dayanımında en fazla artış sağlamıştır.

Çapraz bağlanma ortamındaki stiren miktarının daha düşük olmasından dolayı ön polimerleştirme metodu ile esneme dayanımı ve modülünde daha fazla gelişme elde edilmiştir. Kırılmadaki uzama değerleri, kil miktarı arttıkça azalan bir eğilim izlemiştir, fakat kil tipleri göz önüne alındığında birbirinden belirgin farklılık göstermemiştir.

Anahtar Kelimeler: doymamış poliester, nanokompozit, organokil, yerinde polimerleştirme, ön polimerleştirme.

To my family...

ACKNOWLEDGEMENTS

I would like to express my deepest gratitude to my supervisor Prof. Dr. Ülkü Yilmazer, for his continuous support, encouragement and guidance throughout this study. It was a pleasing honor for me to work with him.

I also wish to extend my acknowledgements and sincere thanks to Çiğdem Zeytin who contributed greatly in my study with her help and support.

I am very grateful to Assoc. Prof. Dr. Göknur Bayram from Department of Chemical Engineering for giving me every opportunity to use the instruments in her laboratory. I also would like to thank Prof. Dr. Teoman Tinçer from Department of Chemistry for providing me the impact test instrument in his laboratory. I appreciate the courtesy of Prof Dr. Güngör Gündüz for providing the ultrasonic mixing apparatus.

Special thanks go to Cengiz Tan from Department of Metallurgical and Materials Engineering for SEM Analysis and Mihrican Açıkgöz from Department of Chemical Engineering for DSC Analysis and İnciser Girgin and Bilgin Çiftçi from General Directorate of Mineral Research and Exploration, for X-Ray Diffraction Analysis.

I also would like to thank all my friends in Polymer Research Group including Gülsüm Özden, Ali Emrah Keyfoğlu, Işıl Işık, Elif Alyamaç, Fatma Işık, İlknur Çakar, Sertan Yeşil, Güralp Özkoç, Aslı Tolga, Mert Kılınc, Çiğdem Başara and Özcan Köysüren for their friendship, and for helping me in all the possible ways. Many thanks to Arcan Erkan for being always right beside me.

And I wish to express my sincere thanks to my family for supporting, encouraging, and loving me all through my life. It would not be possible without their love to complete this study.

TABLE OF CONTENTS

PLAGIARISM	iii
ABSTRACT	iv
ÖZ.....	vi
DEDICATION.....	viii
ACKNOWLEDGEMENTS	ix
TABLE OF CONTENTS	x
LIST OF TABLES	xiv
LIST OF FIGURES	xvi
CHAPTER	
1. INTRODUCTION.....	1
2. BACKGROUND	3
2.1 Composites	3
2.1.1 Matrix	3
2.1.1.1 Thermoplastics.....	4
2.1.1.2 Thermosets.....	4
2.1.2 Reinforcement	4
2.2 Nanocomposites.....	5
2.3 Polymer-Layered Crystal Nanocomposites	5
2.3.1 Layered Silicates	6
2.3.1.1 Cation-Exchange Process	8
2.3.2 Nanocomposite Synthesis Methods	9
2.3.2.1 In-Situ Polymerization Method	9
2.3.2.2 Melt Intercalation Method	10
2.3.2.3 Solution Intercalation Method	10

2.3.3 Nanocomposite Structures	11
2.4 Unsaturated Polyesters	12
2.4.1 History of Unsaturated Polyesters.....	12
2.4.2 Application Areas of Unsaturated Polyesters.....	13
2.4.3 Synthesis of Unsaturated Polyesters	14
2.4.4 Classification of Unsaturated Polyester Resins	14
2.4.5 Curing of Unsaturated Polyester Resins	16
2.5 Casting	19
2.6 Characterization	19
2.6.1 Mechanical Properties	19
2.6.1.1 Flexural Test	19
2.6.1.2 Impact Test	21
2.6.2 Differential Scanning Calorimetry (DSC).....	21
2.6.3 X-Ray Diffraction (XRD)	22
2.6.4 Scanning Electron Microscopy (SEM).....	24
2.7 Previous Studies	24
3. EXPERIMENTAL.....	26
3.1 Materials.....	26
3.1.1 Monomers.....	26
3.1.1.1 Maleic Anhydride	26
3.1.1.2 O-Phthalic Anhydride	27
3.1.1.3 Propylene Glycol	27
3.1.2 Crosslinking Agent	28
3.1.2.1 Styrene	28
3.1.3 Catalyst.....	29
3.1.3.1 Methyl Ethyl Ketone Peroxide (MEKP)	29
3.1.4 Accelerator	29

3.1.4.1 Cobalt Naphthanate	29
3.1.5 Organoclays	29
3.1.5.1 Cloisite 30B	31
3.1.5.2 Cloisite 25A	32
3.1.5.3 Cloisite 15A	33
3.1.6 Release Agent	33
3.2 Experimental Procedure	34
3.2.1 In-Situ Polymerization Method	34
3.2.2 Prepolymerization Method	35
3.2.3 Acid Number Determination	37
3.2.4 Determination of Percentage of Styrene in The Resin	38
3.3 Characterization	38
3.3.1 Mechanical Testing Procedure and Equipment	38
3.3.1.1 Flexural Test.....	38
3.3.1.2 Impact Test.....	39
3.3.2 Morphological Analysis.....	40
3.3.2.1 X-Ray Diffraction (XRD) Analysis	40
3.3.2.2 Scanning Electron Microscopy (SEM)	40
3.3.3 Thermal Analysis	40
3.3.3.1 Differential Scanning Calorimetry (DSC) Analysis	40
4. RESULTS AND DISCUSSION	41
4.1 Morphological Analysis	41
4.1.1 Scanning Electron Microscopy (SEM).....	41
4.1.2 Analysis X-Ray Diffraction (XRD) Analysis.....	48
4.2 Mechanical Analysis	57
4.2.1 Impact Test Analysis	57
4.2.2 Flexural Test Analysis	61
4.3 Thermal Analysis.....	72

4.3.1 Differential Scanning Calorimetry (DSC) Analysis	72
5. CONCLUSIONS	74
REFERENCES	76
APPENDICES	81
A. Mechanical Testing Results	81
B. X-ray Diffraction Patterns of All Formulations	84
C. DSC Thermograms of the Materials	91

LIST OF TABLES

TABLE

3.1 Physical Properties of Maleic Anhydride	26
3.2 Physical Properties of <i>O</i> -Phthalic Anhydride.....	27
3.3 Physical properties of Propylene Glycol	27
3.4 Physical Properties of Styrene	28
3.5 Manufacturer's Physical Data of Cloisite 30B.....	31
3.6 Manufacturer's Physical Data of Cloisite 25A	32
3.7 Manufacturer's Physical Data of Cloisite 15A	33
3.8 Formulations used in the study.....	37
4.1 X-ray diffraction results of all compositions with respect to Cloisite 30B wt. %.....	48
4.2 X-ray diffraction results of the compositions prepared by two methods containing 3 wt. % Cloisite 15A, Cloisite 25A and cloisite 30B.....	54
4.3 % increase in the d-spacings of organoclays with respect to the polymerization method.....	54
4.4 Effect of organoclay (Cloisite 30B) content on the thermal properties of the compositions prepared by the In-Situ and the Prepolymerization Methods.....	72
4.5 Effect of organoclay type on thermal properties of the samples containing 3 wt. % organoclay.....	72
A.1 Impact strength data of samples with respect to polymerization method and organoclay (Cloisite 30B) content.	81
A.2 Impact strength data of samples with respect to polymerization method and organoclay type.	81
A.3 Flexural strength data of samples with respect to polymerization method and organoclay (Cloisite 30B) content.	81
A.4 Flexural modulus data of samples with respect to polymerization method and organoclay (Cloisite 30B) content	82

A.5 Flexural strain at break (%) data of samples with respect to polymerization method and organoclay (Cloisite 30B) content.....	82
A.6 Flexural strength data of samples with respect to polymerization method and organoclay type.....	82
A.7 Flexural modulus data of samples with respect to polymerization method and organoclay type.....	83
A.8 Flexural strain at break (%) data of samples with respect to polymerization method and organoclay type.....	83

LIST OF FIGURES

FIGURE

2.1 The model structure of montmorillonite	6
2.2 Microstructure of montmorillonite	7
2.3 The cation-exchange process between alkylammonium ions and cations initially intercalated between the clay layers	8
2.4 The "in-situ" polymerization	9
2.5 The "melt intercalation" process	10
2.6 The "solution intercalation" method	10
2.7 Scheme of different types of composites arising from the interaction of layered silicates and polymers: (a) phase-separated microcomposite; (b) intercalated nanocomposite and (c) exfoliated nanocomposite.....	11
2.8 Synthesis reaction of UP from maleic anhydride, o-phthalic anhydride and propylene glycol	14
2.9 Schematic view of crosslinking of unsaturated polyester	17
2.10 The stresses on the sample during flexural testing	20
2.11 Principle of X-Ray diffraction	23
3.1 Chemical structure of Maleic Anhydride	26
3.2 Chemical structure of <i>O</i> -Phthalic Anhydride.....	27
3.3 Chemical structure of Propylene Glycol	28
3.4 Chemical structure of Styrene	28
3.5 Chemical structure of MEKP	29
3.6 Cloisite® selection chart from Southern Clay Products.....	30
3.7 Chemical structure of the quaternary ammonium salt used in the manufacture of Cloisite 30B	31
3.8 Chemical structures of the quaternary ammonium and the anion, methyl sulfate used in the manufacture of 25A.....	32

3.9 Chemical structure of the quaternary ammonium salt used in the manufacture of Cloisite 25A.....	33
3.10 Flowcharts of specimen preparation by the In-Situ Method	35
3.11 Flowcharts of specimen preparation by the Prepolymerization Method.....	36
3.12 Charpy-type impact instrument	39
4.1 SEM micrographs of pure Unsaturated Polyester	43
4.2 SEM micrographs of Unsaturated Polyester containing 1 wt. % Cloisite 30B synthesized by (a) In-situ Method ×250, (b) In-Situ Method ×3500; (c) Prepolymerization Method ×250 and (d) Prepolymerization Method ×3500.....	43
4.3 SEM micrographs of Unsaturated Polyester containing 3 wt. % Cloisite 30B synthesized by (a) In-situ Method ×250, (b) In-Situ Method ×3500; (c) Prepolymerization Method ×250 and (d) Prepolymerization Method ×3500.....	44
4.4 SEM micrographs of Unsaturated Polyester containing 5 wt. % Cloisite 30B synthesized by (a) In-situ Method ×250, (b) In-Situ Method ×3500; (c) Prepolymerization Method ×250 and (d) Prepolymerization Method ×3500.....	45
4.5 SEM micrographs of Unsaturated Polyester containing 3 wt. % Cloisite 15A synthesized by (a) In-situ Method ×250, (b) In-Situ Method ×3500; (c) Prepolymerization Method ×250 and (d) Prepolymerization Method ×3500.....	46
4.6 SEM micrographs of Unsaturated Polyester containing 3 wt. % Cloisite 25A synthesized by (a) In-situ Method ×250, (b) In-Situ Method ×3500; (c) Prepolymerization Method ×250 and (d) Prepolymerization Method ×3500.....	47
4.7 X-ray diffraction patterns of nanocomposites synthesized by In-Situ Method containing 1,3 and 5 wt. % organoclay (Cloisite30B).....	49
4.8 X-ray diffraction patterns of nanocomposites synthesized by Prepolymerization Method containing 1, 3 and 5 wt % organoclay (Cloisite 30B).	50
4.9 X-ray diffraction patterns of nanocomposites prepared by the two methods containing 1 wt. % of organoclay (Cloisite 30B).	51
4.10 X-ray diffraction patterns of nanocomposites prepared by the two methods containing 3 wt. % of organoclay (Cloisite 30B).	52
4.11 X-ray diffraction patterns of nanocomposites prepared by the two methods containing 5 wt. % of organoclay (Cloisite 30B).	53

4.12 X-ray diffraction patterns of nanocomposites prepared by the In-Situ Method containing 3 wt. % of organoclays (Cloisite 30B,25A and 15A).	56
4.13 X-ray diffraction patterns of nanocomposites prepared by the Prepolymerization Method containing 3 wt. % of organoclays (Cloisite 30B,25A and 15A).....	56
4.14 Impact strength of nanocomposites prepared by the two methods with respect to the organoclay (Cloisite 30B) content.....	57
4.15 Impact strength of nanocomposites prepared by the two methods containing 3 wt. % organoclay with respect to organoclay type.	59
4.16 Effect of Organoclay (Cloisite 30B) content on the stress-strain curves of nanocomposites prepared by In-Situ Method.	62
4.17 Effect of Organoclay (Cloisite 30B) content on the stress-strain curves of nanocomposites prepared by Prepolymerization Method.....	62
4.18 Effect of polymerization method on the stress-strain curves of nanocomposites containing 1% Cloisite 30B.....	63
4.19 Effect of polymerization method on the stress-strain curves of nanocomposites containing 3% Cloisite 30B.....	64
4.20 Effect of polymerization method on the stress-strain curves of nanocomposites containing 5% Cloisite 30B.	64
4.21 Effect of organoclay type (3 wt. %) on the stress-strain curves of nanocomposites prepared by In-Situ Method.	66
4.22 Effect of organoclay type (3 wt.%) on the stress-strain curves of nanocomposites prepared by Prepolymerization Method.....	66
4.23 Effect of organoclay type (3 wt. %) on the flexural strength of nanocomposites prepared by In-Situ Method and Prepolymerization Method.....	67
4.24 Effect of organoclay type (3 wt. %) on the flexural modulus of nanocomposites prepared by In-Situ Method and Prepolymer Method.	67
4.25 Effect of organoclay type (3 wt. %) on the flexural strain at break (%) values of nanocomposites prepared by In-Situ Method and Prepolymerization Method.	68
4.26 Effect of organoclay (Cloisite 30B) content on the flexural strengths of nanocomposites prepared by In-Situ Method and Prepolymerization Method.	69

4.27 Effect of organoclay (Cloisite 30B) content on the flexural modulus of nanocomposites prepared by In-Situ Method and Prepolymerization Method	70
4.28 Effect of organoclay (Cloisite 30B) content on the flexural strain at break(%) values of nanocomposites prepared by In-Situ Method and Prepolymerization Method.....	71
B.1 X-ray diffraction patterns of pure unsaturated polyester (UP).	84
B.2 X-ray diffraction pattern of UP nanocomposite synthesized by In-Situ Method containing 1 wt. % Cloisite 30B.	84
B.3 X-ray diffraction pattern of UP nanocomposite synthesized by In-Situ Method containing 3 wt. % Cloisite 30B.	85
B.4 X-ray diffraction pattern of UP nanocomposite synthesized by In-Situ Method containing 5 wt. % Cloisite 30B.	85
B.5 X-ray diffraction pattern of UP nanocomposite synthesized by Prepolymerization Method containing 1 wt. % Cloisite 30B.	86
B.6 X-ray diffraction pattern of UP nanocomposite synthesized by Prepolymerization Method containing 3 wt. % Cloisite 30B.	86
B.7 X-ray diffraction pattern of UP nanocomposite synthesized by Prepolymerization Method containing 5 wt. % Cloisite 30B	87
B.8 X-ray diffraction pattern of UP nanocomposite synthesized by In-Situ Method containing 3 wt. % Cloisite 15A.	87
B.9 X-ray diffraction pattern of UP nanocomposite synthesized by In-Situ Method containing 3 wt. % Cloisite 25A.	88
B.10 X-ray diffraction pattern of UP nanocomposite synthesized by Prepolymerization Method containing 3 wt. % Cloisite 15A.	88
B.11 X-ray diffraction pattern of UP nanocomposite synthesized by prepolymerization Method containing 3 wt. % Cloisite 25A.	89
B.12 X-ray diffraction pattern of Cloisite 30B.	89
B.13 X-ray diffraction pattern of Cloisite 25A.	90
B.14 X-ray diffraction pattern of Cloisite 15A.	90
C.1 DSC thermogram of pure unsaturated polyester (UP).	91
C.2 DSC thermogram of UP synthesized by In-Situ Method containing 1 wt. % Cloisite 30B.	91
C.3 DSC thermogram of UP nanocomposite synthesized by In-Situ Method containing 3 wt. % Cloisite 30B.	92

C.4 DSC thermogram of UP nanocomposite synthesized by In-Situ Method containing 5 wt. % Cloisite 30B.	92
C.5 DSC thermogram of UP nanocomposite synthesized by Prepolymerization Method containing 1 wt. % Cloisite 30B.	93
C.6 DSC thermogram of UP nanocomposite synthesized by Prepolymerization Method containing 3 wt. % Cloisite 30B.	93
C.7 DSC thermogram of UP nanocomposite synthesized by Prepolymerization Method containing 5 wt. % Cloisite 30B.	94
C.8 DSC thermogram of UP nanocomposite synthesized by In-Situ Method containing 3 wt. % Cloisite 15A.	94
C.9 DSC thermogram of UP nanocomposite synthesized by In-Situ Method containing 3 wt. % Cloisite 25A.	95
C.10 DSC thermogram of UP nanocomposite synthesized by Prepolymerization Method containing 3 wt. % Cloisite 15A.	95
C.11 DSC thermogram of UP nanocomposite synthesized by Prepolymerization Method containing 3 wt. % Cloisite 25A.	96

CHAPTER 1

INTRODUCTION

A composite material is made by combining two or more materials to give a unique combination of properties. Composites based on a polymer matrix have become more common and are widely used in many industries due to the advantageous properties offered by the polymers [1]. The scope of nanotechnology provides the opportunity to explore unique functionalities beyond those found in conventional composites. The property that differentiates the nanocomposites from typical composites is that the reinforcing phase contains a constituent on the order of a few nanometers [2]. The unique properties obtained in a nanocomposite may be attributed to a well-dispersed reinforcing phase creating a large interfacial surface area.

In the field of polymer based nanocomposites, a wide variety of materials are used as the filler, but much research is focused on layered silicates. Two properties of layered silicates are exploitable in nanocomposite preparation; the first is the fine particles creating a large surface area and the second is the ability to modify their surface chemistry [3]. Montmorillonite, with a special layer charge density and high expandibility is particularly useful [4].

There are three conventional ways of incorporating layered silicates into polymer matrices; these are in-situ polymerization, melt intercalation and solution methods. The nanocomposites of thermoset polymers that can be prepared by the in-situ intercalative polymerization method, phenol resins, epoxy resins and unsaturated polyester resins are included in this category. These thermosetting nanocomposites are prepared by first swelling the organically modified clay with the proper polymerizable monomers followed by crosslinking reactions [5].

Unsaturated polyesters are the most versatile class of thermosetting polymers which are macromolecules consisting of unsaturated dibasic acids (or

anhydrides) dissolved in unsaturated vinyl monomers. Polyesters, if used as matrix for composite production, have improved tensile and flexural values; their sensitivity to brittle fracture is usually improved [6].

In this study, organically treated Na-montmorillonite was used as the filler, and a general purpose unsaturated polyester formulation was used as the matrix in the synthesis of nanocomposites. The nanocomposites were prepared by In-Situ Polymerization and Prepolymerization methods. In the In-Situ Method, the organoclay is added to the reaction medium simultaneously with the monomers. The penetration of the monomers into the clay layers is followed by polymerization. The Prepolymerization Method involved the addition of organoclay to the previously synthesized unsaturated polyester matrix.

X-Ray Diffraction and Scanning Electron Microscopy analyses were performed in order to investigate the extent of dispersion of the filler in the matrix. The glass transition temperatures of the materials were determined by Differential Scanning Calorimetry. Flexural and impact tests were performed to characterize the mechanical properties of the nanocomposites.

CHAPTER 2

BACKGROUND

2.1 Composites

Since the early 1960's, there has been an increasing demand for materials that are stiffer and stronger, yet lighter, in aeronautic, energy, civil engineering and various structural applications. Unfortunately, no monolithic material is available to satisfy them. This need and demand certainly led to the concept of combining different materials in an integral composite structure [6]. The fundamental goal in the production and application of composite materials is to achieve performance from the composite that is not available from the separate constituents or from other materials. The concept of improved performance is broad and includes increased strength or reinforcement of one material by the addition of another material [7].

A composite is a combined material created by the synthetic assembly of two or more components; a selected filler or reinforcing agent and a compatible matrix binder in order to obtain specific characteristics that are related to desired properties.

The matrix can be an engineering material such as ceramic, metal or polymer. Polymers are the most developed matrix materials, and they find widespread applications owing to the ease of fabrication into any large complex shape [8].

2.1.1 Matrix

In a polymer composite, the matrix transfers the load to the reinforcements and distributes the stress among them. It is also responsible for protecting the reinforcement from the environment and allows the necessary positioning of them [9].

All polymers can be divided into two major groups based on their thermal processing behavior.

2.1.1.1 Thermoplastics

Thermoplastic polymers are linear polymers. The bonding occurring along the polymer backbone is covalent. The bonding between the polymer molecules is via secondary forces [10]. These polymers can be softened by heat in order to process into a desired form [11]. Usually, there are higher levels of toughness values and proper damage tolerances for thermoplastics when compared with thermosets. However, being partially crystalline for most cases, the resulting polymer matrix may also suffer from a change in the level of crystallinity during the fabrication and processing of composites due to the variations in the heating and cooling rates, as well as the thickness [6]. Polystyrene is an important example of a commercial thermoplastic. Other major examples are the polyolefins (e.g., polyethylene and polypropylene) and poly(vinyl chloride) [11].

2.1.1.2 Thermosets

Thermosets are polymers whose individual chains have been chemically linked by covalent bonds during polymerization or by subsequent chemical or thermal treatment during fabrication [11]. They are low molecular weight reactive oligomers at the beginning. In general, they contain two or more components, which consist of a proper catalyst and/or a hardener. The subsequent reaction produces a rigid, highly-crosslinked network [6]. Once formed, these crosslinked networks resist heat softening, creep, and solvent attack, but can not be thermally processed. Such properties make thermosets suitable materials for composites, coating and adhesive applications. Principle example of thermosets include epoxy, phenol-formaldehyde resins, and unsaturated polyesters [11].

2.1.2 Reinforcement

Reinforcing agents are a special class of fillers with reinforcement properties of the matrix, and they are either particulates or fibrous in shape, with classification depending mainly on the aspect ratios (ratio of length to breadth) involved [6].

2.2 Nanocomposites

Nanocomposites are a new class of composites in which the filler dimensions are in the nanometer (10^{-9}m) range [12]. The concept of nanoscale reinforcement provides opportunity for synthesis of new polymer materials with unique properties [13]. Conventional composites are based on microscale reinforcement. However, owing to the large interfacial area per unit volume [12], dispersion of the inorganic filler at the nanometer scale have led to significant improvements in the properties of polymer nanocomposites [13].

Three types of nanocomposites can be distinguished, depending on how many dimensions of the dispersed particles are in the nanometer range:

- When three dimensions are in the order of nanometers, they are called isodimensional nanoparticles, such as spherical silica nanoparticles.
- When two dimensions are in the nanometer scale and the third is larger, they form elongated structures like nanotubes or whiskers.
- When only one dimension is in the nanometer range, the filler is in the form of sheets of one to a few nanometers thick, and to hundreds to thousands nanometer long.

The third type constitutes the family of composites, which can be gathered under the name of polymer-layered crystal nanocomposites [14].

2.3 Polymer-Layered Crystal Nanocomposites

These materials are almost exclusively obtained by the intercalation of the polymer (or a monomer subsequently polymerized) inside the galleries of layered host crystals [14].

Owing to the nanocomposite structure, they exhibit concurrent improvements in several material properties, for very moderate inorganic loadings (typically less than 6%). Enhanced properties include improved tensile characteristics, higher heat deflection temperature, higher barrier properties and increased flame retardancy.

At the same time, optical clarity and light weight are largely maintained [15]. Uses for this new class of materials can be found in aerospace, automotive, electronics and biotechnology applications, to list only a few [16].

2.3.1 Layered Silicates

There is a wide variety of both synthetic and natural crystalline fillers that are able, under specific conditions, to intercalate a polymer. Amongst all the potential nanocomposite precursors, those based on clays and layered silicates have been more widely investigated probably because the starting clay minerals are easily available and because their intercalation chemistry has been studied for a long time [14].

Because of its suitable layer charge density [4], montmorillonite is nowadays the most widely used clay as nanofiller. The model structure of montmorillonite is given in Figure 2.1, which consists of two fused silica tetrahedral sheets sandwiching an edge-shared octahedral sheet of either aluminum or magnesium hydroxide.

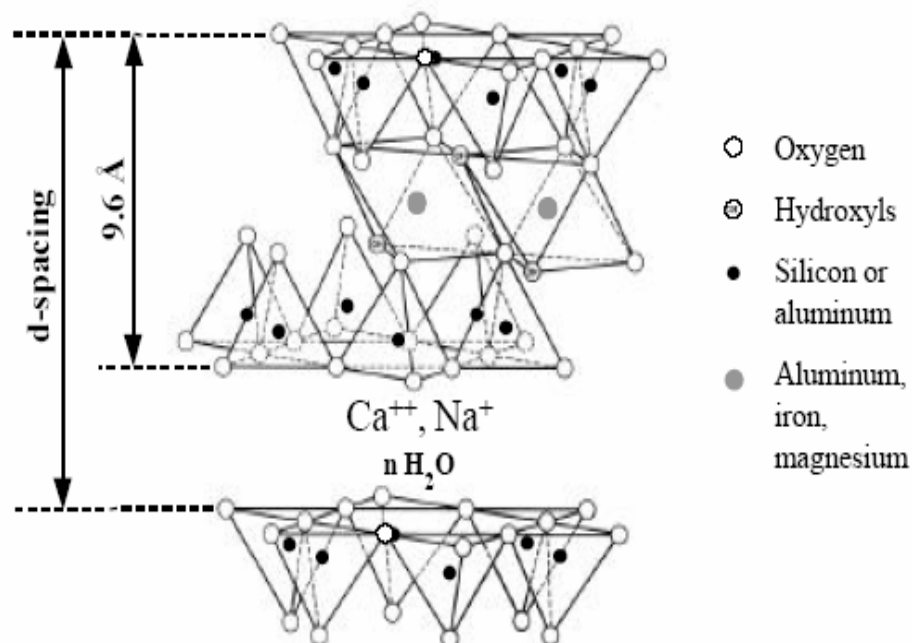


Figure 2.1 The model structure of montmorillonite [4].

They have charge deficiencies partly due to isomorphous substitutions of Al^{3+} and Si^{4+} in each layer, which are counterbalanced by cations, principally sodium and calcium. Water, other hydroxyl-containing groups and amines readily break these ionic bonds. Once the sheets have been parted, many layers can be adsorbed producing a marked expansion of the structure. Under certain conditions, separation of the platelets into primary layers can occur giving very high aspect ratio products [3]. Stacking of the layers leads to regular van der Waals gaps called *interlayers* or *galleries*.

The sum of the single layer thickness (9.6\AA) and the interlayer represents the repeat unit of the multilayer material, so called *d-spacing* or *basal spacing*. The d-spacing between the layers for Na-montmorillonite varies from 9.6\AA for the clay in the collapsed state to approximately 20\AA when the clay is dispersed in the water solution.

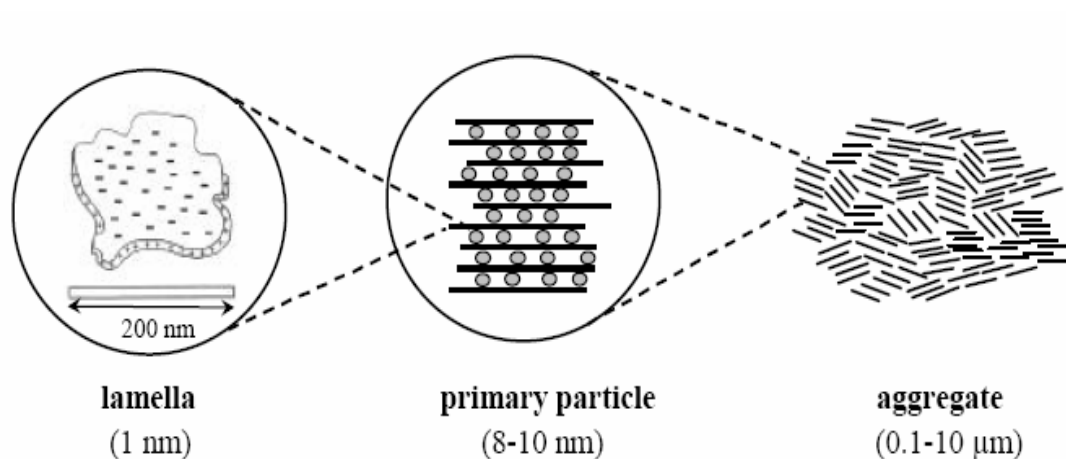


Figure 2.2 Microstructure of montmorillonite [4].

The microstructure of montmorillonite can be seen in Figure 2.2. Clays are in the form of aggregates consisting of primary particles with thickness of 8-10 nm, which contains five to ten lamellae associated by interlayer ions. The grey circles in the primary particle represent the intercalated cations (Na^+ , Ca^{++} , K^+ ,...). On a larger scale, each layer can be seen as a high aspect ratio lamella about 100-200 nm in diameter and 1 nm in thickness [4].

2.3.1.1 Cation-Exchange Process

Although the high aspect ratio of silicate nanolayers is ideal for reinforcement, the nanolayers are not easily dispersed in most polymers due to their preferred face-to-face stacking in agglomerated tactoids. Dispersion of the tactoids into discrete monolayers is further hindered by the intrinsic incompatibility of hydrophilic layered silicates and hydrophobic engineering plastics. However, as was first demonstrated by the Toyota group more than 10 years ago, the replacement of the inorganic exchange cations in the galleries of the native clay by alkylammonium surfactants can compatibilize the surface chemistry of the clay and the hydrophobic polymer matrix.

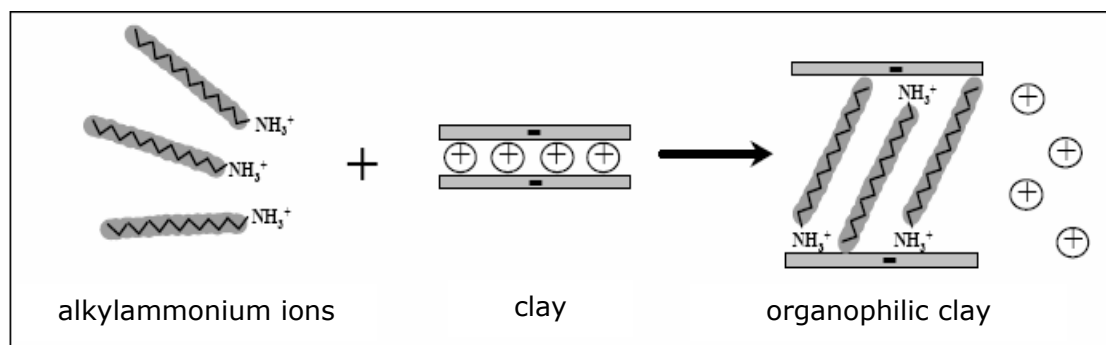


Figure 2.3 The cation-exchange process between alkylammonium ions and cations initially intercalated between the clay layers [4].

By inserting long chain surfactants into the hydrophilic galleries of the native clay, the interlayer distance increases, and the surface chemistry of the clay is modified. In an ideal system, these newly rendered organophilic galleries allow for the intercalation of monomer or prepolymer, and eventually the formation of exfoliated nanocomposites [17]. Additionally, the alkylammonium cations can provide functional groups that can react with the polymer matrix, or in some cases initiate the polymerization of monomers to improve the strength of the interface between the inorganic and the polymer matrix [18].

Depending on the layer charge density of the clay, the alkylammonium ions adopt different structures between the clay layers. For a given clay, the maximum amount of cations that can be taken up is constant and is known as the *cation-exchange capacity* (CEC). It is measured in milliequivalents per gram

(meq/g) and more frequently per 100 g (meq/100g). The CEC of montmorillonite varies from 80 to 150 meq/100g [4].

2.3.2 Nanocomposite Synthesis Methods

2.3.2.1 In-Situ Polymerization Method

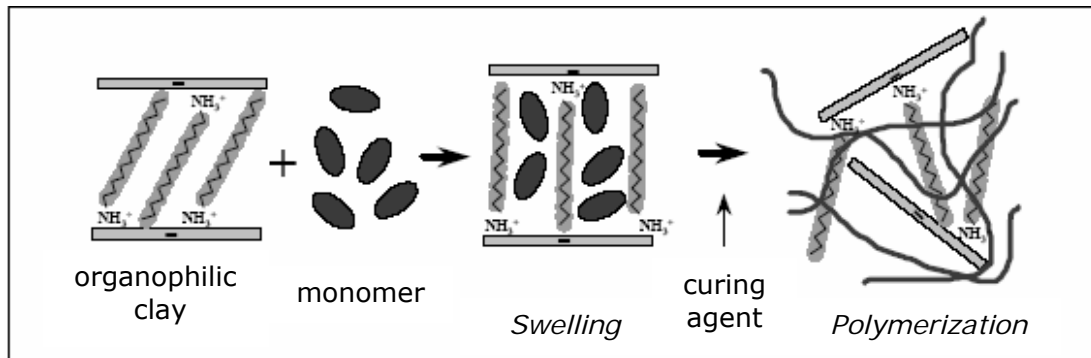


Figure 2.4 The “in-situ” polymerization [4].

It is the conventional process used to synthesize thermoset-clay nanocomposites. First, the organoclay is swollen in the monomer. This step requires a certain amount of time, which depends on the polarity of the monomer molecules, the surface treatment of the organoclay, and the swelling temperature. Then, the reaction is initiated. For thermosets such as epoxies or unsaturated polyesters, a curing agent or a peroxide, respectively, is added to initiate the polymerization. For thermoplastics, the polymerization can be initiated either by the addition of a curing agent or by an increase of temperature.

During the swelling phase, the high surface energy of the clay attracts polar monomer molecules so that they diffuse between the clay layers. When a certain equilibrium is reached the diffusion stops and the clay is swollen in the monomer to a certain extent. When the polymerization is initiated, the monomer starts to react with the curing agent. This reaction lowers the overall polarity of the intercalated molecules and displaces the thermodynamic equilibrium so that more polar molecules are driven between the clay layers. As this mechanism occurs, the organic molecules can eventually delaminate the clay. Polymer-clay

nanocomposites based on epoxy, unsaturated polyester, polyurethanes and polyethylene terephthalate have been synthesized by this method [4].

2.3.2.2 Melt Intercalation Method

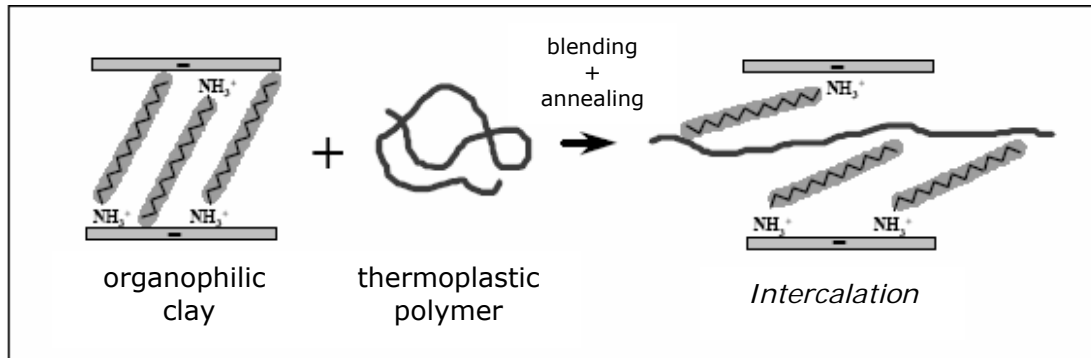


Figure 2.5 The "melt intercalation" process [4].

The layered silicate is mixed with the polymer matrix in the molten state. Under these conditions and if the layer surfaces are sufficiently compatible with the chosen polymer, the polymer can crawl into the interlayer space and form either an intercalated or an exfoliated nanocomposite. In this technique, no solvent is required [14]. Polypropylene nanocomposites are generally synthesized by this method [19].

2.3.2.3 Solution Intercalation Method

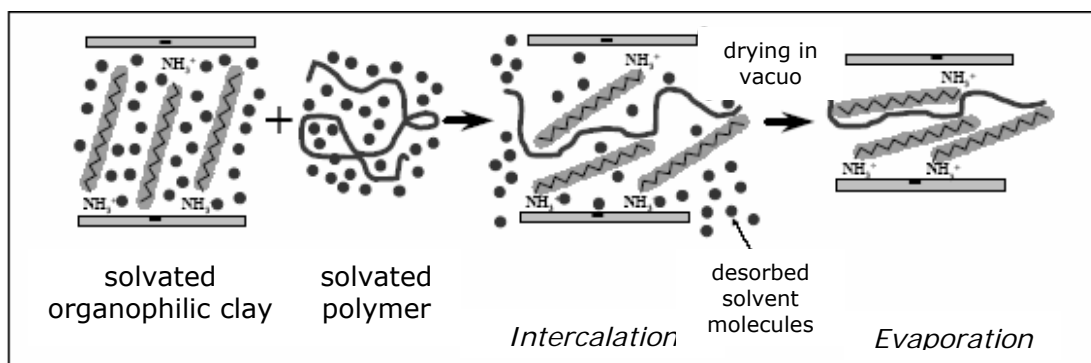


Figure 2.6 The "solution intercalation" method [4].

The layered silicate is exfoliated into single layers using a solvent in which the polymer (or a prepolymer in case of insoluble polymers such as polyimide) is soluble. It is well known that such layered silicates, owing to the weak forces that stack the layers together can be easily dispersed in an adequate solvent. The polymer then adsorbs onto the delaminated sheets, and when the solvent is evaporated (or the mixture precipitated), the sheets reassemble, sandwiching the polymer to form, in the best case, an ordered multilayer structure [14].

2.3.3 Nanocomposite Structures

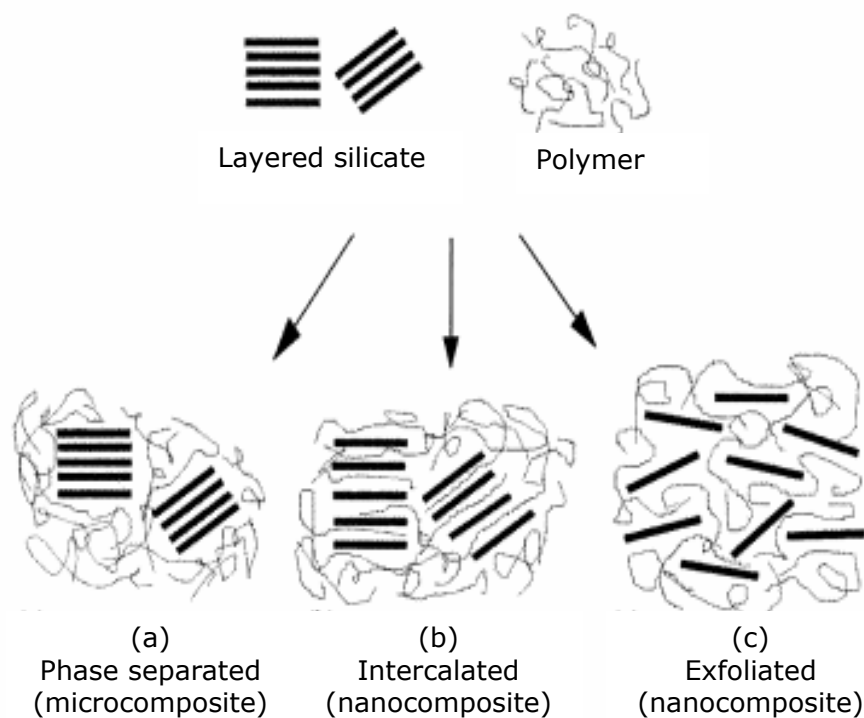


Figure 2.7 Scheme of different types of composites arising from the interaction of layered silicates and polymers: (a) phase-separated microcomposite; (b) intercalated nanocomposite and (c) exfoliated nanocomposite.

The key to the performance of nano-clays is how well they can be dispersed into a polymer matrix. Types of dispersion that can be achieved need to be considered. Three types of structures can be recognised [3].

- Conventional composite: Silicate tactoids exist in their original aggregated state with no intercalation of the polymer matrix into the galleries. For this case, the particles act as microscale fillers [13].
- Intercalated Nanocomposite: A single (or sometimes more than one) extended polymer chain is intercalated between the silicate layers resulting in a well ordered multilayer morphology built up with alternating polymeric and inorganic layers [14].
- Exfoliated/Delaminated Nanocomposite: Extensive polymer penetration, resulting in disorder and eventual delamination of the silicate layer, produces exfoliated structures consisting of individual 1 nm thick silicate layers suspended in the polymer matrix [5].

The fully dispersed form is most useful for the majority of commercial applications, and is the one that is normally aimed for, although conventional processing methods often give mixed structures [3].

2.4 Unsaturated Polyesters

Unsaturated polyesters (UP) are linear polycondensation products based on unsaturated and saturated acids/anhydrides and diols or oxides dissolved in unsaturated vinyl monomers. They comprise a versatile family of thermosetting materials which are generally pale yellow oligomers with a low degree of polymerization. Depending on the chemical composition and the molecular weight (1200-3000 g/mol), these oligomers may be viscous, liquids or brittle solids. The unsaturation in the backbone provides sites for reaction with vinyl monomers using free-radical initiators, leading to the formation of a three-dimensional network. The solutions of unsaturated polyesters and vinyl monomers which are reactive diluents are known as UP resins [20].

2.4.1 History of Unsaturated Polyesters

The actual preparation of the first polyester resin is accredited to both Berzelius in 1847 and Gay-Lussac and Pelouze in 1883. The unsaturated polyester resins used in today's reinforced plastics (RP) are combinations of reactive monomers. Carleton Ellis, in the 1930's, discovered that unsaturated polyester resins made

by reacting glycols with maleic anhydride could be cured to insoluble solids simply by adding a peroxide catalyst. He applied for a patent on this idea in 1936.

Ellis later discovered that a more useful product could be made by combining the unsaturated polyester alkyd with such reactive monomers as vinyl acetate or styrene, which makes it easier to add the catalyst and apply the resin [21].

The beginning of the second world war accelerated development in the field of polyesters, as it did in many other fields of research and development. In 1942, the United States Rubber Company discovered the reinforcement that glass fibers convey to plastics of the polyester type. This, then, was the beginning of the large scale commercial use of unsaturated polyesters. The first successful application of glass-reinforced products was in the use of radomes for aircraft industry. This derived from a great need for protective coverings over radar scanning apparatus, thus permitting a minimum hindrance of radar transmission and reception [22].

2.4.2 Application Areas of Unsaturated Polyesters

UP resins either in the form of pure resin or in the compounded form with fillers find a wide range of applications. Their main applications are in the construction industry (non-reinforced or glass-fiber-reinforced products), automotive industry, and industrial wood and furniture finishing.

Some of the important products based on UP resins are cast items such as pearl buttons, knife and umbrella handles, and encapsulated electronic assemblies. Polyester compounds have been formulated for the manufacture of bathroom fixtures. Floor tiles have been manufactured by mixing UP resin with fillers such as limestone, silica, china clay, and more.

The applications of UP resins in a variety of areas such as transportation, electrical appliances, and building and construction are largely due to development of bulk and sheet molding compounds using glass fibers [20].

2.4.3 Synthesis of Unsaturated Polyesters

The polyester backbone is composed of three basic types of structural units. They are synthesised by the polycondensation reaction of a saturated acid or anhydride, an unsaturated acid or anhydride and a glycol. In the case of the general-purpose polyester, these components usually consist of phthalic acid, maleic acid and propylene glycol. Figure 2.8 shows an unbalanced reaction scheme for the synthesis of unsaturated polyesters.

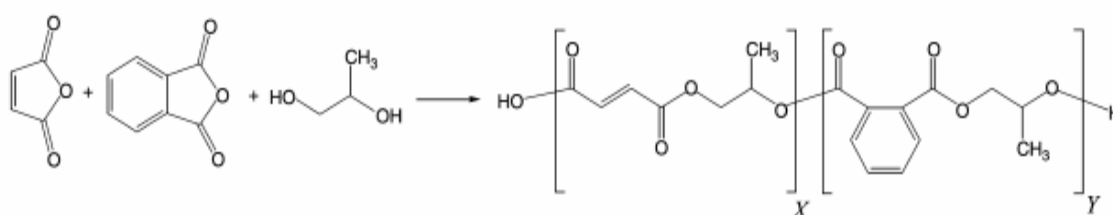


Figure 2.8 Synthesis reaction of UP from maleic anhydride, o-phthalic anhydride and propylene glycol

The unsaturated acid provides the sites for the cross-linking, the saturated acid determines the degree of spacing or concentration of the unsaturated acid molecules along the polyester chains, and the glycol, of course, provides the means for esterification and for bridging the acids to form a prepolymer [22].

The obtained unsaturated prepolymer is then diluted in styrene, and the resin solution is cross-linked by the addition of a peroxide initiator. Unsaturated polyesters are versatile, since a large amount of different glycols and unsaturated as well as saturated acids can be used to design different polymers. The composition of the prepolymer and the curing process can be tailored for a specific purpose [23].

2.4.4 Classification of Unsaturated Polyester Resins

Polyester resins can be classified on the basis of their structure as *ortho*-resins, *iso*-resins, bisphenol-A fumarates, chlorendics, and vinyl ester resins.

a. *Ortho*-Resins

They comprise the largest group of polyester resins which are known as the general-purpose resins. They are synthesized with *ortho*-phthalic anhydride (PA), maleic anhydride (MA) and glycols. PA is relatively low in price and provides an inflexible link in the backbone. Among the glycols, 1,2-propylene glycol is the most important one. Due to the presence of the pendant methyl group, the resulting resins are less crystalline and more compatible with commonly used reactive diluent (styrene) and those obtained using ethylene glycol, diethylene glycol (DEG), and triethylene glycol [20]. Maleic anhydride does not appear to have a competitor other than its isomer fumaric acid since there does not seem to be another unsaturated dibasic acid that can match both the cost and quality of these isomers [22].

b. *Iso*-Resins

They are prepared using *iso*-phthalic acid, MA/fumaric acid, and glycol. These resins are higher in cost than *ortho*-resins and also have considerably higher viscosities, hence a higher proportion of reactive diluent (styrene) is needed. The presence of higher quantities of styrene imparts improved water and alkali resistance to the cured resins. *Iso*-phthalic resins are thus of higher quality since they have better thermal and chemical resistance and mechanical properties [20].

c. Bisphenol-A Fumarates

They are synthesized by reacting ethoxy-based bisphenol-A with fumaric acid. The introduction of bisphenol-A in the backbone imparts a higher degree of hardness and rigidity and improvement in the thermal performance [20].

d. Chlorendics

To enhance flame retardency, chlorine/bromine-containing anhydrides or phenols are used in the preparation of UP resins. For example, reaction of chlorendic anhydride/chlorendic acid with MA/fumaric acid and glycol yields the resin with better flame retardency than general-purpose UP resin. Other monomers also include tetrachloro or tetrabromophthalic anhydride [20].

e. Vinyl Ester (VE) Resins

Bisacryloxy or bismethacryloxy derivatives of epoxy resins contain unsaturated sites only in the terminal position and are prepared by reaction of acrylic acid or methacrylic acid with epoxy resin. The viscosity of neat resin is high; hence, reactive diluent (e.g., styrene) is added to obtain a lower viscosity of solution. Notable advances in VE resin formulations are low-styrene-emission resins, automotive grades with high tensile strength, heat deflection temperature and corrosion resistance [20].

2.4.5 Curing of Unsaturated Polyester Resins

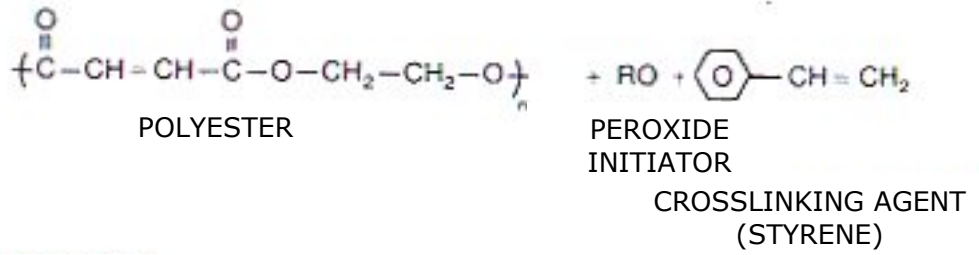
The curing of unsaturated polyester resins can be described as a free-radical copolymerization reaction. As there are several double bonds per polyester molecule, the polymerization proceeds with extensive crosslinking and results in a three-dimensional network [24].

Hydroquinone is widely used in commercial resins to provide stability during the dissolution of the hot prepolymer in styrene. The addition polymerization reaction between the unsaturated polyester and the styrene monomer is initiated by free-radical catalysts usually benzoyl peroxide (BPO) or methyl ethyl ketone peroxide (MEKP), which can be dissociated by heat or redox metal activators like cobalt naphthanate into peroxy and hydroperoxy free radicals.

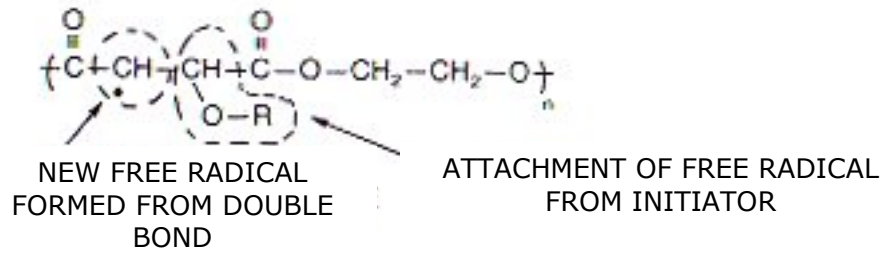


This catalyst system is temperature sensitive and does not function effectively at temperatures below 10°C, but at temperatures over 35°C the generation of free radicals can be too prolific, giving rise to incomplete cross-linking formation [25]. Figure 2.9 shows a schematic view of crosslinking reaction of unsaturated polyester.

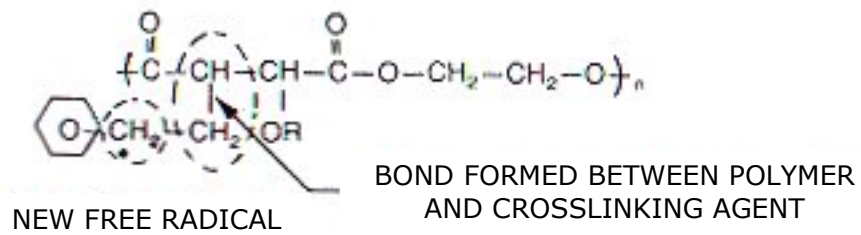
REACTANTS



INITIATION STEP



BRIDGING STEP



CROSSLINKED POLYMERS

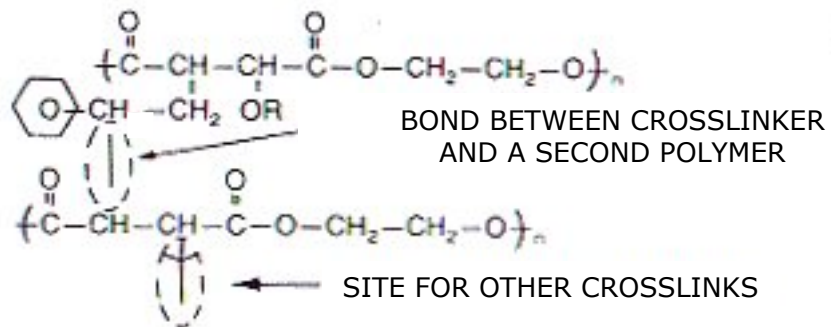


Figure 2.9 Schematic view of crosslinking of unsaturated polyester [26]

The curing process of unsaturated polyester resins can be divided into five stages;

a. Induction Stage

This stage is caused by the presence of inhibitor which consumes the radicals generated by initiators. Because of the high reaction rate constant between the radical and the inhibitor, propagation of radicals is suppressed by the inhibition effect. Radical concentration remains at a constant value because of the balance between radical generation and inhibition effect [27]. This temporary induction period between catalysis and the change to a semisolid gelatinous mass is referred to as "gelation time" and can be controlled between 1-60 min by varying stabilizer and catalyst levels [25].

b. Primary Polymer (Microgel) Formation Stage

As the amount of inhibitor is reduced to a very low level at the end of the induction period, monomeric radicals gain the chance to link with adjacent monomers and form primary polymers. The microgels can be described as weakly crosslinked networks. The radical concentration starts to increase gradually and reaches a constant rate because of the formation of stable radicals during the microgel formation stage [27].

c. Transition Stage

The number of microgels reaches a high level and the amount of unreacted UP monomers decreases to such a level that the ratio between the pendant vinylene and the unreacted UP monomers is very high [27]. Consequently, the double bonds buried inside the microgel undergo intramolecular crosslinking, while those on the surface react with monomers or microgels [25].

d. Macrogelation Stage

As the polymerization progresses, more and more microgels form and the resin system reaches the gel point and a polymer network is formed through chemical cross-linking. The reaction exotherm increases gradually and the system enters the early stage of major reaction exotherm [27].

d. Post-Gelation Stage

The radical concentration increases at a constant rate at the beginning of the post-gelation stage then gradually levels off at the end of reaction. The styrene-end stable radicals appear in this stage and dominate the radical population. The major reaction exotherm appears in this stage.

2.5 Casting

In the casting process, a liquid material is poured into a mold and allowed to solidify by chemical (e.g., polymerization) means resulting in a rigid object that generally reproduces the mold cavity detail with great fidelity. A large number of resins are available and a variety of molds and casting methods are used in casting processes. Therefore the choice of material, mold type and casting technique is determined by the particular application.

In casting processes, the resin is added with an appropriate amount of hardener, catalyst, or accelerator, mixed manually or mechanically, and then poured into a mold, which is normally coated with a mold-release agent. Air is removed if necessary, and the resin is allowed to solidify. The casting process is relatively slow and employs comparatively cheap equipment. To facilitate the removal of the cast part from the mold, mold releasing agents such as high melting waxes, silicone oils, greases and some film-forming agents are used to coat the mold. Among other considerations, the choice of mold-release agents is based upon the absence of interaction between the resin system and the release agent [28].

2.6 Characterization

2.6.1 Mechanical Properties

2.6.1.1 Flexural Tests

Flexural test is performed in order to measure the material's resistance to bending. The test method identifies the three point or four point loading system to determine the flexural properties of the polymers. In the three point loading system, the specimen of a known length is placed on a two supporting mounds separated by a distance L . The perpendicular load is applied at the mid-point of the support. The maximum stress in the specimen occurs at midspan [29].

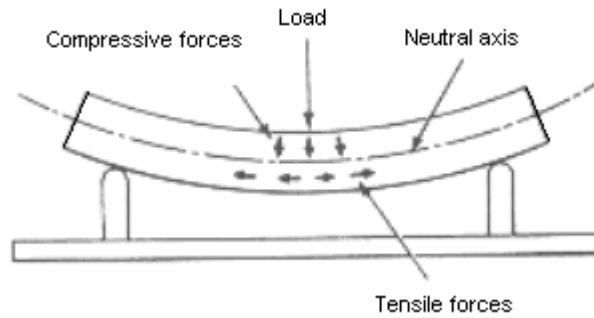


Figure 2.10 The stresses on the sample during flexural testing [30].

When the material is subjected to a bending force, the maximum stress developed is called as *flexural strength*. It is calculated by the following equation;

$$S = \frac{3PL}{2bd^2} \quad (2.1)$$

where S is the stress in the outer fibers at midspan (MPa), P is the load at a given point on the load-deflection curve (N), L is the support span (mm), b and d are the width and the depth of beam tested, respectively (mm).

The deflection at the breaking point is called *flexural strain at break* and may be calculated as follows;

$$r = \frac{6Dd}{L^2} \quad (2.2)$$

where r is the maximum strain in the outer fibers (mm/mm), D is the maximum deflection of the center of the beam (mm), L is the support span (mm), and d is the depth of the sample (mm).

Flexural modulus is the property used to indicate the bending stiffness of a material. It is calculated by drawing a tangent to the initial straight line portion of the load-elongation curve. The slope of this curve is substituted in Equation 2.3.

$$E_b = \frac{L^3 m}{4bd^3} \quad (2.3)$$

where E_b shows the modulus of elasticity in bending (MPa), L is the support span (mm), b and d are the width and the depth of beam tested, respectively (mm), and m is the slope of the tangent to the initial straight line portion of the load-deflection curve (N/mm) [29].

Flexural stress-strain curves can be drawn by using Equation 2.1 for the stress and Equation 2.2 for the strain.

2.6.1.2 Impact Tests

Impact test is applied to measure the energy to break the sample and therefore gives an idea about the toughness of the material. In impact test, a known weight strikes the sample and the energy is measured by the loss in the kinetic energy of the weight.

There are many types of special purpose impact tests. But the most popular impact tests are *izod* and *charpy impact tests* specified in ASTM D256.

Izod Impact test: The specimen is held vertically at the base of the test stand. The weight falls through a known height and breaks the sample. The specimen can be tested without a notch [10].

Charpy Impact test: The specimen is supported horizontally and broken by a single swing of the pendulum with impact line midway between the supports.

In this study, charpy impact test was applied to the test specimens in order to determine their impact strengths.

2.6.2 Differential Scanning Calorimetry (DSC)

Differential scanning Calorimetry (DSC) is a technique of non-equilibrium calorimetry in which the heat flow into or away from the polymer compared with the heat flow into or away from a reference is measured as a function of

temperature or time. Presently, available DSC equipment measures the heat flow by maintaining a thermal balance between the reference and the sample by changing a current passing through the heaters under the two chambers [31].

Two identical small sample pans are instrumented to operate at the same temperature and can be programmed up or down in temperature at the same rate. A sample is placed in one pan and the other is left empty [32]. A known weight of polymer, typically 3 to 10 mg is placed in a pan and the pan is placed into a test cell. The heating or cooling rate is selected, usually 10 or 20 °C/min, and the initial and the final temperatures are preset [10]. If a temperature is encountered at which the sample undergoes a change of phase or state, more or less power will be needed to keep the sample pan at the same temperature as the reference pan (depending on whether the reaction is exothermic or endothermic) [32]. For instance, at T_g , the heat capacity of the sample suddenly increases requiring more power (relative to reference) to maintain the temperatures the same, the differential heat flow to the sample (endothermic) causes a drop in the DSC curve [33].

In order to obtain useful thermodynamic data, the DSC heating or cooling rate must be sufficiently slow for the sample to respond to the temperature change [10].

The advantages of DSC include speed, low cost, and the ability to use small samples.

2.6.3 X-Ray Diffraction (XRD)

X-Ray Diffraction (XRD) is a versatile method that gives information about the order of crystallinity of the material. In the spectrum of electromagnetic radiation, X-Rays lie between the ultraviolet rays and gamma rays. Those X-Rays used for structure analysis have wavelengths λ in the range of 0.05-0.25 nm.

Most work on polymers is done with the Cu $K\alpha$ emission line with an average wavelength equal to 0.154 nm [34]. When electrons are accelerated in an electric field and impinge on a metal target, X-Rays are generated.

Diffraction is essentially a scattering phenomena in which phase relations are such that destructive interference occurs in most directions of scattering, but in a few directions constructive interference takes place and diffracted beams are formed. The two essentials of XRD are a wave motion capable of interference (X-Rays) and a set of periodically arranged scattering centers [35].

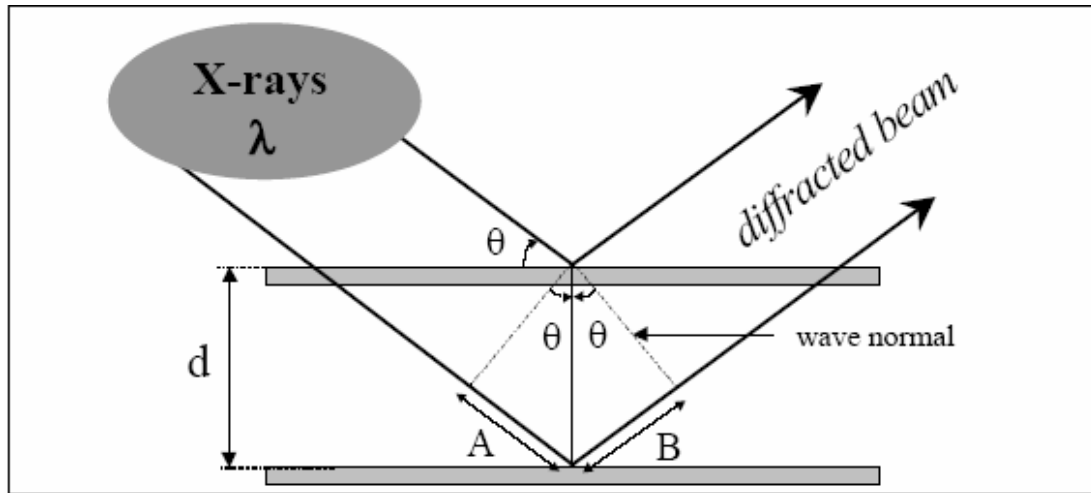


Figure 2.11 Principle of X-Ray diffraction.

Figure 2.11 shows the diffraction from two scattering planes (i.e. two consecutive clay layers or other crystallographic planes of the layers themselves) that are separated by a distance d (i.e. interlamellar spacing or d -spacing) and intercept X-rays of wavelength λ at the incident angle θ . The experimental 2θ value is the angle between the diffracted and incoming X-ray waves. The wave normals connect points of identical phase for incident and diffracted waves. Since the direction of d is normal to the planes, and the wave normal is normal to the wavelets, the angles opposite A and B are also θ . Thus, $\sin \theta = A/d = B/d$ so that $(A+B) = 2d\sin\theta$. Thus, a constructive interference occurs when:

$$n\lambda = 2d\sin\theta \quad (2.4)$$

This equation is known as the Bragg Law. The integer n refers to the degree of the diffraction [4].

2.6.4 Scanning Electron Microscopy (SEM)

The Scanning Electron Microscope permits the materials to be examined in three dimensions. It is an extension of the reflected light microscope and because of its depth of focus and greater resolution, it fills the gap between the light and electron optics. In a Scanning Electron Microscope, a current is passed through a filament and the filament is heated sufficiently to emit electrons [32]. The basic components of the SEM are the lens system, electron gun, electron collector, visual and recording cathode ray tubes and the electron associated with them [37]. The electrons are accelerated by applying a high voltage (1-30 kV) and the electron beam is focused with a series of electromagnetic lenses [32].

In Scanning Electron Microscope, high resolution is achieved by scanning a very finely focused beam of short-wave length electrons across a surface and by the detection of either the back-scattered or secondary electrons [36].

In SEM, if the specimen is not a good conductor it should be coated with a thin layer of conducting material. This coating is done by placing the specimen in a high vacuum evaporator and vaporizing a suitable material such as gold, silver or aluminum [36].

Some advantages of SEM are simple image interpretation and ease of sample preparation [32].

2.7 Previous Studies

Kornmann X. et al. [13] investigated the possibility to synthesize materials with nanocomposite structure based on MMT (montmorillonite) and UP (unsaturated polyester). The results confirmed the formation of a nanocomposite material and the mechanical properties were improved even with 1.5 vol% MMT content.

Suh D.J et al. [5] studied the effects of different mixing methods (simultaneous and sequential) on the property and the formation mechanism of UP/MMT nanocomposites. In the simultaneous mixing process, the unsaturated polyester chains, styrene monomers and organophilic-treated MMTs were simultaneously mixed for 3h at 60°C.

In the Sequential mixing process, at first the preintercalates of UP and MMT nanocomposites were prepared. This mixture was then dissolved in styrene. It was observed that the total crosslinking density of the samples decreased in the simultaneous mixing method due to the low concentration of styrene in uncured UP chains as a result of its high diffusion coefficient ($10^{-5} \text{ m}^2/\text{s}$) when compared to UP ($10^{-7} \text{ m}^2/\text{s}$). However in the sequential mixing method, the crosslinking reaction took place homogeneously inside and outside of the silicate layers and crosslinking density reached the degree of the crosslinking density of the cured pure UP.

Suh D.J. et al. [38] studied the properties of unsaturated polyester based on the glycolized PET with various glycol compositions and found that the extent of decomposition of PET decreases with increasing amount of DEG (diethylene glycol) and the gelation time is also delayed. The tensile toughness of the cured resin was greatly enhanced by incorporating DEG units.

Bharadwaj R.K. et al. [39] investigated the structure-property relationships in crosslinked polyester and found that although there is a firm evidence showing the formation of a nanocomposite structure, the tensile modulus, loss and storage modulus exhibit a progressively decreasing trend with increasing clay concentration due to the decrease in the degree of crosslinking with increasing clay concentration.

Gamstedt E.K. et al. [23] studied the effect of adjusting the chemical composition of unsaturated polyester on the interfacial strength between the carbon fibers and the polymer matrix. The strongest interface was obtained with the highest degree of unsaturation which is controlled by the relative amount of maleic anhydride.

Yilmazer Ü. and İnceoğlu B. [40] investigated the effects of unmodified and organically modified MMT and ultrasonic mixing on the mechanical properties of MMT/UP nanocomposites. Modified montmorillonites showed improvements on the mechanical properties with the maximum degree of exfoliation at approximately 3% - 5% clay content. The degree of exfoliation was lower in the unmodified one. It was also observed that ultrasonic bath after mechanical mixing has a positive effect on the Young's modulus, tensile and impact strength of the composites.

CHAPTER 3

EXPERIMENTAL

3.1 Materials

3.1.1 Monomers

3.1.1.1 Maleic Anhydride

The Maleic Anhydride (MA) used in this study was purchased from Poliya A.Ş. It is available as white powder. It provided the unsaturation sites which take part in the crosslinking reaction. Some of its physical properties are given in Table 3.1 and its chemical structure is shown in Figure 3.1.

Table 3.1 Physical Properties of Maleic Anhydride

Molecular Weight (g/mol)	98.05
Boiling Point (°C)	200
Freezing Point (°C)	52.6

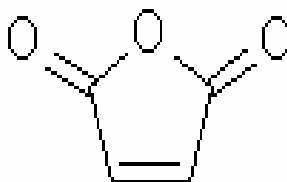


Figure 3.1 Chemical structure of Maleic Anhydride

3.1.1.2 *O*-Phthalic Anhydride

O-Phthalic Anhydride (PA) used in this study was purchased from Poliya A.Ş. It provides an inflexible ring to the backbone of unsaturated polyester. Some of its physical properties are given in Table 3.2 and its chemical structure is shown in Figure 3.2.

Table 3.2 Physical Properties of *O*-Phthalic Anhydride

Molecular Weight (g/mol)	148.118
Boiling Point (°C)	286.85
Freezing Point (°C)	130.85

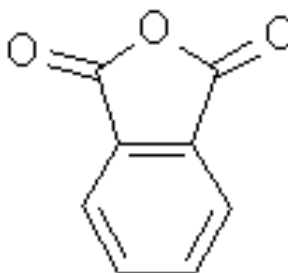


Figure 3.2 Chemical structure of *O*-Phthalic Anhydride

3.1.1.3 Propylene Glycol

The Propylene Glycol (PG) used in this study was supplied by Solventas Company. In the synthesis of unsaturated polyester, it was used to impart flexibility to the backbone. Some of its properties are given in Table 3.3 and its chemical structure is shown in Figure 3.3.

Table 3.3 Physical properties of Propylene Glycol

Molecular Weight (g/mol)	76.1
Specific Gravity (20/20c)	1.38-1.39
Water % max	0.2
Boiling Point (°C)	188.2

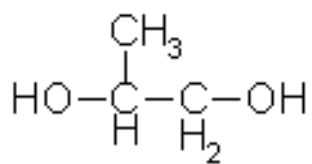


Figure 3.3 Chemical structure of Propylene Glycol

3.1.2 Crosslinking Agent

3.1.2.1 Styrene

In this study, styrene was used as the solvent and the crosslinking agent. It was obtained from Solventaş Company. Some of its properties are given in Table 3.4 and its chemical structure is shown in Figure 3.4.

Table 3.4 Physical Properties of Styrene

Molecular Weight (g/mol)	104.15
Boiling Point (°C)	145
Specific Gravity (20/20c)	0.9

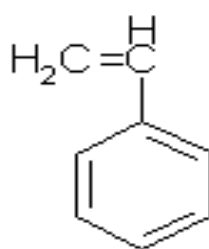


Figure 3.4 Chemical Structure of Styrene

3.1.3 Catalyst

3.1.3.1 Methyl Ethyl Ketone Peroxide (MEKP)

Methyl Ethyl Ketone Peroxide was used as the catalyst for the crosslinking reaction of the unsaturated polyester resin. It was purchased from Poliya A.Ş. and is available as liquid. Its chemical structure is given in Figure 3.5.

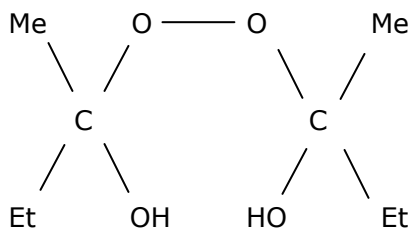


Figure 3.5 Chemical structure of MEKP

3.1.4 Accelerator

3.1.4.1 Cobalt Naphthanate

The Cobalt Naphthanate was purchased from Poliya A.Ş. and is available as 1% solution. It was used as the accelerator in the crosslinking reaction of unsaturated polyester resin.

3.1.5 Organoclays

Experiments were carried out with natural clay montmorillonite organically modified with three different quaternary ammonium salts. These organoclays were purchased from Southern Clay Products. Figure 3.6 shows the organoclay (Cloisite® Nanoclays) selection chart based on polymer/monomer chemistry.

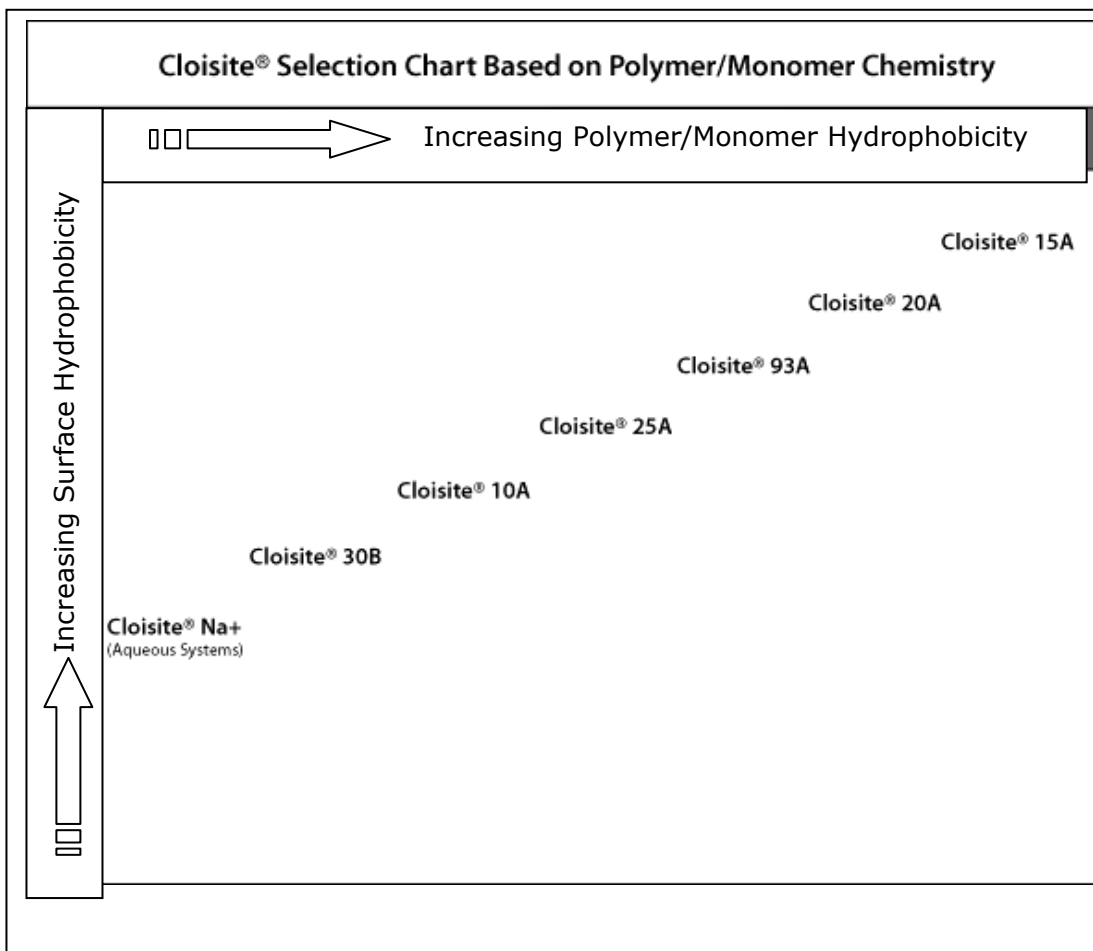


Figure 3.6 Cloisite® selection chart from Southern Clay Products.

Cloisite® Nanoclays are surface treated to be compatible with a whole host of systems. The chart above indicated relative hydrophobicity of the products.

3.1.5.1 Cloisite 30B

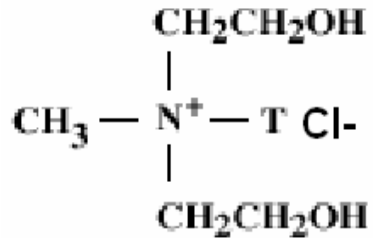


Figure 3.7 Chemical structure of the quaternary ammonium salt used in the manufacture of Cloisite 30B

Figure 3.7 shows the chemical structure of the quaternary ammonium with its anion, chloride used in Cloisite 30B. Some physical data of Cloisite 30B are given in Table 3.5

Table 3.5 Manufacturer's Physical Data of Cloisite 30B

Properties	Cloisite®30B
Organic Modifier	MT2EtOH
Modifier Concentration	90meq/100g clay
% Moisture	< 2%
% Weight loss on ignition	30%
Specific gravity	1.98
Color	Off white
Typical Dry Particle Sizes (microns, by volume)	10% less than 2μ 50% less than 6μ 90% less than 13μ
Initial d-spacing	18.5 Å

* HT = hydrogenated tallow (~65%C18; ~30%C16; ~5%C14),
M = Methyl, 2EtOH = bis-2hydroxyethyl.

3.1.5.2 Cloisite 25A

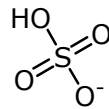
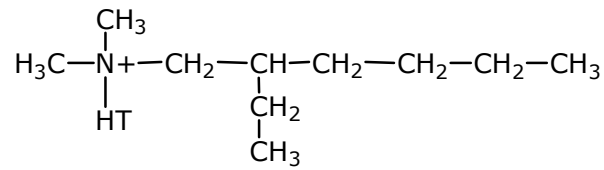


Figure 3.8 Chemical structures of the quaternary ammonium and the anion, methyl sulfate used in the manufacture of 25A

Figure 3.8 shows the chemical structure of the quaternary ammonium with its anion, methyl sulfate used in Cloisite 25A. Some physical data of Cloisite 25A are given in Table 3.6

Table 3.6 Manufacturer's Physical Data of Cloisite 25A

Properties	Cloisite®25A
Organic Modifier	2MHTL8
Modifier Concentration	95meq/100g clay
% Moisture	< 2%
% Weight loss on ignition	34%
Specific gravity	1.87
Color	Off white
Typical Dry Particle Sizes (microns, by volume)	10% less than 2μ 50% less than 6μ 90% less than 13μ
Initial d-spacing	18.6 Å

* HT = hydrogenated tallow (~65%C18; ~30%C16; ~5%C14),
2 M = dimethyl, L8 = 2-ethylhexyl.

3.1.5.3 Cloisite 15A

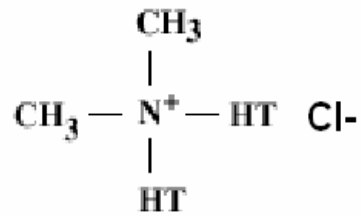


Figure 3.9 Chemical structure of the quaternary ammonium salt used in the manufacture of Cloisite 25A

Figure 3.9 shows the chemical structure of the quaternary ammonium with its anion, chloride used in Cloisite 15A. Some physical data of Cloisite 15A are given in Table 3.7.

Table 3.7 Manufacturer's Physical Data of Cloisite 15A

Properties	Cloisite®15A
Organic Modifier	2M2HT
Modifier Concentration	125meq/100g clay
% Moisture	< 2%
% Weight loss on ignition	43%
Specific gravity	1.66
Color	Off white
Typical Dry Particle Sizes (microns, by volume)	10% less than 2μ 50% less than 6μ 90% less than 13μ
Initial d-spacing	31.5 Å

* 2HT = dihydrogenated tallow (~65%C18; ~30%C16; ~5%C14),
2M = dimethyl.

3.1.6 Release Agent

Polywax SV-6 from Poliya A.Ş. was used as the release agent in order to make it easy to take the cured specimens out of the molds.

3.2 Experimental Procedure

3.2.1 In-Situ Polymerization Method

The flowchart of the specimen preparation procedure by the In-Situ Method is shown in Figure 3.10. First, the monomers and the clay were fed together to the reactor. The relative molar ratios of the monomers were 1:3.6:5.4 (PA:MA:PG). The composites contained 0, 1, 3 or 5 % wt. organoclay with different modifiers. The reaction took place for nearly 14h at 160°C. Each hour, 20ml toluene was used as an azeotropic solvent to assist water removal. During the reaction, the acid number of the polymer obtained was determined to monitor the molecular weight of the unsaturated polyester. The procedure of the acid number determination will be explained following the experimental procedure part. When the acid number reached nearly 40 mgKOH/g resin, vacuum was applied for 1 hour in order to remove the residual water and the unreacted monomers from the reactor. 50ppm hydroquinone was added to styrene which was heated up to 50°C to prevent premature gelation of the resin. Then the prepolymer and clay mixture was dissolved in 35% wt. styrene. It was mechanically mixed for 3 hours. The resin was cooled to room temperature and the styrene content in the resin was determined by a procedure which will be explained in the latter part of the experimental procedure section. After determining the deficient amount of styrene, the amount of styrene to obtain 35% wt. of the resin was added to the mixture and mechanically mixed for a while (~15min). An additional ultrasonic mixing with a frequency of 35 kHz was applied for 0.5h. After the addition of cobalt naphthanate as the initiator (0.16% of the resin), the resin and the initiator was mixed for few minutes and vacuum was applied for ~20min. Then MEKP, as the catalyst, was added (0.54% of the resin) and mixed for ~10s. Finally, after the release agent was applied to the aluminum mold surfaces, the resin was casted into the molds which are shaped according to ASTM standards. Materials were cured for 4 h at 120°C. The temperature was gradually increased from room temperature to 120°C at the beginning and then cooled from 120°C to room temperature at the end of the curing stage in order to prevent craze and cracks due to sudden crosslinking and cooling.

3.2.2 Prepolymerization Method

When compared to the In-Situ Method, the Prepolymerization method differs such that the clay was not fed to the reactor with the monomers but added to the resin after dissolving the prepolymer in styrene. The rest of the procedure is just the same. The flowchart of the specimen preparation by the Prepolymerization Method is shown in Figure 3.11.

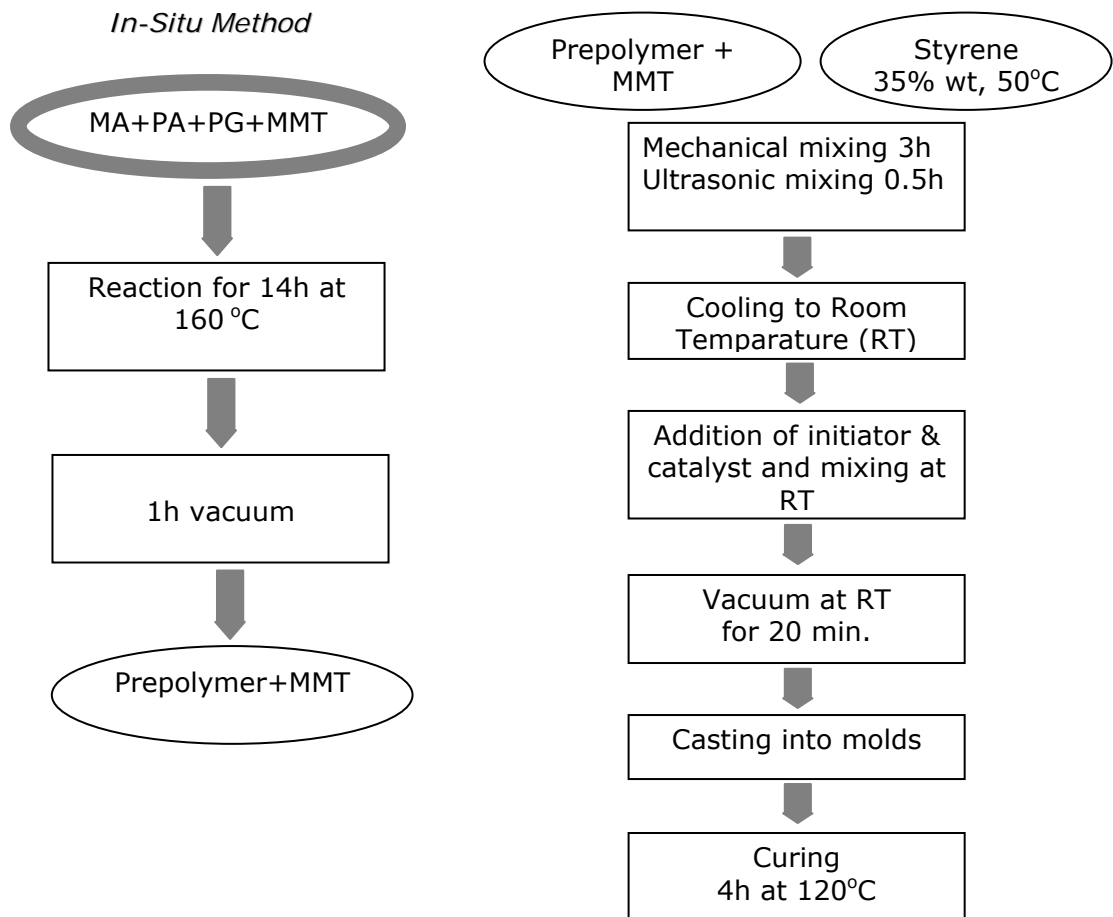


Figure 3.10 Flowcharts of specimen preparation by the In-Situ Method

Prepolymerization Method

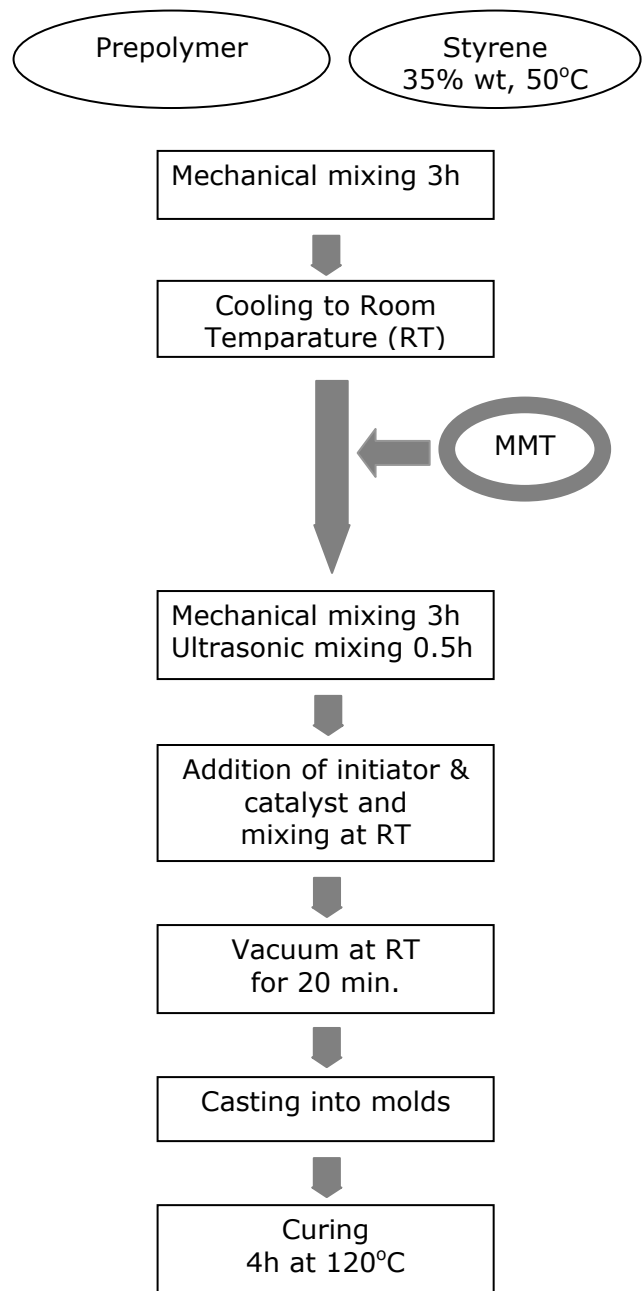
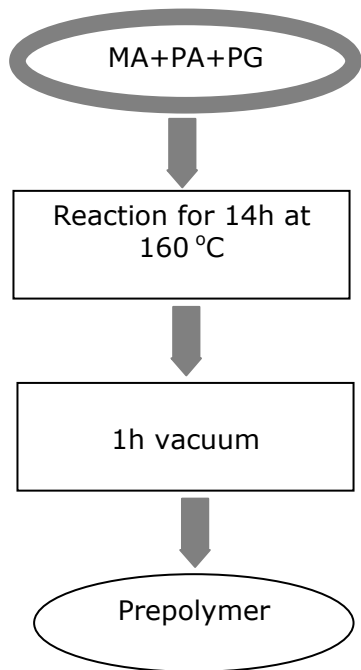


Figure 3.11 Flowcharts of specimen preparation by the Prepolymerization Method

Table 3.8 shows the formulations applied in this study. First, neat unsaturated polyester containing 0 wt.% clay was synthesized. Then, Cloisite 30B was used in the synthesis with the clay loadings of 1, 3, and 5 wt. %. In order to investigate the effect of clay type on the properties of the nanocomposites, 3 wt.% Cloisite 25A and Cloisite 15A were used. These formulations were applied to both the In-Situ and the Prepolymerization methods.

Table 3.8 Formulations applied in the study.

Organoclay Type	Cloisite 30B	Cloisite 25A	Cloisite 15A
Organoclay Content (wt. %)	1	-	-
	3	3	3
	5	-	-

3.2.3 Acid Number Determination

Acid number of a resin is defined as the milligrams of potassium hydroxide (KOH) required to neutralize the free or unreacted carboxyl groups in 1 gram of the resin. It is determined by the following formula [41]:

$$AN = \frac{\text{ml. of KOH} \times \text{normality of KOH} \times 56.1}{\text{wt. of sample in grams}} \quad (3.1)$$

In order to determine the acid number of the resin obtained by the polycondensation reaction, ~1 g of the prepolymer was dissolved in 1/2 (v/v) ethanol/toluene solution and titrated with 0.1N ethanolic KOH solution by using thymol blue indicator until the yellow colour turned blue.

The Molecular Weight (MW_{av}) was calculated by the following formula [41];

$$MW_{av} \text{ (approx.)} = \frac{56\,000}{\text{Acid Number}} \quad (3.2)$$

3.2.4 Determination of Percentage of Styrene In The Resin

The styrene in which the prepolymer would dissolve was calculated as 25 % of the resin. In order to determine the actual amount of styrene in the resin obtained, ~1 g of resin was taken and mixed with 0.1 ml 20% (w/w) hydroquinone/acetone solution by the help of a metal paper clip on a glass petri dish. The mixture was then heated at 150°C for 1 h.

Since;

$$M_1 = m_{\text{petri}} + m_{\text{paper clip}}$$

$$M_2 = m_{\text{resin}} = \sim 1 \text{ g}$$

$$M_3 = (m_{\text{petri}} + m_{\text{paper clip}} + m_{\text{resin}})_{\text{after 1 h}}$$

The following equation gives the actual ratio of styrene in the resin (S/R).

$$\frac{(M_2 + M_1) - M_3}{M_2} = S/R \quad (3.3)$$

3.3 Characterization

In order to elucidate the influence of type, amount and the addition sequence of the organoclay on the final properties of the composites, their characterizations were made by mechanical, morphological and thermal analyses.

3.3.1 Mechanical Testing Procedure and Equipment

All mechanical tests were performed at room temperature. At least five samples were tested. Their average results and the standart deviations are reported for each group of composites.

3.3.1.1 Flexural Tests

Three-point bending tests were performed according to Test Method-I Procedure A of ASTM D790M-92 (Standard Test Methods for Flexural Properties of Unreinforced and Reinforced Plastics and Electrical Insulating Materials) on rectangular specimens by using a Lloyd 30K Universal Testing Machine. The

three-point loading diagram is shown in Figure 2.10. The dimensions of the specimens were $80 \times 6 \times 4$ mm and the support span was 50 mm. The rate of cross-head motion was 10.47 mm/min as calculated to obtain a strain rate of 0.1 min^{-1} .

3.3.1.2 Impact Tests

Charpy Impact Tests were performed by using a Pendulum Impact tester of Coesfeld Material Test, according to the Test Method-I Procedure A in ASTM D256-91a (Standard Test Methods for Impact Resistance of Plastics). Dimensions of the unnotched samples were $50 \times 6 \times 4$ mm. During the test, the sample is supported at both ends and a part of the impact testing machine strikes the sample as shown in Figure 3.12.

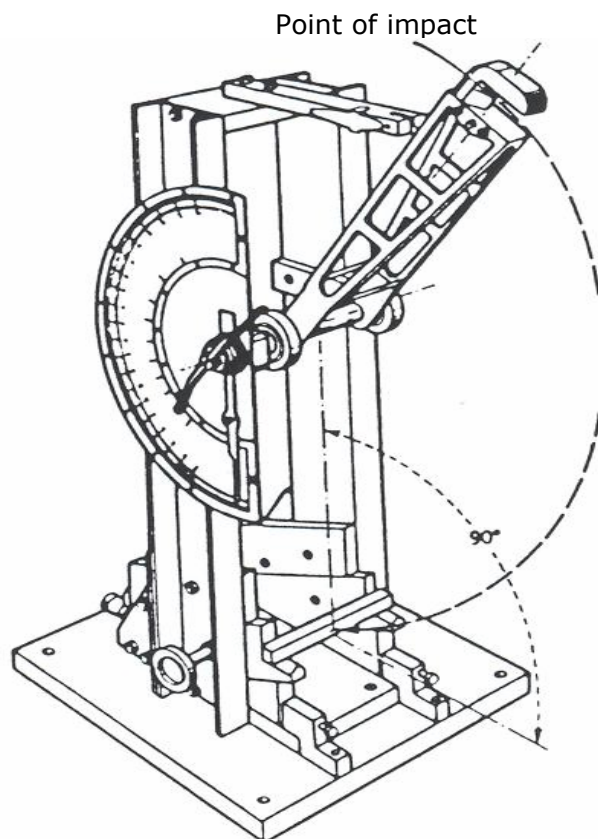


Figure 3.12 Charpy-type impact instrument

3.3.2 Morphological Analysis

3.3.2.1 X-Ray Diffraction (XRD) Analysis

The composites were analyzed by using a Philips PW3710 X-ray diffractometer. Cu K α ($\lambda = 1.54\text{\AA}$) radiation, generated at a voltage of 40 kV and current of 55mA was used as the X-Ray source. The diffraction patterns were collected at a diffraction angle 2θ from 1° to 10° at a scanning rate and step size of $3^\circ/\text{min}$ and 0.02° , respectively.

3.3.2.2 Scanning Electron Microscopy (SEM)

A low voltage SEM (JEOL JSM-6400) was used to analyze the impact fracture surfaces of the composites. The fracture surfaces were coated with a thin layer of gold before SEM to provide conductive surfaces. The SEM photographs were taken at $\times 250$ and $\times 3500$ magnifications.

3.3.3 Thermal Analysis

3.3.3.1 Differential Scanning Calorimetry (DSC) Analysis

Differential Scanning Calorimetry (DSC) analyses were performed with a General V4.1.C DuPont 2000. Measurements were carried out in a temperature range of $20\text{-}280^\circ\text{C}$ with $20^\circ\text{C}/\text{min}$ heating rate under nitrogen atmosphere. The changes in the glass transition (T_g) temperatures were observed.

CHAPTER 4

RESULTS AND DISCUSSION

4.1 Morphological Analysis

4.1.1 Scanning Electron Microscopy (SEM)

In order to investigate the effect of the polymerization method, clay content and the clay type on the morphological structure of the impact fractured surfaces; Scanning Electron Microscopy (SEM) analysis was performed.

The structure of the crack propagation lines gives idea about the impact strength of the material investigated. Figure 4.1 shows the impact surfaces of the neat unsaturated polyester (UP) resin with 250 and 3500 magnifications. It is obvious that the impact surface is smooth and few straight crack propagation lines are observed which explains the low impact strength of this material.

Figures 4.2, 4.3 and 4.4 show the impact surfaces of the nanocomposites prepared by the In-Situ and Prepolymerization methods containing 1, 3 and 5 wt. % of organoclay (Cloisite 30B) respectively. In Figures 4.2 and 4.3, it is observed that the crack propagation lines are approaching a shorter and closer structure with increasing clay loading which means that the crack propagation path is tortuous preventing easy propagation of cracks. This results in higher impact strength of the samples prepared by both the In-Situ Method and the Prepolymerization Method as shown later. In Figure 4.4, the crack propagation lines have also shorter and closer structure in comparison to Figure 4.1 which shows the SEM micrograph of neat UP. However, with the addition of 5 weight % organoclay, the decrease in the impact strength can be attributed to the agglomeration of the clay particles (Figure 4.4), which act as stress concentrators at higher clay loadings.

In Figures 4.2 through 4.4, the presence of more agglomerates in samples synthesized by the Prepolymerization Method is confirmed by the SEM micrographs when the two methods are compared. This may be the reason of obtaining lower impact strength in the samples prepared by the "Prepolymerization Method" in comparison to the samples prepared by the "In-Situ Method".

Figures 4.5 and 4.6 show the impact fractured surfaces of samples containing 3 wt. % Cloisite 15A and Cloisite 25A synthesized by the two methods. In Figures 4.3, 4.5 and 4.6, it is not easy to differentiate the effect of clay type on the morphological structure of the nanocomposites, because these micrographs exhibit similar structures. A more powerful technique like Transmission Electron Microscopy (TEM) should be used since it allows a more precise observation of nanostructures with an exceptional resolution (about 0.2 nm) [4].

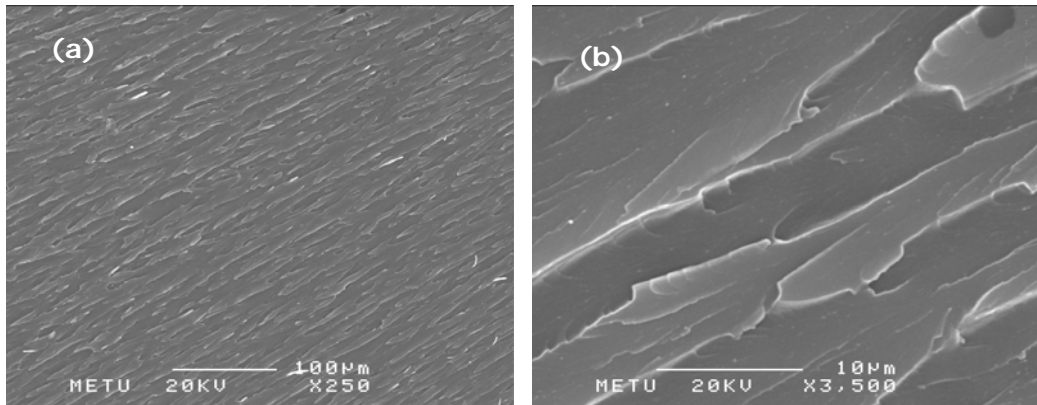


Figure 4.1 SEM micrographs of pure Unsaturated Polyester.

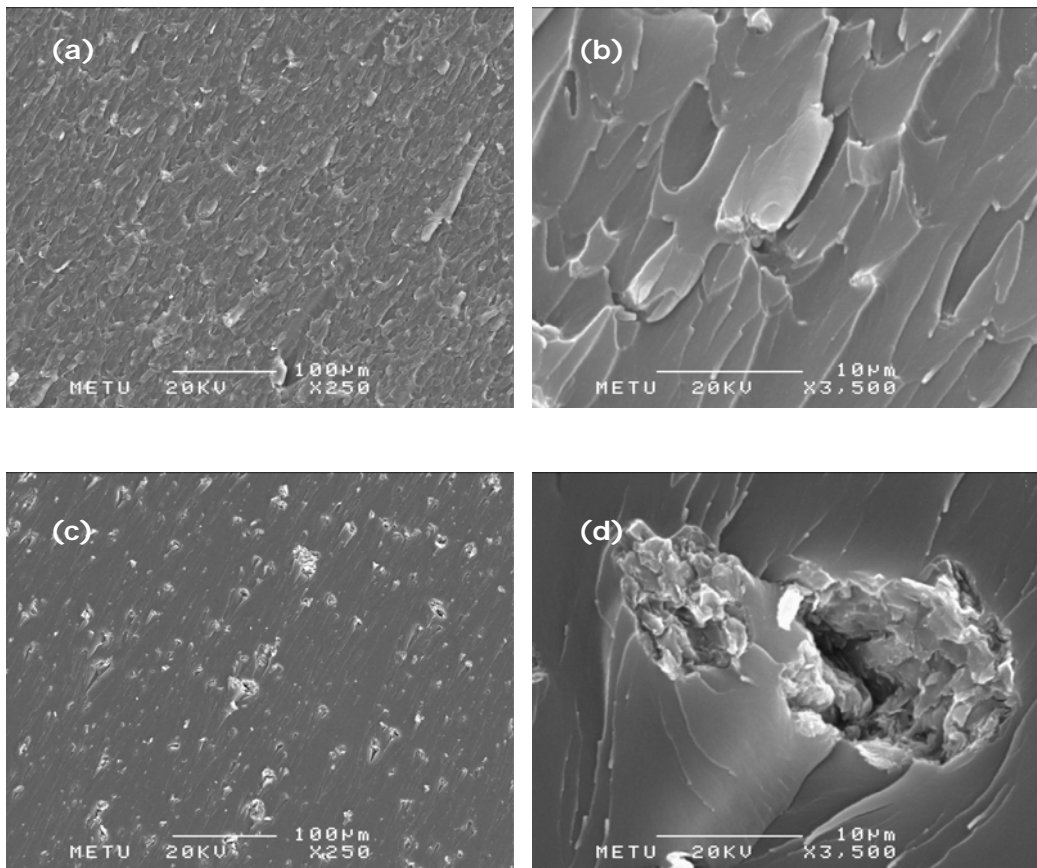


Figure 4.2 SEM micrographs of Unsaturated Polyester containing 1 wt. % Cloisite 30B synthesized by (a) In-situ Method $\times 250$, (b) In-Situ Method $\times 3500$; (c) Prepolymerization Method $\times 250$ and (d) Prepolymerization Method $\times 3500$.

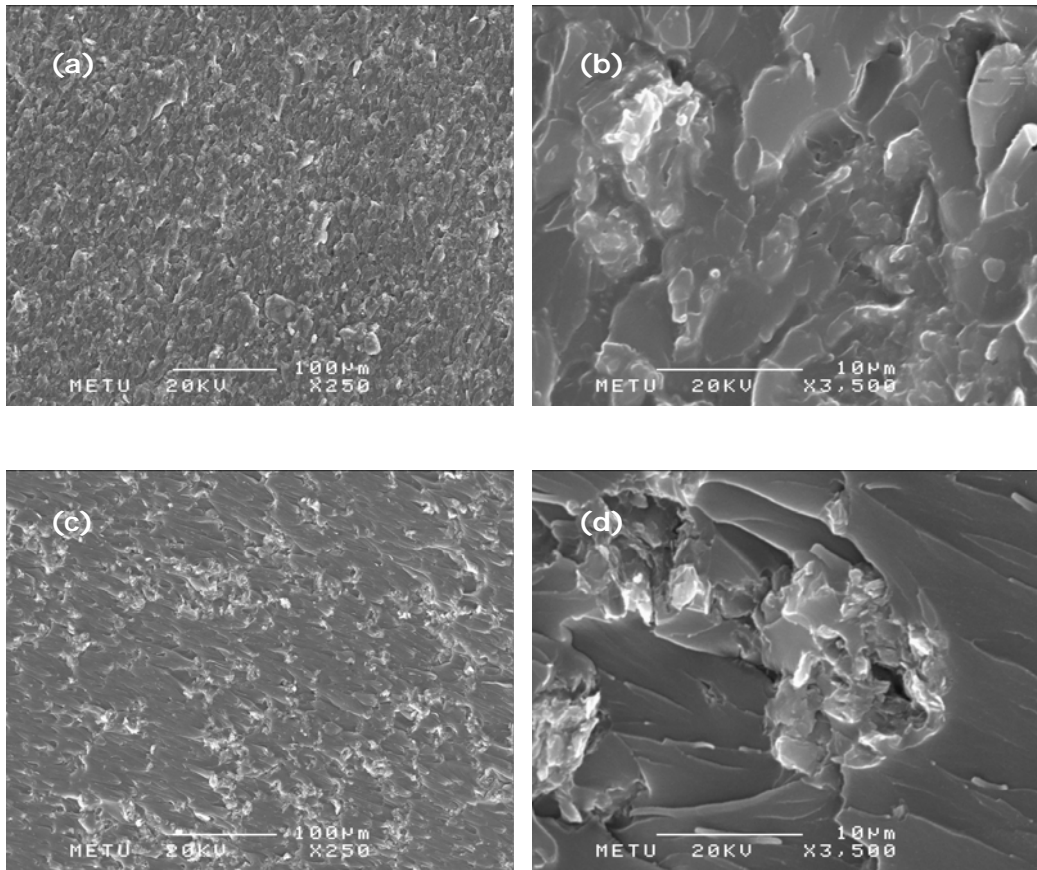


Figure 4.3 SEM micrographs of Unsaturated Polyester containing 3 wt. % Cloisite 30B synthesized by (a) In-situ Method $\times 250$, (b) In-Situ Method $\times 3500$; (c) Prepolymerization Method $\times 250$ and (d) Prepolymerization Method $\times 3500$.

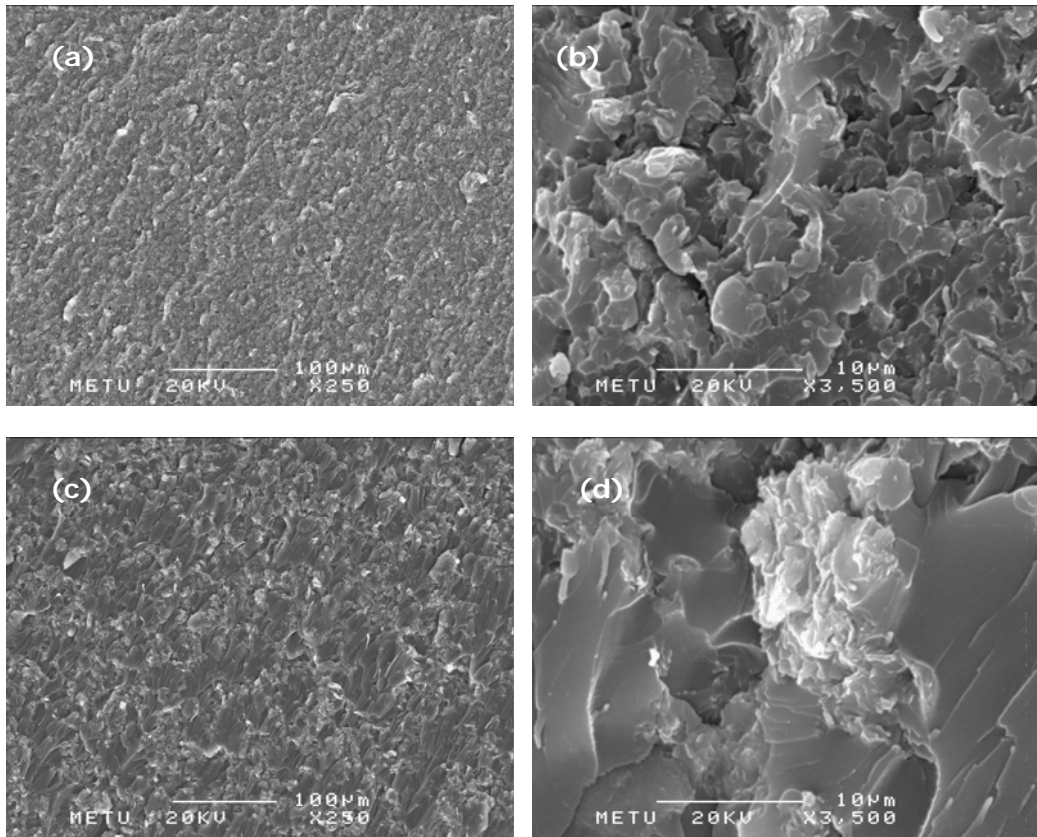


Figure 4.4 SEM micrographs of Unsaturated Polyester containing 5 wt. % Cloisite 30B synthesized by (a) In-situ Method $\times 250$, (b) In-Situ Method $\times 3500$; (c) Prepolymerization Method $\times 250$ and (d) Prepolymerization Method $\times 3500$.

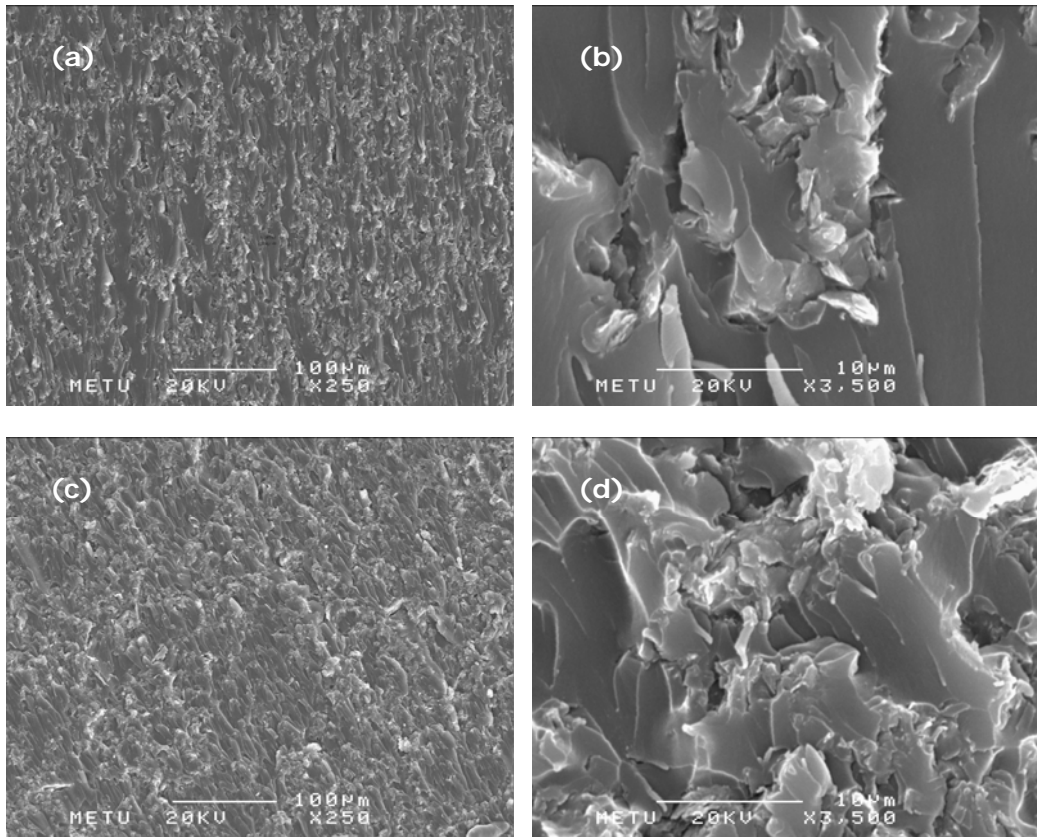


Figure 4.5 SEM micrographs of Unsaturated Polyester containing 3 wt. % Cloisite 15A synthesized by (a) In-situ Method $\times 250$, (b) In-Situ Method $\times 3500$; (c) Prepolymerization Method $\times 250$ and (d) Prepolymerization Method $\times 3500$.

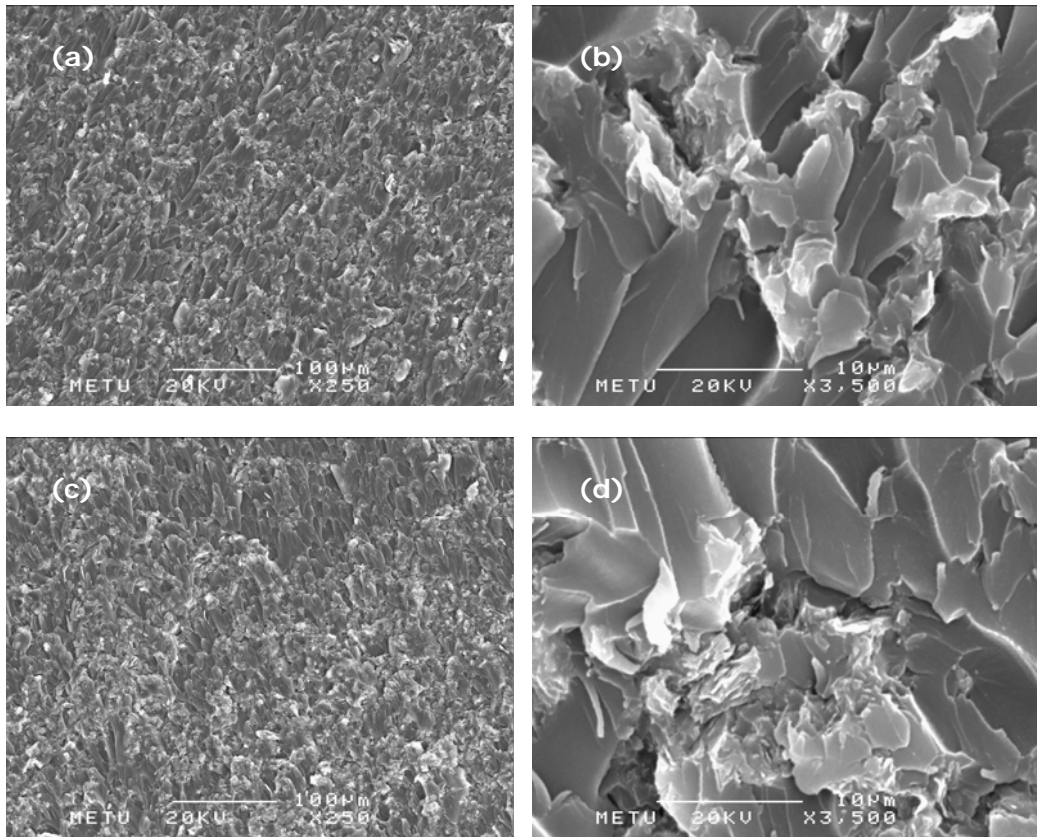


Figure 4.6 SEM micrographs of Unsaturated Polyester containing 3 wt. % Cloisite 25A synthesized by (a) In-situ Method $\times 250$, (b) In-Situ Method $\times 3500$; (c) Prepolymerization Method $\times 250$ and (d) Prepolymerization Method $\times 3500$.

4.1.2 X-ray Diffraction Analysis

The gallery space between the clay platelets within an aggregate structure is indicative of their extent of intercalation and can be determined with XRD analysis [42]. The final d-spacings obtained from the XRD data of the samples of the silicate sheets are given in Table 4.1 with respect to the sample preparation method and clay loading.

Table 4.1 X-ray diffraction results of all compositions with respect to *Cloisite 30B wt. %.

Polymerization Method	Organoclay Weight %	d-spacing (Å)	2theta (deg)
In-Situ	1	exfoliated	-
	3	39	2.27
	5	39.1	2.26
Prepolymerization	1	40.1	2.2
	3	exfoliated	-
	5	38.9	2.27

* The original d-spacing of Cloisite 30B is 18.4 Å and 2 θ value is 4.81 deg.

Figure 4.7 displays the XRD patterns of the unintercalated organoclay (Cloisite 30B) and the in-situ polymerized nanocomposites containing 1, 3 and 5 wt. % organoclay Cloisite 30B. The y-axis of the patterns are shifted for clarity. As seen in the figure; no peak is observed in the XRD pattern of the nanocomposites containing 1 wt. % organoclay. In the case of well dispersed polymer layered clay nanocomposites, the absence of the basal reflections is the evidence of exfoliated layers (19). Considering this phenomenon; it can be claimed that an exfoliated structure is obtained in this case. At 3 wt. % and 5 wt. % clay contents, it is observed that the characteristic interlayer spacing of Cloisite 30B is increased to 39 Å and 39.1 Å respectively indicating the intercalation of the polymer chains within the silicate sheets expanding the galleries.

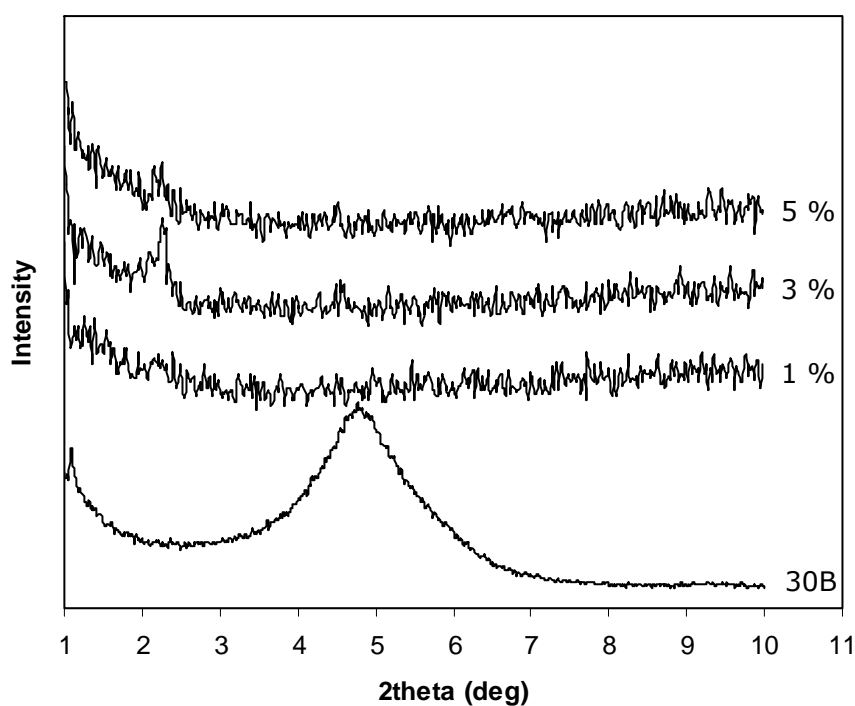


Figure 4.7 X-ray diffraction patterns of nanocomposites synthesized by In-Situ Method containing 1, 3 and 5 wt. % organoclay (Cloisite 30B).

In Figure 4.8, XRD patterns of the compositions synthesized by the Prepolymerization Method containing 1, 3 and 5 wt. % organoclay (Cloisite 30B) are seen. It can be stated that the optimum organoclay content for this method is 3 wt. % in terms of obtaining an exfoliated structure. From Table 4.1 a slight decrease in the d-spacing at 5 wt. % organoclay loading is observed. This decrease can be attributed to the tendency of clay particles to agglomerate at high clay contents.

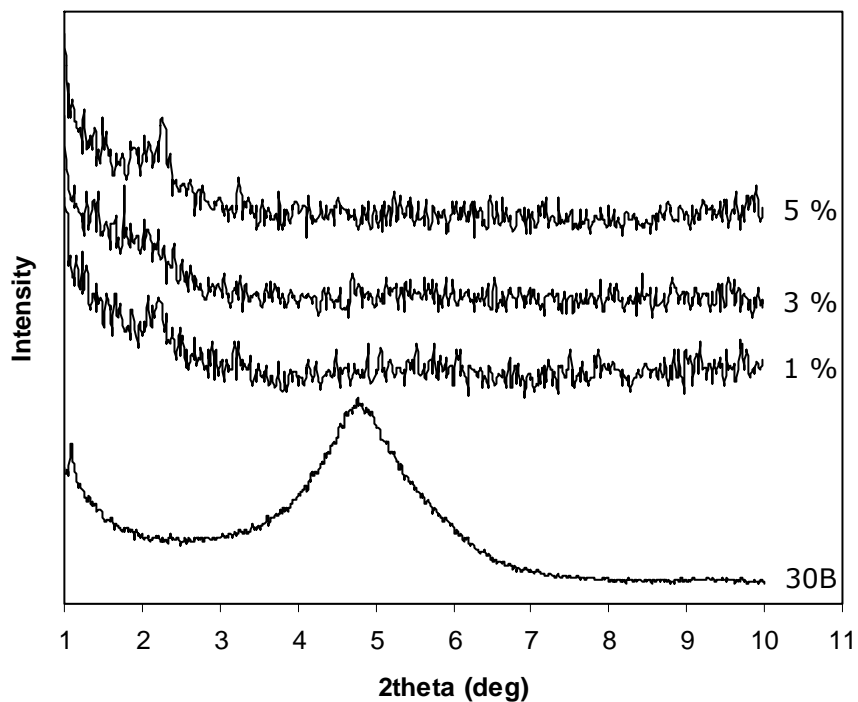


Figure 4.8 X-ray diffraction patterns of nanocomposites synthesized by Prepolymerization Method containing 1, 3 and 5 wt % organoclay (Cloisite 30B).

Figure 4.9 shows the XRD patterns of nanocomposites containing 1 wt. % of organoclay (Cloisite 30B) prepared by both the In-Situ Method and the Prepolymerization Method. In the pattern of the samples prepared by the Prepolymerization Method, a peak occurs corresponding to the d-spacing value of 40.1 Å which verifies the formation of an intercalated structure. In the pattern of the In-Situ Method at the same clay content, no peak is observed indicating further delamination of the silicate layers and formation of an exfoliated structure. Beyond a certain d-spacing the interlayer attractive forces may not be able to hold the clay layers parallel to each other. Thus exfoliation would start at higher d-spacings.

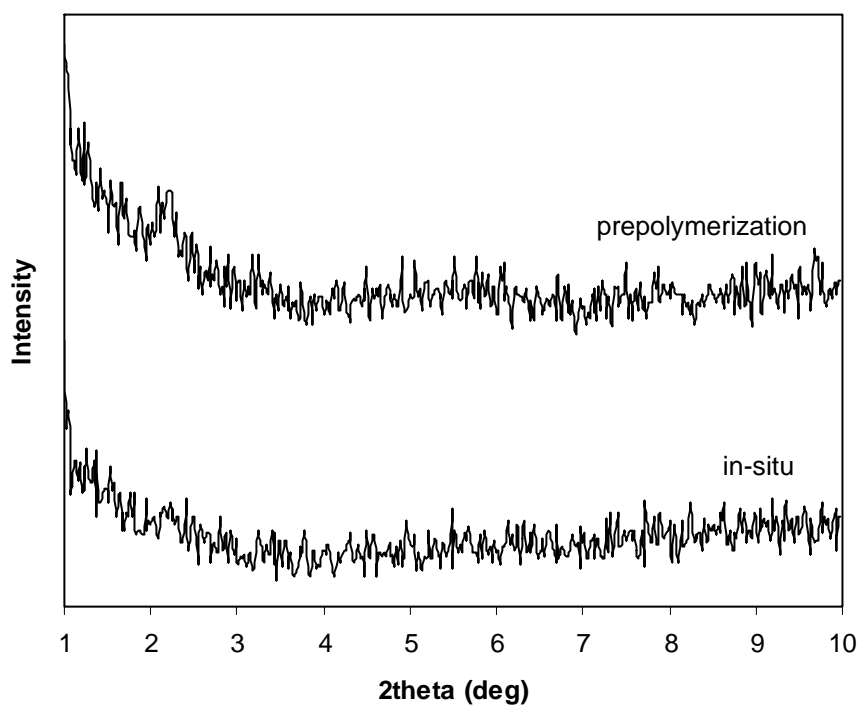


Figure 4.9 X-ray diffraction patterns of nanocomposites prepared by the two methods containing 1 wt. % of organoclay (Cloisite 30B).

In Figure 4.10, the XRD patterns of the nanocomposites containing 3 wt. % organoclay (Cloisite 30B) prepared by both the In-situ Method and the Prepolymerization Method are seen. A peak can be detected at $2\theta=2.27$ corresponding to a d-spacing of 39 \AA which confirms the formation of intercalated structure for the nanocomposites prepared by the In-Situ Method. However, in the Prepolymerization Method, the formation of an exfoliated structure is confirmed with the absence of a basal reflection. In the Prepolymerization Method, clay is introduced to previously synthesized unsaturated polyester resin which has higher molecular weight than the monomers. Owing to the higher molecular weight, higher viscosity and shear-stress are attained. In this context, it can be concluded that high shear-stress is effective in overcoming the forces holding the silicate sheets together.

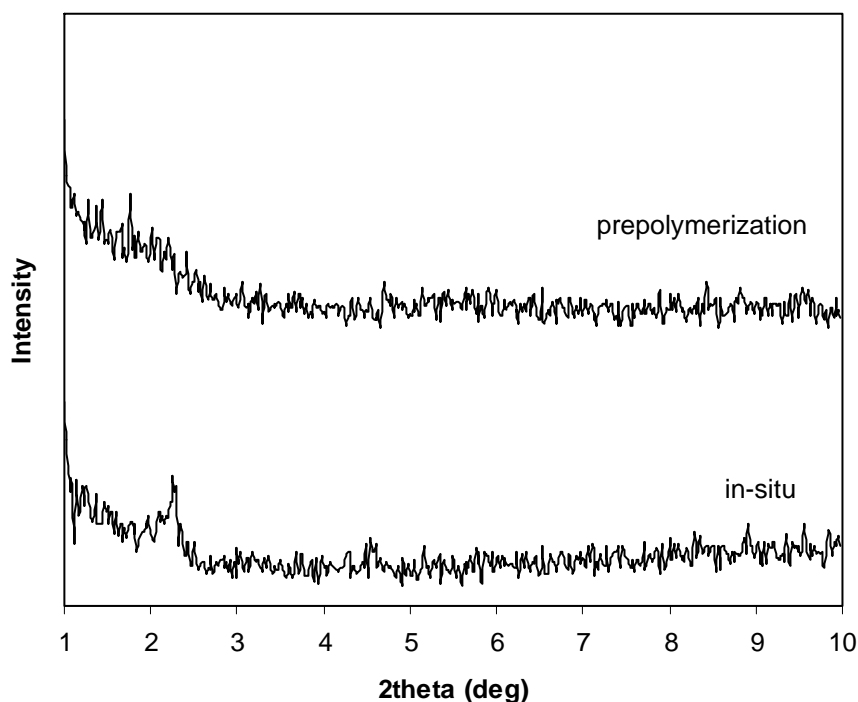


Figure 4.10 X-ray diffraction patterns of nanocomposites prepared by the two methods containing 3 wt. % of organoclay (Cloisite 30B).

Figure 4.11 shows the XRD patterns of the samples prepared by both methods containing 5 wt. % organoclay (Cloisite 30B). When Figure 4.11 is observed, it is seen that two basal reflections are located at nearly the same 2θ values for both the Prepolymerization Method and the In-Situ Method corresponding to the d-spacing values of 38.9 Å and 39.1 Å respectively. It is observed that beyond 3 wt. % clay loading, high levels of exfoliation is not obtained.

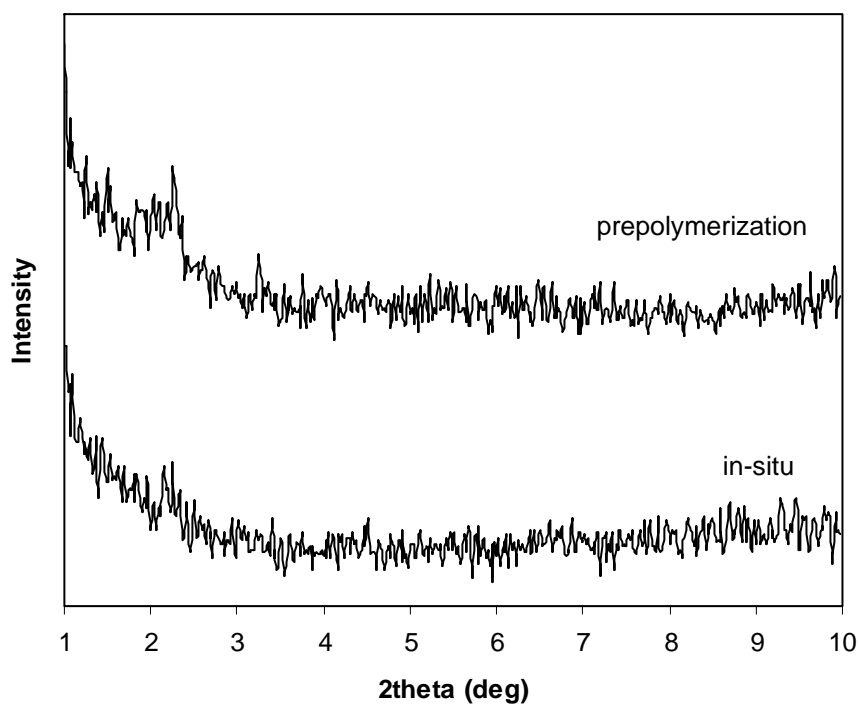


Figure 4.11 X-ray diffraction patterns of nanocomposites prepared by the two methods containing 5 wt. % of organoclay (Cloisite 30B).

In Table 4.2, the final d-spacings of the silicate sheets are given with respect to the polymerization methods and clay type. Table 4.3 gives the percent increase in the width of the galleries of the organoclays in comparison to the initial gallery width and is calculated by the following formula;

$$\left(\begin{array}{l} \% \text{ increase in} \\ \text{the d-spacing} \end{array} \right) = \frac{(\text{final d-spacing}) - (\text{initial d-spacing})}{\text{initial d-spacing}} \times 100 \quad (4.1)$$

Table 4.2 X-ray diffraction results of the compositions prepared by two methods containing 3 wt. % Cloisite 15A, Cloisite 25A and Cloisite 30B.

Polymerization Method	Organoclay Type	d-spacing (Å)	2theta (deg)
In-Situ	*Cloisite 15A	38.6	2.29
	*Cloisite 25A	34	2.6
	*Cloisite 30B	39	2.27
Prepolymerization	*Cloisite 15A	38.9	2.27
	*Cloisite 25A	39.2	2.25
	*Cloisite 30B	exfoliated	-

* The original d-spacing of Cloisite 15A is 32.9 Å and 2θ value is 2.68 deg.

* The original d-spacing of Cloisite 25A is 17.9 Å and 2θ value is 4.92 deg.

* The original d-spacing of Cloisite 30B is 18.4 Å and 2θ value is 4.81 deg.

Table 4.3 % increase in the d-spacings of organoclays with respect to the polymerization method.

Organoclay Type	Polymerization Method	
	In-Situ	Prepolymerization
Cloisite 15A	17 %	18 %
Cloisite 25A	90 %	119 %
Cloisite 30B	112 %	exfoliated

The basal reflection of the nanocomposites prepared by both the In-Situ Method and the Prepolymerization Method with 3 wt. % organoclays (Cloisite 30B, 25A and 15A) are shown in Figures 4.12 and 4.13. In agreement with Table 4.3, it can be concluded that the maximum increase in the gallery size of the silicate sheets appears to be in Cloisite 30B in both methods. The increase in the d-spacing is 112 % for the In-Situ Method and an exfoliated structure is obtained when the Prepolymerization Method is applied. The increase in the d-spacing of Cloisite 25A for the In-Situ and the Prepolymerization Methods are 90 % and 119 % respectively. The minimum increase in the gallery size is observed with Cloisite 15A in both methods with an increase of 17 % for the In-Situ Method and 18 % for the Prepolymerization Method.

From the above mentioned results, it can be concluded that the expansion of the interlayer spacings of all three kinds of organoclay are higher in the Prepolymerization Method when compared with the In-Situ Method. As discussed previously, in the Prepolymerization Method, clay is mechanically mixed at room temperature with previously synthesized unsaturated polyester resin. Since UP resin has higher molecular weight than the monomers, higher shear-stress and viscosity can be attained when compared to the In-Situ Method. When the clay layers are subjected to high shear-stress, platelets are easily delaminated by peeling apart [42]. Also, in the In-Situ Method, the reaction temperature is 160 °C. Since the viscosity of the polymer decreases at high temperatures, low shear-stresses are obtained in the In-Situ Method.

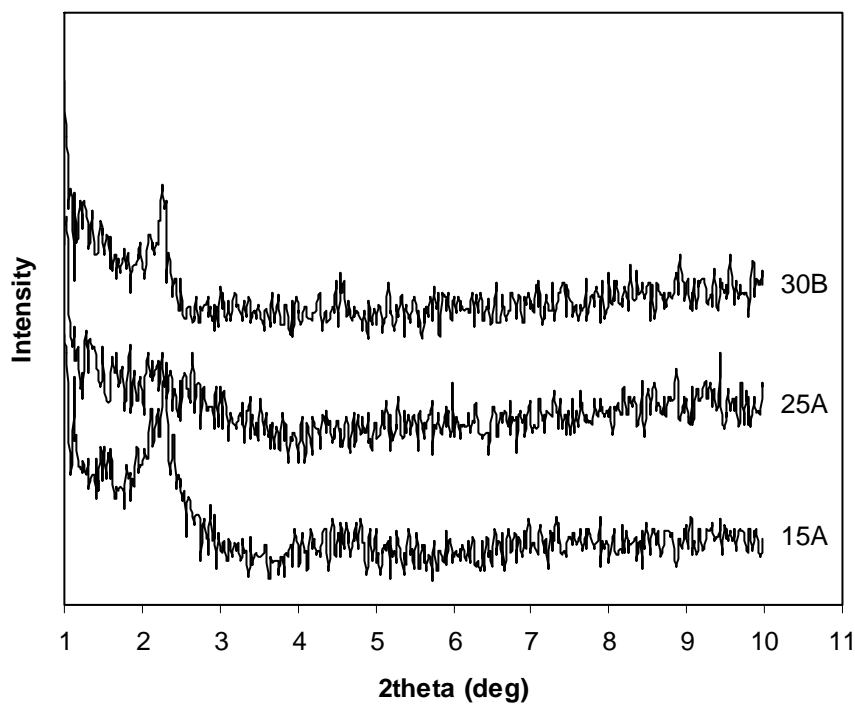


Figure 4.12 X-ray diffraction patterns of nanocomposites prepared by the In-Situ Method containing 3 wt. % of organoclays (Cloisite 30B, 25A and 15A).

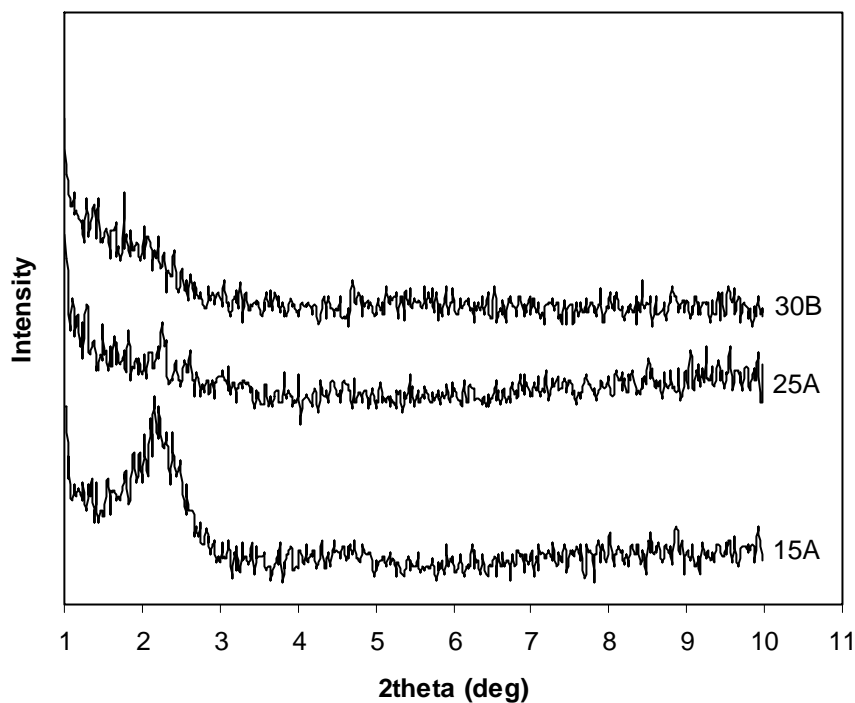


Figure 4.13 X-ray diffraction patterns of nanocomposites prepared by the Prepolymerization Method containing 3 wt. % of organoclays (Cloisite 30B, 25A and 15A).

4.2 Mechanical Analysis

4.2.1 Impact Test Analysis

Fillers can either decrease or increase the impact strength compared to the unfilled polymer. As a general rule, large particles give rise to a loss of impact strength because the particles act as stress concentrators initiating the cracks. In contrast, well dispersed nano-particles are able to improve the impact strength by a crack-pinning mechanism [3]. Figure 4.14 shows the impact strength of the samples with respect to the polymerization method and organoclay content.

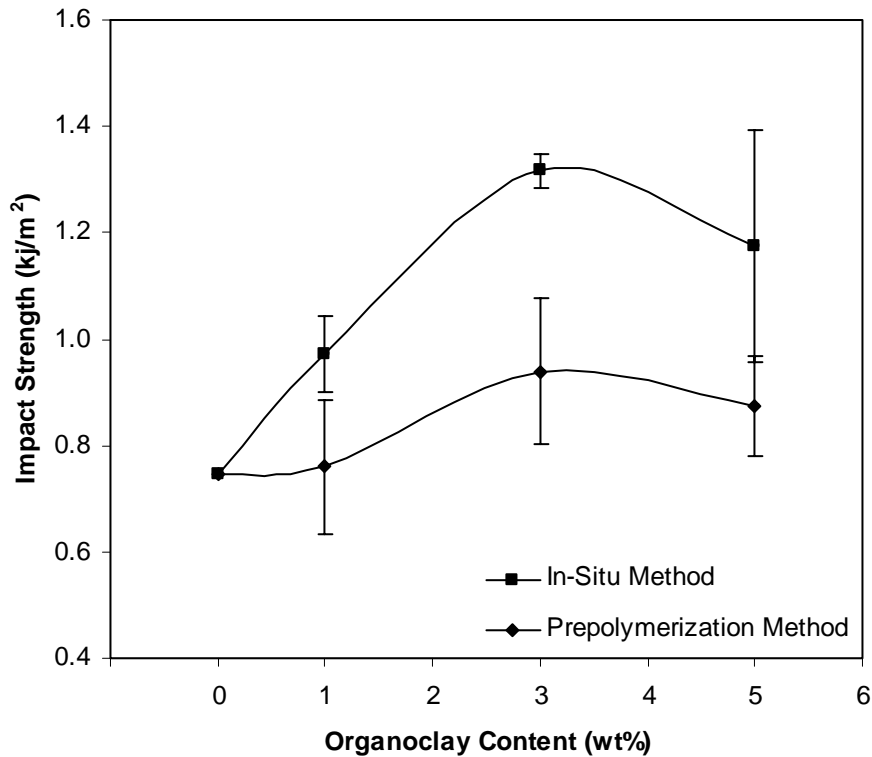


Figure 4.14 Impact strength of nanocomposites prepared by the two methods with respect to the organoclay (Cloisite 30B) content.

In the Prepolymerization Method, styrene and the prepolymer are simultaneously introduced with the organoclay. Since styrene has a smaller molecular structure than the prepolymer, it can diffuse through the galleries of the organoclay more easily. This mechanism reduces the styrene amount available for crosslinking in

the medium. Because of this reason, the molecular weight of the chains between the crosslink sites happens to be smaller in the Prepolymerization Method resulting in restrictions in chain mobility and decreasing the impact strength. Also, since the styrene between the silicate layers has the possibility to polymerize with the styrene in the crosslinking medium outside the layers, adhesion between the polymer and the silicate sheets would increase leading to restrictions in the chain mobility and decrease the impact strength. As seen from Figure 4.14, the impact strength of the samples prepared by the In-Situ method are higher than that of the samples prepared by the Prepolymerization Method owing to the higher styrene content in the medium when the In-Situ Method is used. When the number of the crosslink sites are constant, the increase in the average molecular weight between the crosslink sites promotes chain mobility between the crosslinks [43]. This results in better sharing of the impact force along the polymer chain by causing more atoms to rotate, vibrate and stretch to absorb the energy of the impact [44].

Also in agreement with the SEM analysis of the impact fractured surfaces of the nanocomposites, more agglomerates are seen in the micrographs of the samples synthesized by the Prepolymerization Method resulting in lower impact strength when the two methods are compared. When the clay agglomerates are present, the stress acting on a small part of the material surface would be much greater than the average stress applied to the test specimen. This stress concentration phenomena results in breaking of the material at a stress which is less than the expected value [43].

The impact strength of the samples prepared by both the In-Situ Method and the Prepolymerization Method increased up to a certain clay loading with increasing clay concentration and showed a decrease at higher clay loading (5 wt.%). This result may be due to the presence of larger agglomerates at higher clay contents which act as stress concentrators.

Figure 4.15 displays the impact strength of the samples prepared by the two methods containing 3 wt. % of different types of organoclay. It is seen that the impact strength of the samples prepared by the Prepolymerization Method is lower due to the lower styrene content in the crosslinking medium as discussed previously.

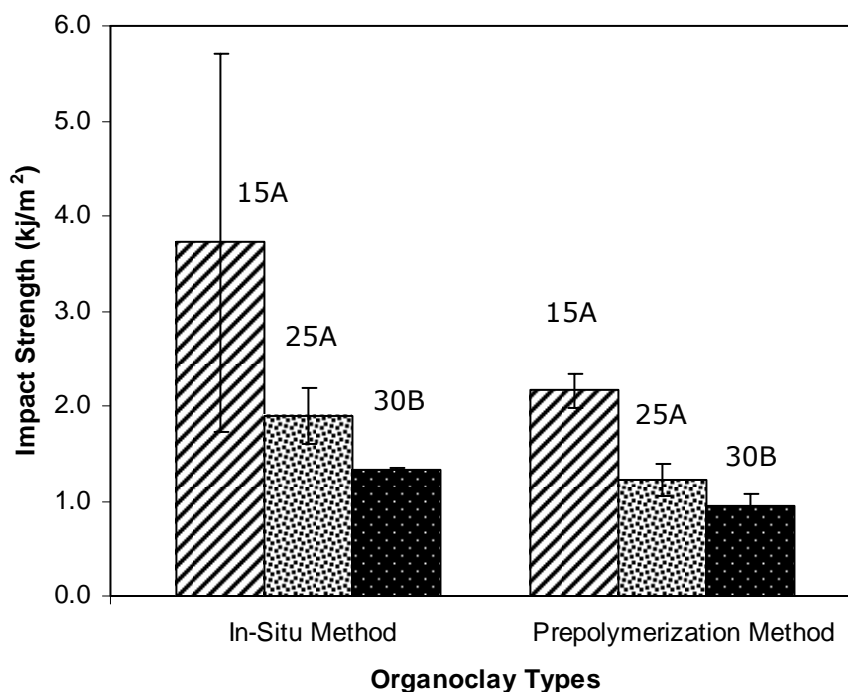


Figure 4.15 Impact strength of nanocomposites prepared by the two methods containing 3 wt. % organoclay with respect to organoclay type.

When the organoclay types are considered, it is observed that maximum impact strength is obtained with Cloisite 15A and minimum impact strength is obtained with Cloisite 30B. The only difference of these organoclays are the organic modifiers used to render their structure from hydrophilic to organophilic and increase the distance between the platelets so that polymer molecules can easily get intercalated through the gap. According to the modifier used, the nanocomposites attain different d-spacings. Therefore, from the XRD patterns of the organoclay powders given in Appendix B, it can be said that Cloisite 15A has the maximum and Cloisite 30B has the minimum d-spacing. In Figure 3.6, it can be seen that the organic modifier of Cloisite 30B has two OH groups. These groups distinguishes Cloisite 30B as more polar in comparison to Cloisite 15A and Cloisite 25A. The hydroxyl group increases the possibility of reaction

between the modifier and the acid used in the synthesis of unsaturated polyester. This possible reaction between UP resin and the modifier would result in higher adhesion between the polymer and the clay surface which decreases the chain mobility. Since chain mobility is directly related to the impact strength, the impact strength of the samples prepared by Cloisite 30B are the lowest in both the In-Situ and the Prepolymerization methods.

As seen from Figure 4.13 and Table 4.3, in the Prepolymerization Method, maximum increase in the d-spacing is obtained with Cloisite 30B. Samples prepared by Cloisite 15A have the sharpest peak intensity indicating well-ordered structures. The peak intensity starts to diminish in the XRD pattern of the Cloisite 25A containing samples. For the samples containing Cloisite 30B, the basal reflection disappears which is an indication of exfoliation. When exfoliation is obtained, polymer-clay interaction increases, decreasing the chain mobility and the impact strength.

When the XRD patterns of the samples prepared by the In-Situ Method containing Cloisite 15A and Cloisite 30B are compared using Figure 4.12, it is observed that the pattern of Cloisite 15A exhibits a broader peak indicating a disordered structure. At this point, it can be claimed to have a partially exfoliated structure leading to an increase in the impact strength by a crack-pinning mechanism (3). This reason can also be verified by the fact that being maximum, the d-spacing of Cloisite 15A is very suitable for the radius of gyration of the monomers which may lead to further delamination of the platelets when the polymerization reaction takes place.

4.2.2 Flexural Test Analysis

Figures 4.16 and 4.17 show the stress-strain curves of nanocomposites prepared by the In-Situ and the Prepolymerization methods containing different amounts of organoclay (Cloisite 30B). Equation 2.1 was used to obtain the stress and Equation 2.2 was used to obtain the strain data. Since modulus is defined as the slope of the stress-strain plot [31], it can be seen from the Figures 4.16 and 4.17 that the modulus of the compositions prepared by both methods increase with increasing clay concentration up to 3 wt. % clay content. This is a result of the high surface area attained by adding nano-clays to the pristine polymer. Polymers interact with the filler surface forming an interphase of adsorbed polymer and the overall polymer-filler adhesion increases as a function of high surface area and thereby improves the modulus [3].

With the support of Figure 4.27, it can be concluded from Figures 4.16 and 4.17 that the modulus shows a decreasing trend above the clay loading of 3 wt.%. This decrease can be attributed to the agglomeration of the clay particles at higher clay contents decreasing the surface area available for the polymer-clay interaction.

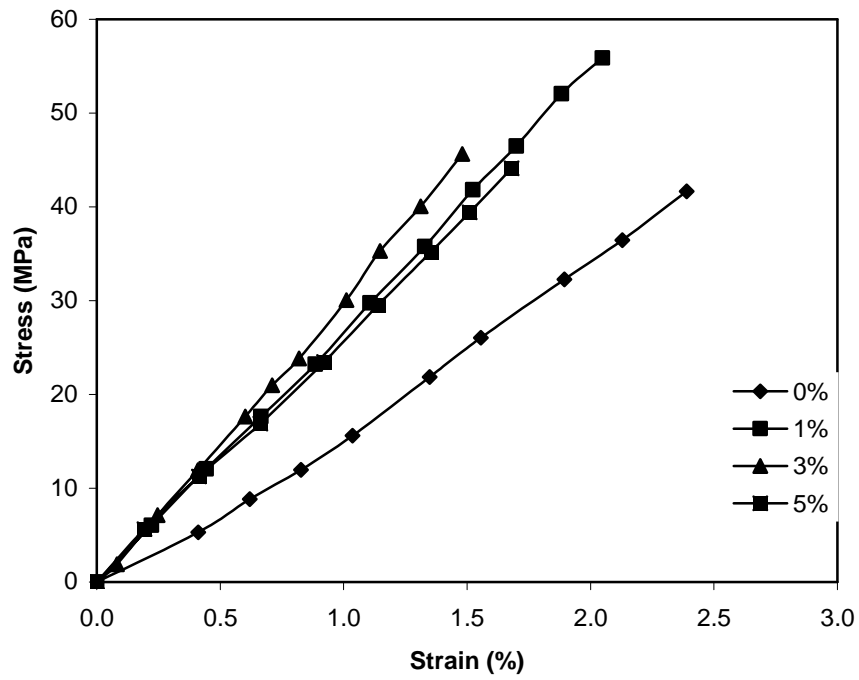


Figure 4.16 Effect of Organoclay (Cloisite 30B) content on the Stress-Strain curves of nanocomposites prepared by In-Situ Method.

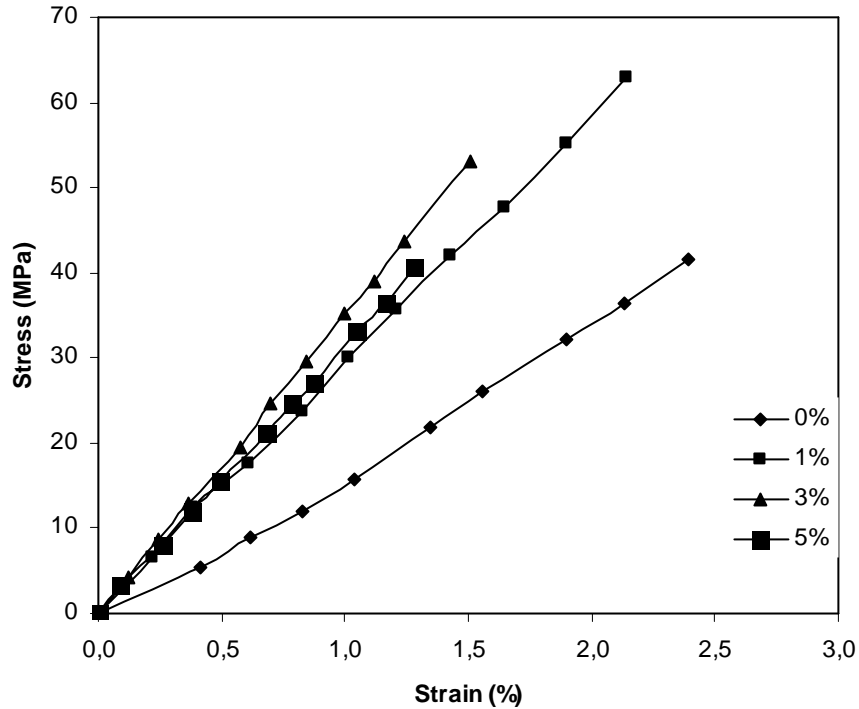


Figure 4.17 Effect of Organoclay (Cloisite 30B) content on the Stress-Strain curves of nanocomposites prepared by Prepolymerization Method.

The effect of polymerization method can be seen from Figure 4.18 through Figure 4.20. As mentioned previously, in the Prepolymerization Method, the prepolymer and styrene is mixed with the organoclay at the same time. Styrene diffuses through the galleries of the organoclay more easily owing to its smaller molecular structure than the polymer. This reduces the styrene amount available for crosslinking in the medium which is the reason of lower molecular weight between the crosslinking sites leading to restrictions for chain mobility and increasing the stiffness, flexural modulus and flexural strength [45].

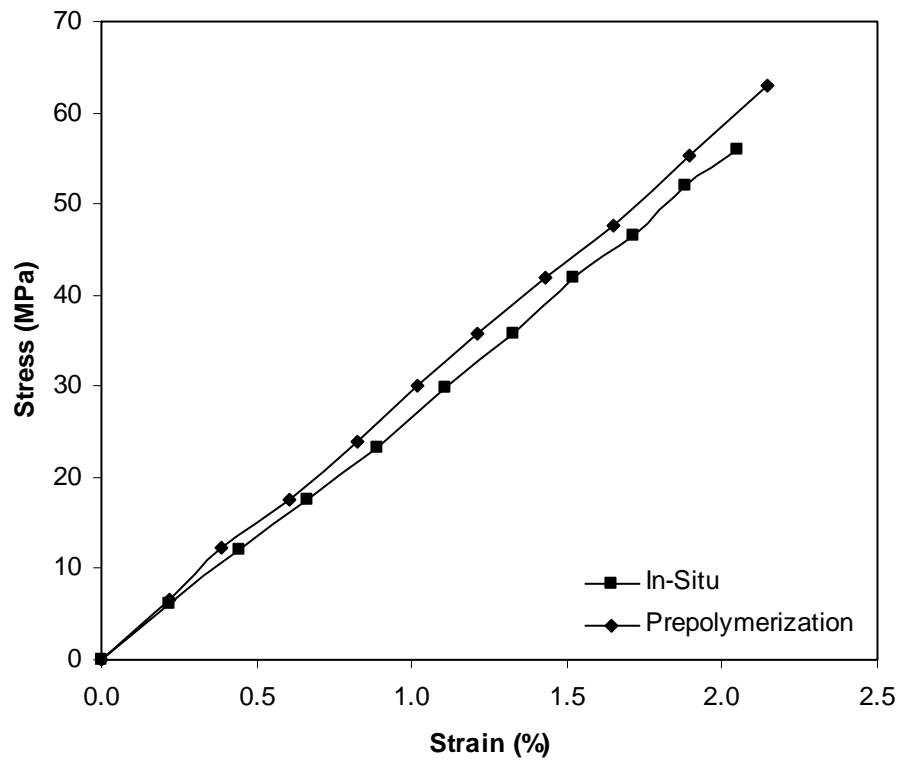


Figure 4.18 Effect of polymerization method on the stress-strain curves of nanocomposites containing 1% Cloisite 30B.

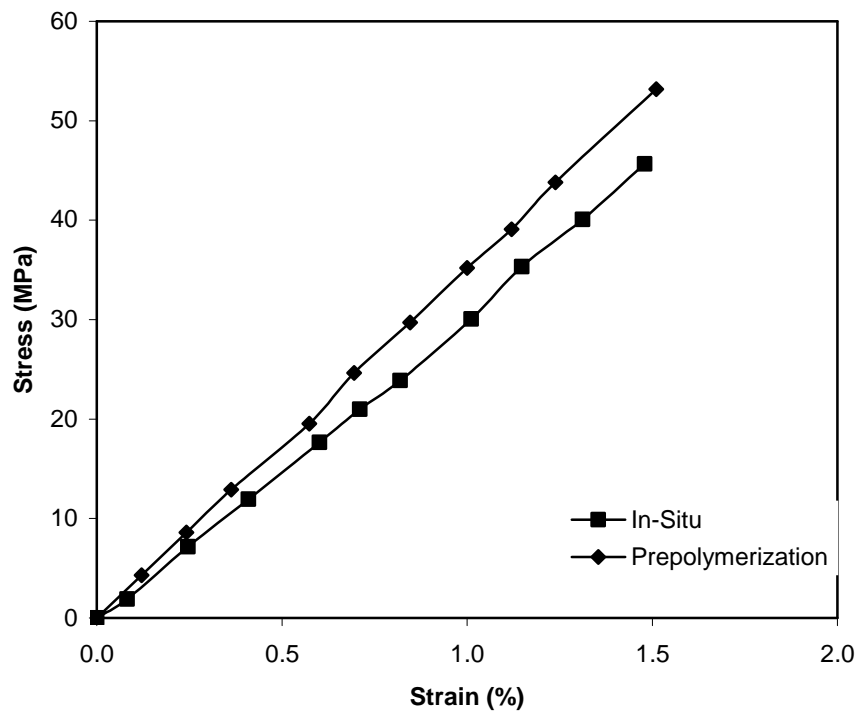


Figure 4.19 Effect of polymerization method on the stress-strain curves of nanocomposites containing 3% Cloisite 30B.

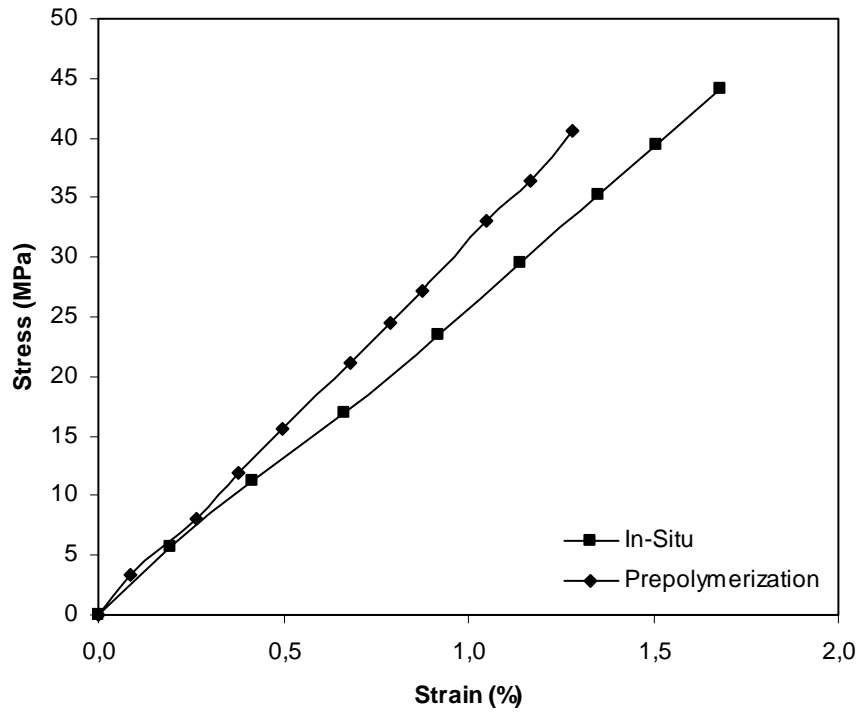


Figure 4.20 Effect of polymerization method on the stress-strain curves of nanocomposites containing 5% Cloisite 30B.

Figures 4.21 and 4.22 display the stress-strain curves of the samples containing different clay types prepared by In-Situ and the Prepolymerization methods. The modulus of the samples are obtained by the slope of the stress-strain curves and are given in Figure 4.24.

The effect of organoclay type on the flexural properties of the nanocomposites prepared by both methods are seen from Figure 4.23 through 4.25. As it is confirmed by the XRD data for the In-Situ Method (Figure 4.12), a nearly exfoliated structure is obtained with Cloisite 25A. Based on the previous discussion, owing to the high surface area obtained by the exfoliation of the silicate sheets, overall polymer-filler adhesion would increase resulting in higher flexural strength and flexural modulus.

In the In-Situ Method, when the samples prepared with Cloisite 15A and Cloisite 30B are compared, by the existence of a broader peak for Cloisite 25A containing samples, Figure 4.12 indicates a more disordered structure for nanocomposites with Cloisite 15A as verified by the XRD data. This may be the reason of higher flexural strength and the modulus of the samples prepared with Cloisite 15A in comparison to the samples prepared with Cloisite 30B as seen in Figures 4.23 and 4.24.

In Figures 4.23 and 4.24, samples containing Cloisite 30B prepared by the Prepolymerization Method have the highest flexural strength and modulus. From the XRD patterns of the samples prepared by the Prepolymerization Method (Figure 4.13), it can be seen that maximum exfoliation is obtained by using Cloisite 30B, leading to maximum flexural strength and flexural modulus owing to higher level of polymer-clay adhesion and possible reactions between the clay modifier and the unsaturated polyester resin.

As mentioned previously, in the Prepolymerization Method the prepolymer is introduced into the layers of the organoclay rather than the monomers. Since the prepolymer has a larger molecular structure than the monomer, it can get intercalated into the galleries of the silicate sheets more easily which have larger d-spacing values like Cloisite 15A, so that more clay-polymer interaction can occur. In other words; Cloisite 15A has more suitable gallery distance for the radius of gyration of the polymer. This may be the reason of higher flexural strength and modulus obtained by Cloisite 15A in comparison to Cloisite 25A.

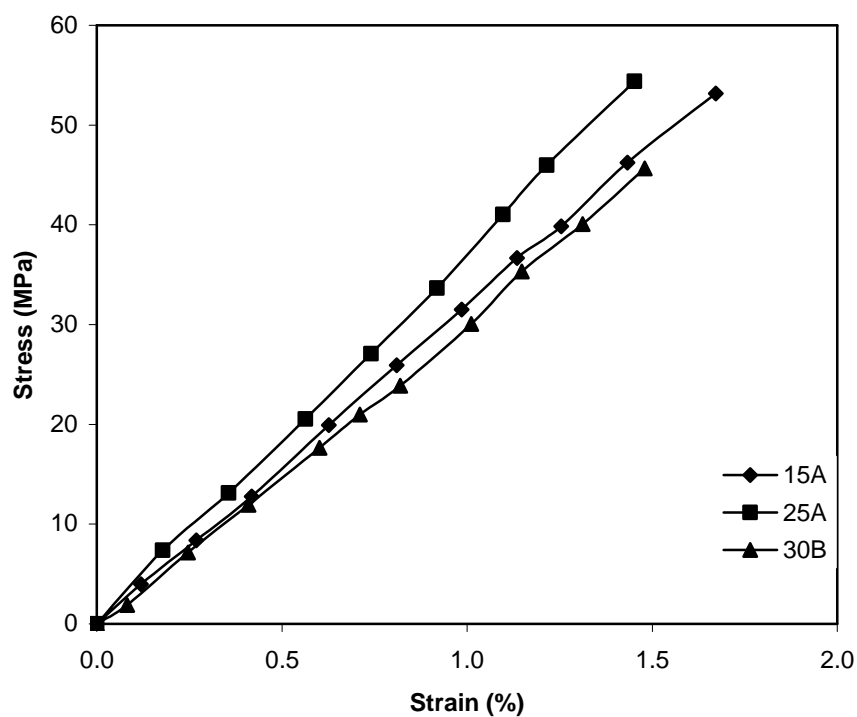


Figure 4.21 Effect of organoclay type (3 wt. %) on the stress-strain curves of nanocomposites prepared by In-Situ Method.

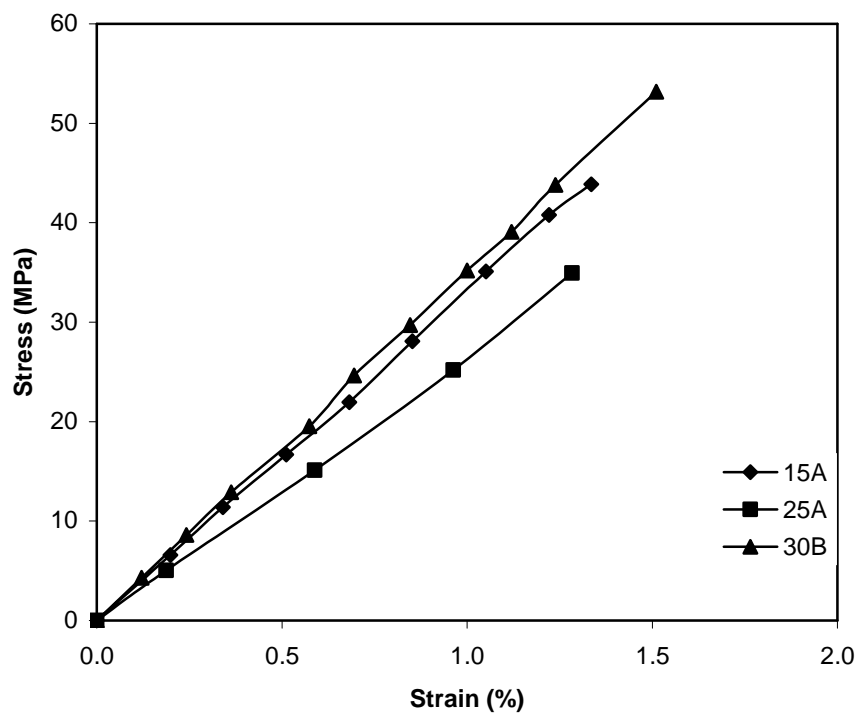


Figure 4.22 Effect of organoclay type (3 wt.%) on the stress-strain curves of nanocomposites prepared by Prepolymerization Method.

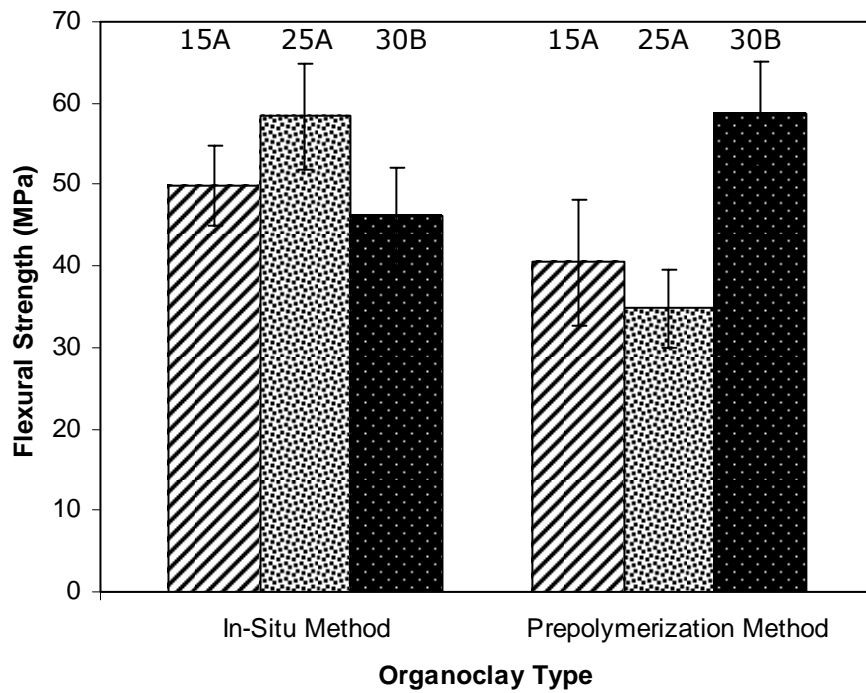


Figure 4.23 Effect of organoclay type (3 wt. %) on the flexural strength of nanocomposites prepared by In-Situ Method and Prepolymerization Method.

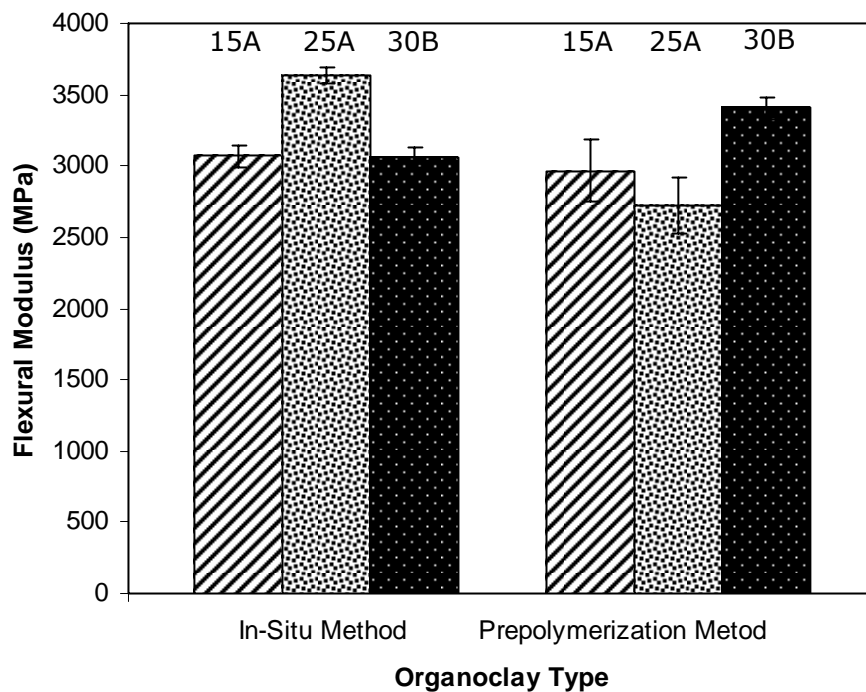


Figure 4.24 Effect of organoclay type (3 wt. %) on the flexural modulus of nanocomposites prepared by In-Situ Method and Prepolymer Method.

Figure 4.25 shows the flexural strain at break (%) values of the samples with respect to the polymerization method and the organoclay type. As Figure 4.25 shows, there is not significant difference between the flexural strain at break (%) values of the samples when different organoclay types were used. A high value is only seen for the samples prepared by the Prepolymerization Method using Cloisite30B. This result can be attributed to the exfoliation of the silicate sheets and thus existence of good adhesion between the polymer and the clay. Addition of rigid particulate fillers to a polymer matrix decreases the elongation at break since a more brittle structure is obtained. Only in rare instances, if there is a good adhesion between the polymer and the filler the fracture goes from particle to particle rather than following a direct path, in this case the filled polymers have higher elongations at break compared to neat resin (43).

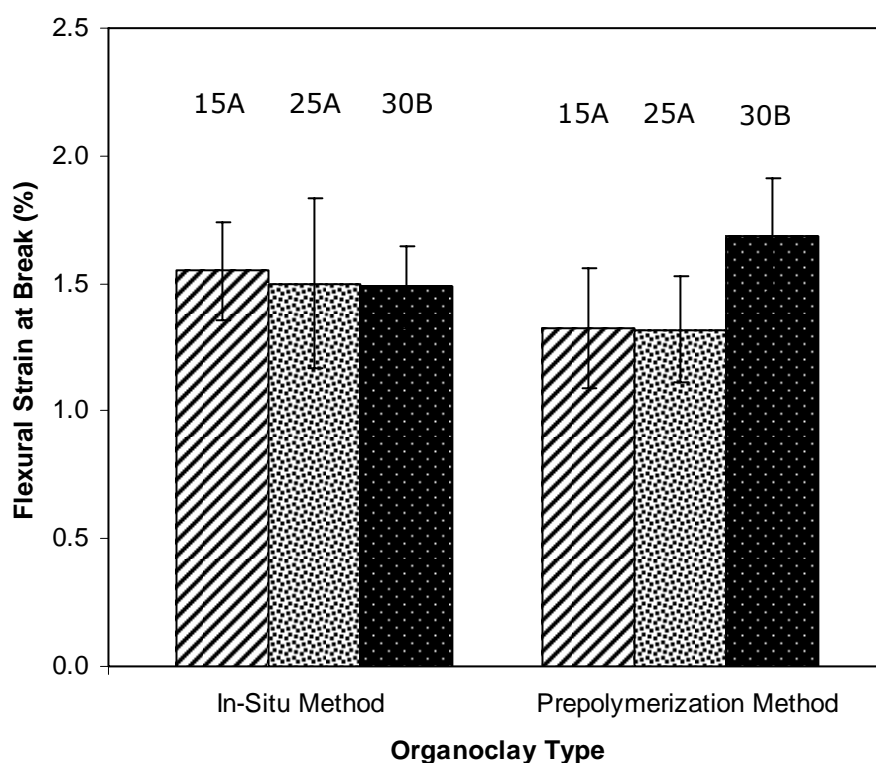


Figure 4.25 Effect of organoclay type (3 wt. %) on the flexural strain at break (%) values of nanocomposites prepared by In-Situ Method and Prepolymerization Method.

Figures 4.26 and 4.27 display the flexural strength and modulus of the samples prepared by both methods containing 0, 1, 3, and 5 wt. % organoclay (Cloisite 30B). As discussed previously, since the radius of gyration of styrene monomer is smaller than a polymer, in the Prepolymerization Method, it diffuses into the galleries of the organoclay easily resulting in a decrease in the amount of styrene available for crosslinking in the medium. This decreases the chain length between the crosslink sites leading to higher flexural strength and modulus.

From the XRD data, it was observed that exfoliation is obtained with 1 wt. % and 3 wt.% organoclay contents for the In-Situ and Prepolymerization methods, respectively. It can be seen from Figure 4.26 that maximum flexural strengths are also obtained at these clay contents. At higher clay loadings, the decrease in the flexural strength can be attributed to the decrease in the crosslink density of the material, because high amount of organoclay can create a restriction to obtaining high crosslinking density, thus leading to lower strength and modulus.

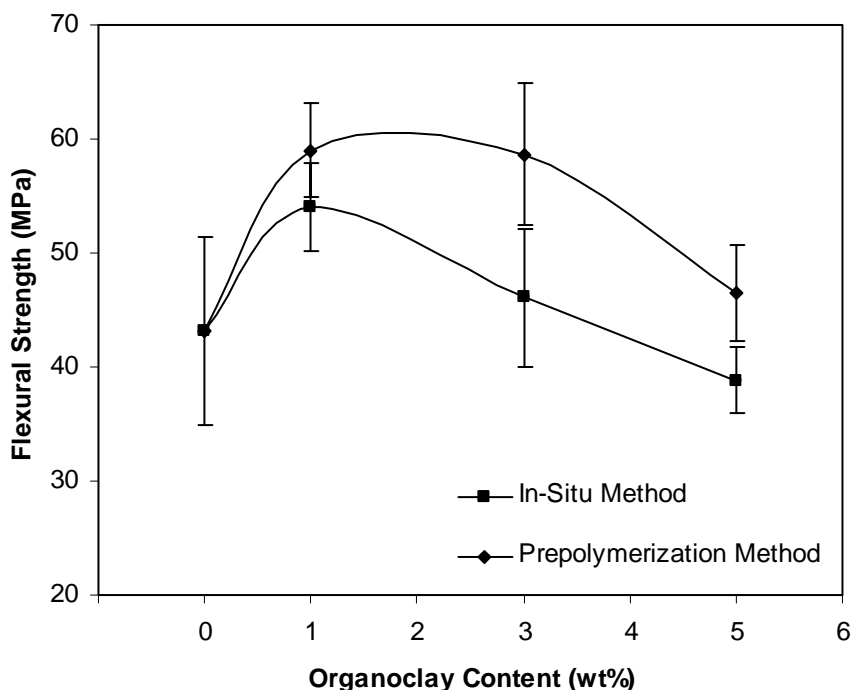


Figure 4.26 Effect of organoclay (Cloisite 30B) content on the flexural strengths of nanocomposites prepared by In-Situ Method and Prepolymerization Method.

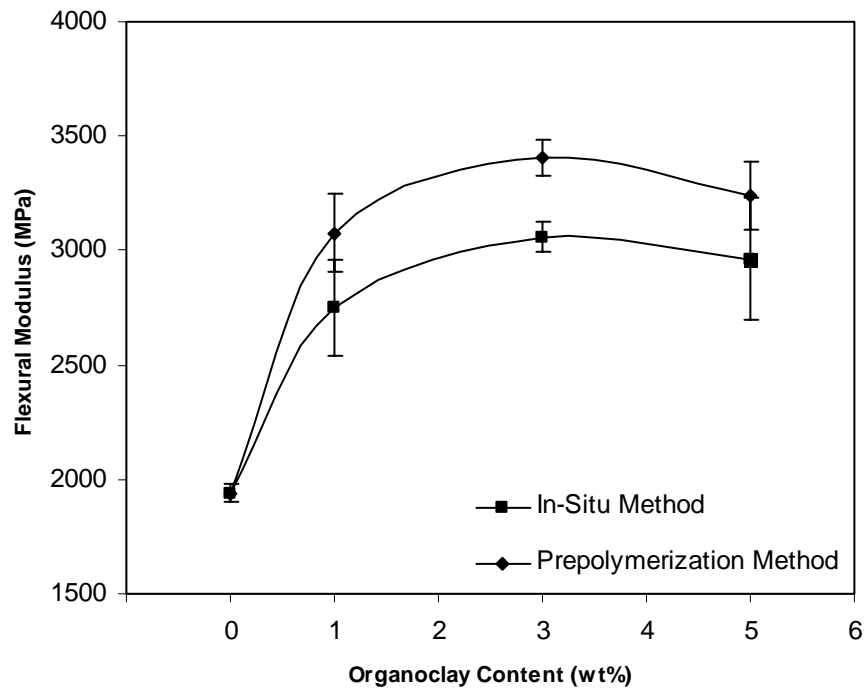


Figure 4.27 Effect of organoclay (Cloisite 30B) content on the flexural modulus of nanocomposites prepared by In-Situ Method and Prepolymerization Method.

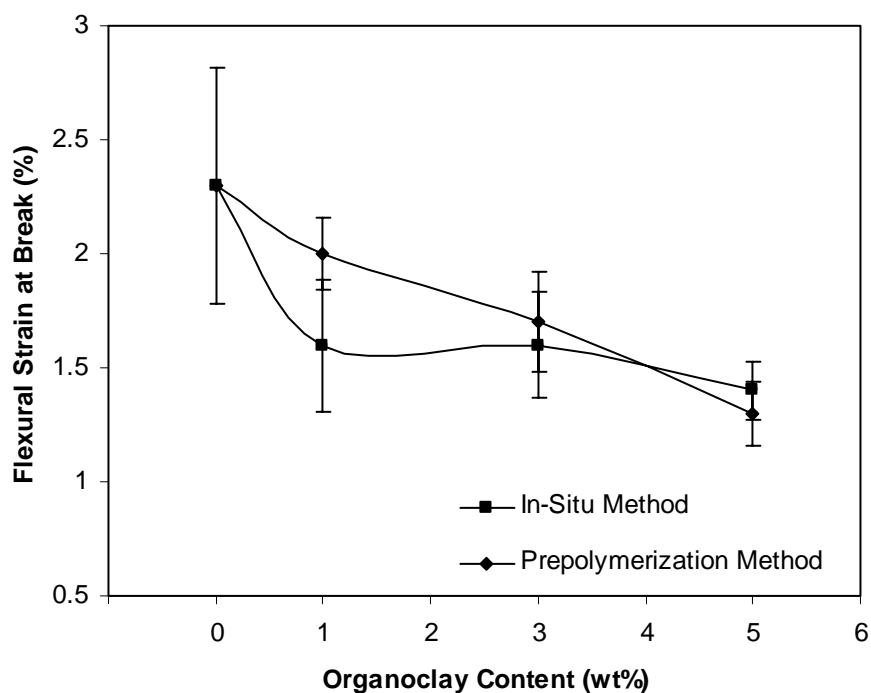


Figure 4.28 Effect of organoclay (Cloisite 30B) content on the flexural strain at break(%) values of nanocomposites prepared by In-Situ Method and Prepolymerization Method.

Addition of organoclay causes a decrease in the strain at break values. At low filler content, the decrease in the strain at break value arises from the fact that the composition material consists part of unsaturated polyester and part of organoclay and all the elongation comes from unsaturated polyester since the organoclay is a rigid filler. Thus the actual elongation experienced by the unsaturated polyester is much greater than the measured elongation of the composite. However, at high clay loadings, the increase in the clay content may lead to lower crosslink density and thus elongation at break value may increase as observed at 3 wt.% clay content for the In-Situ Method [12].

4.3 Thermal Analysis

4.3.1 Differential Scanning Calorimetry (DSC) Analysis

Table 4.4 Effect of organoclay (Cloisite 30B) content on the thermal properties of the compositions prepared by the In-Situ and the Prepolymerization Methods.

Polymerization Method	Organoclay Weight %	Glass Transition Temperature, T_g (°C)
In-Situ	0	56.2
	1	57.5
	3	55.9
	5	58.3
Prepolymerization	1	57.5
	3	63.5
	5	55.6

Table 4.5 Effect of organoclay type on thermal properties of the samples containing 3 wt. % organoclay.

Polymerization Method	Organoclay Type	Glass Transition Temperature, T_g (°C)
In-Situ	Cloisite 15A	57.6
	Cloisite 25A	56.3
	Cloisite 30B	55.9
Prepolymerization	Cloisite 15A	55.6
	Cloisite 25A	55.9
	Cloisite 30B	63.5

Table 4.4 lists the glass transition temperature (T_g) values of the samples prepared by both the In-Situ Method and the Prepolymerization Method. It is seen that the T_g values of the compositions prepared by the In-Situ method remain almost the same with only slight deviations from the neat resin.

Since T_g is related with chain mobility, crosslinking is an important factor that affects T_g of polymers. Crosslinking increases the glass transition by introducing restrictions on the molecular motion of a chain (43). In addition, the intercalation of the polymer chains between the layers of the clay particles and the exfoliation of the silicate sheets can also hinder the crosslinking mechanism. This hindrance decreases the crosslinking density which in turn decreases the glass transition temperature of the polymer. These two phenomena may compensate each other and would be the reasons of the T_g values remaining nearly unchanged.

The same reason is valid for the T_g values of the samples prepared by the Prepolymerization Method. Nevertheless, with 3 wt. % clay (Cloisite 30B) loading, an increase in the T_g value (63.5 °C) is observed. From the XRD patterns of the samples containing 3 wt.% clay (Cloisite 30B) prepared by the Prepolymerization Method, the absence of a basal reflection can be interpreted as an exfoliated behavior of the silicate sheets which will give rise to strong surface interactions between the polymer matrix and the silicate sheets.

In Table 4.5, the glass transition temperature (T_g) values of samples prepared by the two methods containing 3 wt. % different types of organoclay are seen. When the clay types are considered, there is not significant difference between the T_g of the neat unsaturated polyester and the T_g of the other compositions containing Cloisite 15A and Cloisite 25A. The only increase in T_g is seen in the Prepolymerization Method with the Cloisite 30B owing to the exfoliation of the clay layers and increasing the adhesion between the polymer and the clay layers as mentioned earlier. Adhesion would also increase by the possible reactions between the polar modifier constituent of the organoclay and the unsaturated polyester.

CHAPTER 5

CONCLUSIONS

From SEM micrographs, it is seen that the impact fractured surface of neat unsaturated polyester is smooth and straight crack propagation lines are observed explaining low impact strength observed in this sample. As the organoclay (Cloisite 30B) loading was increased, the crack propagation lines approach a shorter and closer structure resulting in higher impact strength for both the In-Situ and the Prepolymerization methods. At 5 wt.% clay content, the organoclay forms agglomerates acting as stress concentrators. In the SEM micrographs of the samples synthesized by the Prepolymerization Method, more agglomerates are seen in comparison to the ones synthesized by the In-Situ Method. The effect of clay type on the morphological structure of the nanocomposites can not be investigated due to the similar structures exhibited by the micrographs.

In XRD analysis, for the In-Situ polymerized samples containing 1 wt. % organoclay (Cloisite 30B) and the samples prepared by the Prepolymerization Method containing 3 wt. % organoclay, no peak is detected by XRD, which suggests that exfoliated structures are obtained. For the In-Situ Method, the characteristic interlayer spacing of Cloisite 30B is increased to 39 Å and 39.1 Å at 3 wt. % and 5 wt. % clay loadings respectively indicating the intercalation of the polymer chains within the silicate sheets expanding the galleries. The increase in the d-spacing values in the Prepolymerization Method is higher than the In-Situ Method owing to the shear stress acting on the silicate sheets, since in the Prepolymerization Method the medium contains polymer of higher molecular weight than the monomers of the In-Situ Method. Comparing the organoclay types, maximum increase in the gallery size is obtained by Cloisite 30B, 112 % increase and an exfoliated structure is observed for the In-Situ and the Prepolymerization methods respectively. With an increase of 17 % and 18 % for the In-Situ and the Prepolymerization methods respectively, Cloisite 15A exhibited the minimum increase in the d-spacing.

The mechanical properties including the impact strength, flexural strength and flexural modulus are improved with increasing clay concentration up to a certain clay loading (<3 wt. %). Considering the impact strength, the optimum organoclay (Cloisite 30B) concentration is found to be 3 wt. % for the two methods. When the In-Situ Method is applied, the samples exhibited higher improvements than the Prepolymerization Method. This improvement can be attributed to the higher mobility of the chains obtained by the In-Situ method owing to the higher styrene content in the crosslinking medium in comparison to the Prepolymerization Method. In the comparison of the clay types, Cloisite 15 is found to exhibit the highest and Cloisite 30B is found to exhibit the lowest impact strength values in both methods.

The flexural strength and the flexural modulus values are higher for the Prepolymerization Method than the In-Situ method indicating the stiffness of the material. When the clay types are considered, it is observed that the tendency of a disordered level leads to improvement in the flexural strength and the flexural modulus of the material. However, this tendency is not valid for the samples prepared by the Prepolymerization method with Cloisite 15A and Cloisite 25A. It is seen that higher level of polymer-clay interaction is achieved with Cloisite 15A owing to its larger initial d-spacing permitting higher amounts of long molecular to intercalate through the silicate sheets. According to the statements mentioned, Cloisite 25A and Cloisite 30B give rise to highest flexural improvement for the In-Situ and the Prepolymerization methods respectively. It is also observed that addition of organoclay decreases the elongation at break values.

The glass transition temperature (T_g) values of the nanocomposites prepared by the two methods remains almost the same with only slight deviations from the neat resin. Only at 3 wt. % clay loading for the Prepolymerization Method, an increase in the T_g value (63.5°C) is observed. It can also be seen that the organoclay type does not affect the T_g values significantly.

REFERENCES

1. Mazumdar S.K., "Composites Manufacturing Materials, Product, and Process Engineering", CRC Press, USA, 2002.
2. Tolle T.B. and Anderson D.P., "Morphology development in layered silicate thermoset nanocomposites", *Composites Science and Technology*, vol.62, 1033-1041, 2002.
3. Rothon R.N., "Particulate-Filled Polymer Composites", 2nd. Edition, Rapra Technology Ltd., United Kingdom, 2003.
4. Kornmann X., "Synthesis and Characterization of Thermoset-Clay Nanocomposites", Ph. D. Thesis, Lulea University of Technology, Sweden, 2000.
5. Suh D.J., Lim Y.T. and Park O.O., "The property and formation mechanism of unsaturated polyester-layered silicate nanocomposite depending on fabrication methods", *Polymer*, vol.41, 8557-8563, 2000.
6. Akovali G., "Handbook of Composite Fabrication", Rapra Technology Ltd., 2001.
7. "Kirk-Othmer Encyclopedia of Chemical Technology", 4th ed., vol.7, 1-27, John Wiley and Sons, Inc., New York, 1993.
8. Lubin G., "Handbook of Composites", Van Norstrand Reinhold, New York, 1982.
9. "Polymeric Materials Encyclopedia", vol.9, 6806-6813, CRC Press, New York, 1996.
10. Progelhof R.C. and Throne J.L., "Polymer Engineering Principles: Properties, Process, Tests for Design", Hanser/Gardner Publications, Inc., Cincinnati, 1993.
11. Fried J.R., "Polymer Science and Technology", Prentice Hall PTR, 1995.

12. Inceoglu A.B., "Synthesis and Mechanical Properties of Unsaturated Polyester Based Nanocomposites", M.S. Thesis, Department of Chemical Engineering, METU, Ankara, 2001.
13. Kornmann X., Berglund L.A., Sterte J. and Giannelis E.P., "Nanocomposites Based on Montmorillonite and Unsaturated Polyester", Polymer Engineering and Science, vol.38, no.8, 1998.
14. Alexandre M. and Dubois P., "Polymer-layered silicate nanocomposites: preparation, properties and uses of a new class of materials", Materials Science and Engineering, vol.28, 1-63, 2000.
15. Manias E., "Origins of the Materials Properties Enhancements in Polymer/Clay Nanocomposites", Department of Materials Science and Engineering, The Pennsylvania University.
16. Schmidt D., Shah D. And Giannelis E.P., "New advances in polymer/layered silicate nanocomposites", Current Opinion in Solid State and Materials Science", vol.6, 205-212, 2002.
17. LeBaron P.C., Wang Z. and Pinnavaia T.J., "Polymer-layered silicate nanocomposites: an overview", Applied Clay Science, vol.15, 11-29, 1999.
18. Ray S.S. and Okamoto M., "Polymer/layered silicate nanocomposites: a review from preparation to processing", Progress in Polymer Science, 2003.
19. Pinnavaia T.J., Beall G.W., "Polymer-Clay Nanocomposites", John Wiley and Sons, Ltd., England, 2000.
20. Malik M., Choudhary V. and Varma I.K., "Current Status of Unsaturated Polyester Resins", rev. Macromol. Chem. Phys., c40(2&3), 139-165, 2000.
21. British Plastics Federation, Unsaturated Polyester UP, www.bpf.co.uk/bpfindustry/plastics_materials_polyester_unsaturated_PU.cmf, 2003.

22. Boeing H.V., "Unsaturated Polyesters. Structure and Properties", Elsevier Publishing Company, Amsterdam, 1964.
23. Gamstedt E.K., Skrifvars M., Jacobsen T.K. and Pyrz R., "Synthesis of unsaturated polyesters for improved interfacial strength in carbon fibre composites", Composites: Part A, vol.33, 1239-1252, 2002.
24. Jacobs P.M. and Jones F.R., "The influence of heterogeneous crosslink density on the thermomechanical and hygrothermal properties of an unsaturated polyester resin: 1. Thermomechanical response", Polymer, vol.33, no.7, 1418-1422, 1992.
25. "Kirk-Othmer Encyclopedia of Chemical Technology", vol.19, 4th ed., 655-678, John Wiley and Sons, Inc., New York, 1993.
26. Strong A.B., "Fundamentals of Composites Manufacturing: Materials, Methods and Applications", Society of Manufacturing Engineers, Publications Development Department, Reference Publications Division, Dearborn, 1989.
27. Hsu C.P. and Lee L.J., "Free-radical crosslinking copolymerization of styrene/unsaturated polyester resin: 3. Kinetics-gelation mechanism", Polymer, vol.34, no.21, 4516-4523, 1993.
28. Ebewele R.O., "Polymer Science and Technology", CRC Prsss LLC, 2000.
29. "Annual Book of ASTM Standarts", Vol.08.01, American society for testing and Materials ASTM D790M, Philadelphia, USA, 1993.
30. Shah V., "Handbook of Plastic Testing Technology", 2nd ed., Wiley-Interscience Publication, USA, 1998.
31. Seymour R.B. and Carraher C.E., "Structure-Property Relationships in Polymers", Plenum Press, New York, 1984.
32. "Encyclopedia of Polymer science and Technology", vol.15, 79-509, John Wiley and Sons, Inc., New York, 1971.

33. Rosen S.L., "Fundamental Principles of Polymeric Materials", 2nd ed., John Wiley and Sons, Inc., New York, 1993.
34. "Kirk-Othmer Encyclopedia of Chemical Technology", 4th ed., vol.6, 381-409, John Wiley and Sons, Inc., New York, 1993.
35. Cullity B.D., "Elements of X-Ray Diffraction", 2nd ed., Addison-Wesley Publishing Company, Inc., U.S.A., 1978.
36. "Kirk-Othmer Encyclopedia of Chemical Technology", 4th ed., John Wiley and Sons, Inc., New York, 1993.
37. Goldstein J.I., Newbury D.E., Echlin P., Joy D.C., Fiory C. and Lifshin E., "Scanning Electron Microscopy and X-Ray Microanalysis", Plenum Press, U.S.A., 1981.
38. Suh D.J., Park O.O. and Yoon K.H., "The properties of unsaturated polyester based on the glycolized poly(ethylene terephthalate) with various glycol compositions", *Polymer*, vol.41, 461-466, 2000.
39. Bharadvaj R.K., Mehrabi A.R., Hamilton C., Trujillo C., Murga M., Fan R., Chavira A. and Thompson A.K., "Structure-property relationships in cross-linked polyester-clay nanocomposites", *Polymer*, vol.43, 3699-3705, 2002.
40. Inceoglu A.B. and Yilmazer U., "Synthesis and mechanical properties of unsaturated polyester based nanocomposites", *Polymer Engineering and Science*, vol.43, no.3, 661-669, 2003.
41. Curtis L.G., Edwards D.L., Simons R.M., Trent P.J. and Von Bramer P.T., "Investigation of maleate-fumarate isomerization in unsaturated polyesters by nuclear magnetic resonance", *I&EC Product Research and Development*, vol.3, no.3, 218-221, 1964.
42. Artzi N., Nir Y., Narkis M. and Siegmann A., "Melt Blending of Ethylene-Vinyl Alcohol Copolymer/Clay Nanocomposites: Effect of Clay Type and Processing Conditions", *Journal of Polymer Science: Part B: Polymer Physics*, vol.40, 1741-1753, 2002

43. Nielsen L.E. and Landel R.F., "Mechanical Properties of Polymers and Composites", 2nd ed., Marcel Dekker Inc., U.S.A., 1993.

44. Strong A.B., "Plastics Materials and Processing", 2nd ed., Prentice Hall, USA, 2000.

45. Nielsen L.E., "Mechanical Properties of Polymers", Reinhold Publishing Corporation, USA, 1962.

APPENDIX A

Table A.1 Impact strength data of samples with respect to polymerization method and organoclay (Cloisite 30B) content.

Organoclay Weight %	In-Situ		Prepolymerization	
	Avg. Impact Strength (kJ/m ²)	Standard Deviation	Avg. Impact Strength (kJ/m ²)	Standard Deviation
0	0.75	0.26	0.75	0.26
1	0.97	0.07	0.76	0.13
3	1.32	0.03	0.94	0.14
5	1.17	0.22	0.87	0.1

Table A.2 Impact strength data of samples with respect to polymerization method and organoclay type.

Organoclay type	In-Situ		Prepolymerization	
	Avg. Impact Strength (kJ/m ²)	Standard Deviation	Avg. Impact Strength (kJ/m ²)	Standard Deviation
Cloisite 15A	3.72	2.00	2.16	0.17
Cloisite 25A	1.90	0.30	1.22	0.17
Cloisite 30B	1.32	0.03	0.94	0.14

Table A.3 Flexural strength data of samples with respect to polymerization method and organoclay (Cloisite 30B) content.

Organoclay Weight %	In-Situ		Prepolymerization	
	Avg. Flexural Strength (MPa)	Standard Deviation	Avg. Flexural Strength (MPa)	Standard Deviation
0	43.2	8.18	43.2	8.18
1	54.1	3.83	59.0	4.13
3	46.1	6.12	58.6	6.21
5	38.9	2.92	46.5	4.25

Table A.4 Flexural modulus data of samples with respect to polymerization method and organoclay (Cloisite 30B) content.

Organoclay Weight %	In-Situ		Prepolymerization	
	Avg. Flexural Modulus (MPa)	Standard Deviation	Avg. Flexural Modulus (MPa)	Standard Deviation
0	1941	41	1941	41
1	2751	212	3077	171
3	3059	67	3406	76
5	2963	269	3238	147

Table A.5 Flexural strain at break (%) data of samples with respect to polymerization method and organoclay (Cloisite 30B) content.

Organoclay Weight %	In-Situ		Prepolymerization	
	Avg. Flexural Strain at Break (%)	Standard Deviation	Avg. Flexural Strain at Break (%)	Standard Deviation
0	2.33	0.52	2.33	0.52
1	1.64	0.29	1.98	0.16
3	1.55	0.23	1.69	0.22
5	1.39	0.13	1.33	0.14

Table A.6 Flexural strength data of samples with respect to polymerization method and organoclay type.

Organoclay Type	In-Situ		Prepolymerization	
	Avg. Flexural Strength (MPa)	Standard Deviation	Avg. Flexural Strength (MPa)	Standard Deviation
Cloisite 15A	49.9	4.92	40.4	7.66
Cloisite 25A	58.4	6.55	34.8	4.84
Cloisite 30B	46.1	6.12	58.8	6.21

Table A.7 Flexural modulus data of samples with respect to polymerization method and organoclay type.

Organoclay Type	In-Situ		Prepolymerization	
	Avg. Flexural Modulus (MPa)	Standard Deviation	Avg. Flexural Modulus (MPa)	Standard Deviation
Cloisite 15A	3068	79	2966	216
Cloisite 25A	3631	54	2718	198
Cloisite 30B	3059	67	3406	76

Table A.8 Flexural strain at break (%) data of samples with respect to polymerization method and organoclay type.

Organoclay Type	In-Situ		Prepolymerization	
	Avg. Flexural Strain at Break (%)	Standard Deviation	Avg. Flexural Strain at Break (%)	Standard Deviation
Cloisite 15A	1.55	0.19	1.33	0.24
Cloisite 25A	1.50	0.34	1.32	0.20
Cloisite 30B	1.49	0.16	1.69	0.22

APPENDIX B

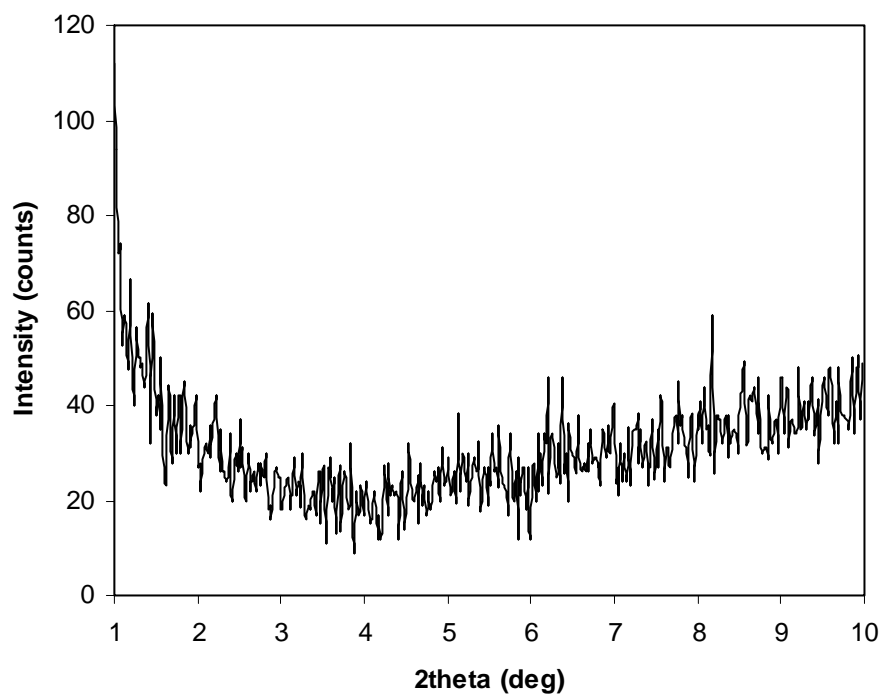


Figure B.1 X-ray diffraction patterns of pure unsaturated polyester (UP).

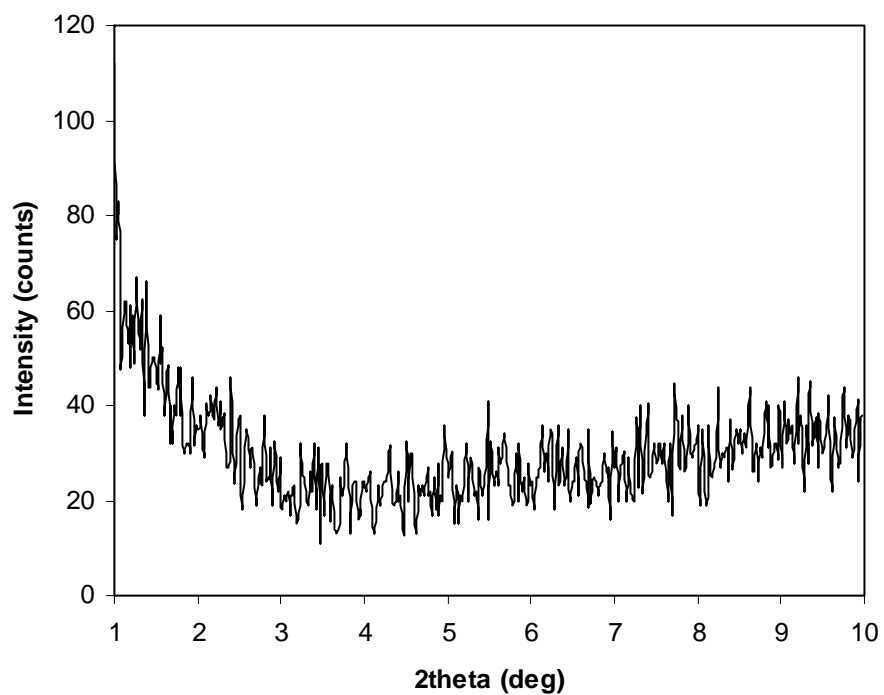


Figure B.2 X-ray diffraction pattern of UP nanocomposite synthesized by In-Situ Method containing 1 wt. % Cloisite 30B.

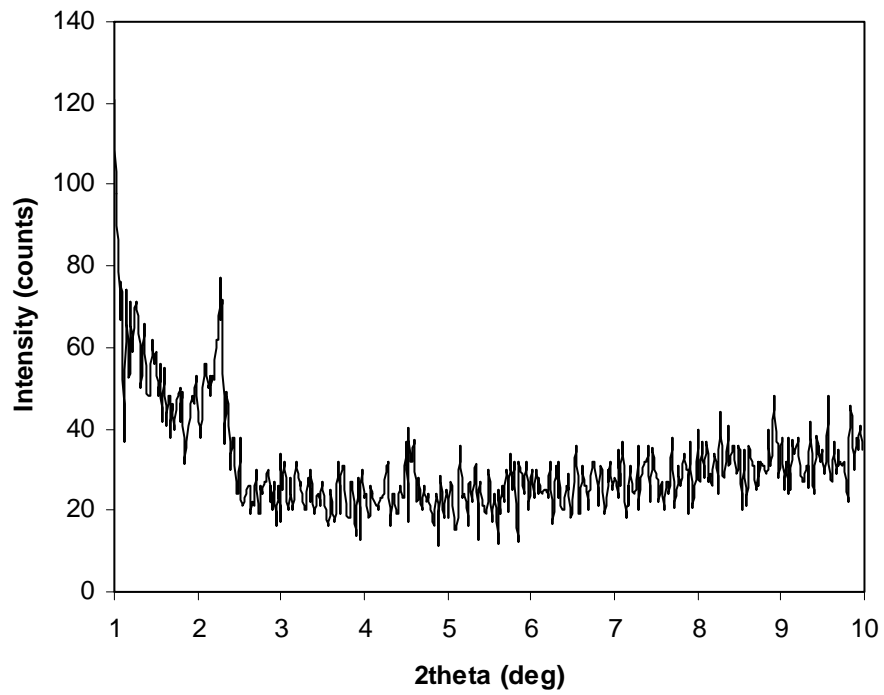


Figure B.3 X-ray diffraction pattern of UP nanocomposite synthesized by In-Situ Method containing 3 wt. % Cloisite 30B.

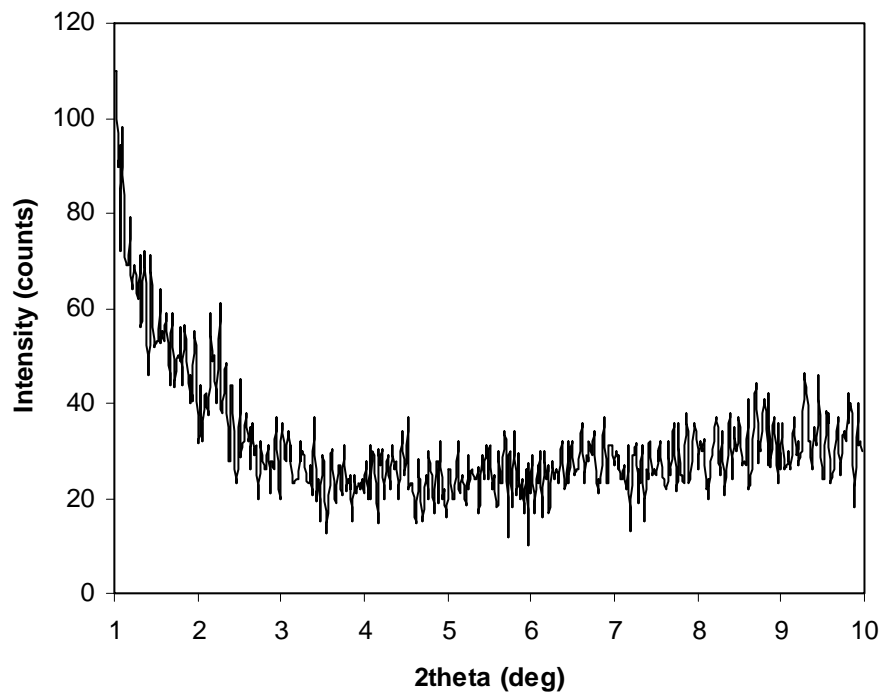


Figure B.4 X-ray diffraction pattern of UP nanocomposite synthesized by In-Situ Method containing 5 wt. % Cloisite 30B.

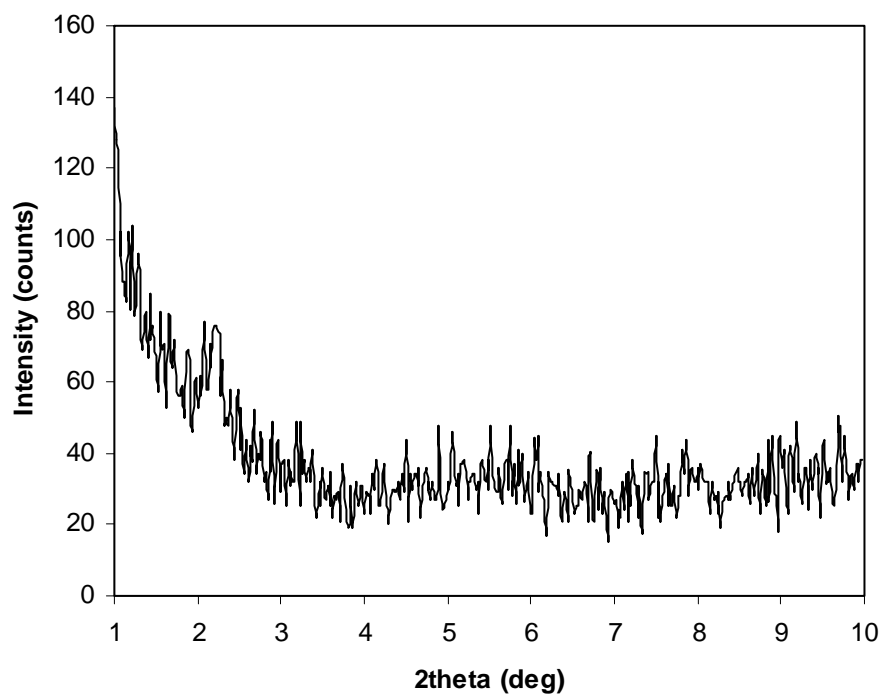


Figure B.5 X-ray diffraction pattern of UP nanocomposite synthesized by Prepolymerization Method containing 1 wt. % Cloisite 30B.

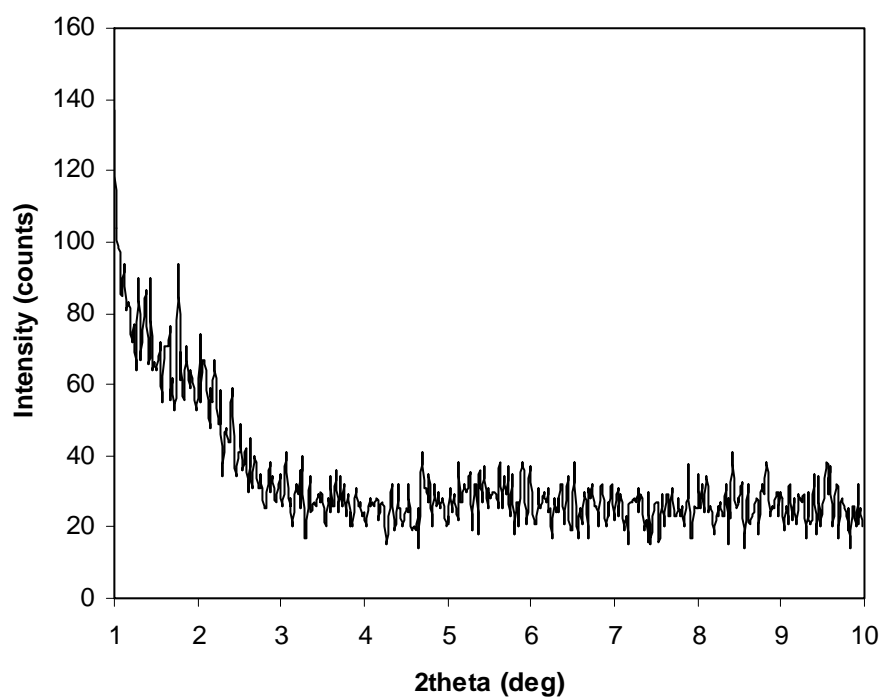


Figure B.6 X-ray diffraction pattern of UP nanocomposite synthesized by Prepolymerization Method containing 3 wt. % Cloisite 30B.

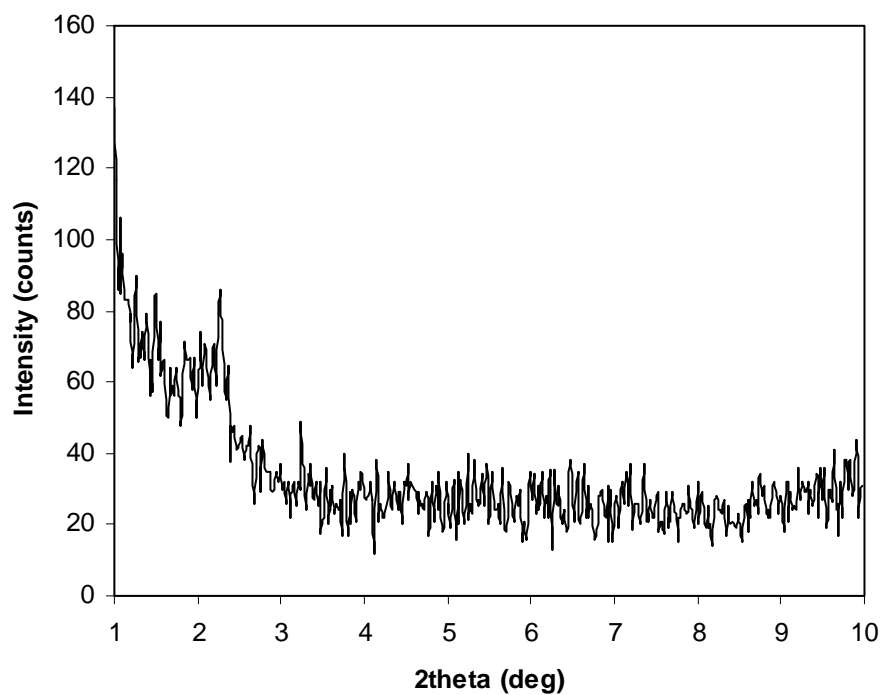


Figure B.7 X-ray diffraction pattern of UP nanocomposite synthesized by Prepolymerization Method containing 5 wt. % Cloisite 30B.

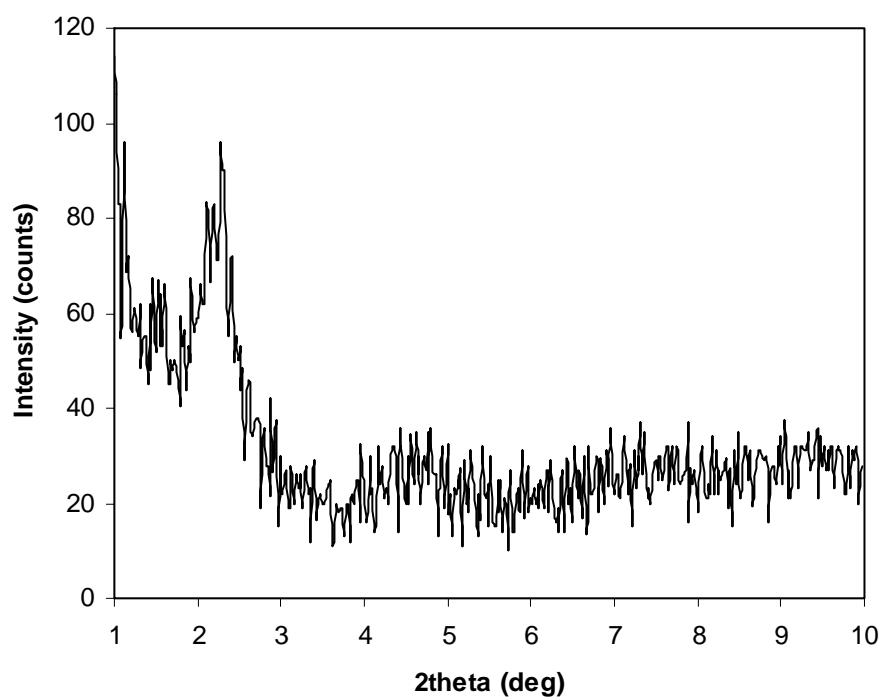


Figure B.8 X-ray diffraction pattern of UP nanocomposite synthesized by In-Situ Method containing 3 wt. % Cloisite 15A.

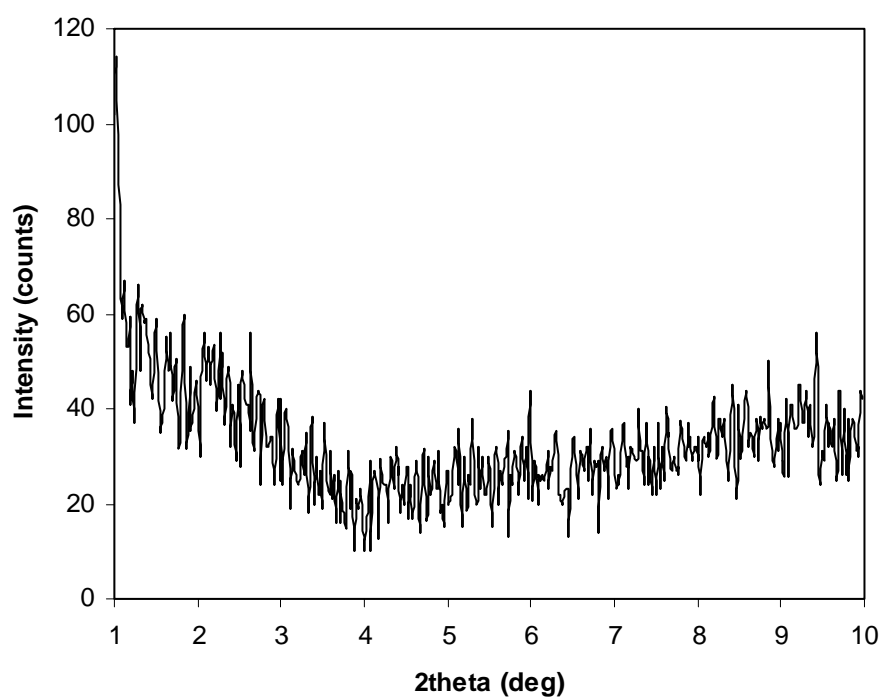


Figure B.9 X-ray diffraction pattern of UP nanocomposite synthesized by In-Situ Method containing 3 wt. % Cloisite 25A.

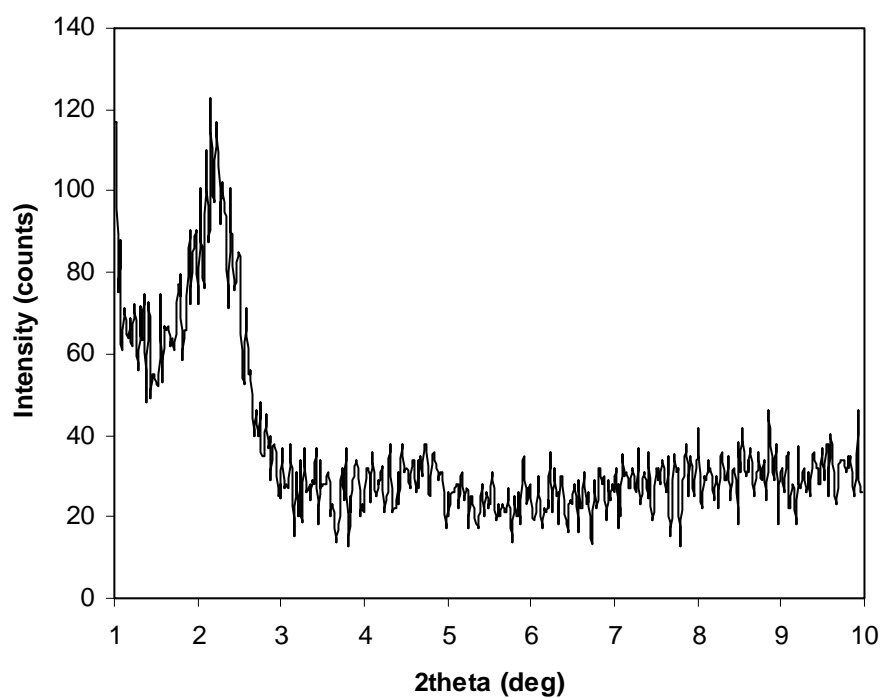


Figure B.10 X-ray diffraction pattern of UP nanocomposite synthesized by Prepolymerization Method containing 3 wt. % Cloisite 15A.

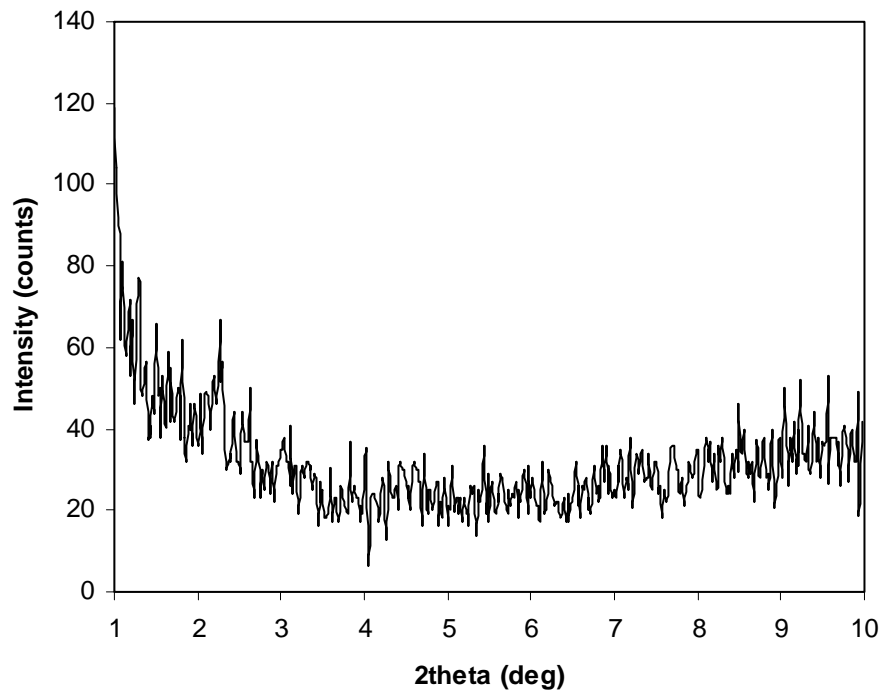


Figure B.11 X-ray diffraction pattern of UP nanocomposite synthesized by prepolymerization Method containing 3 wt. % Cloisite 25A.

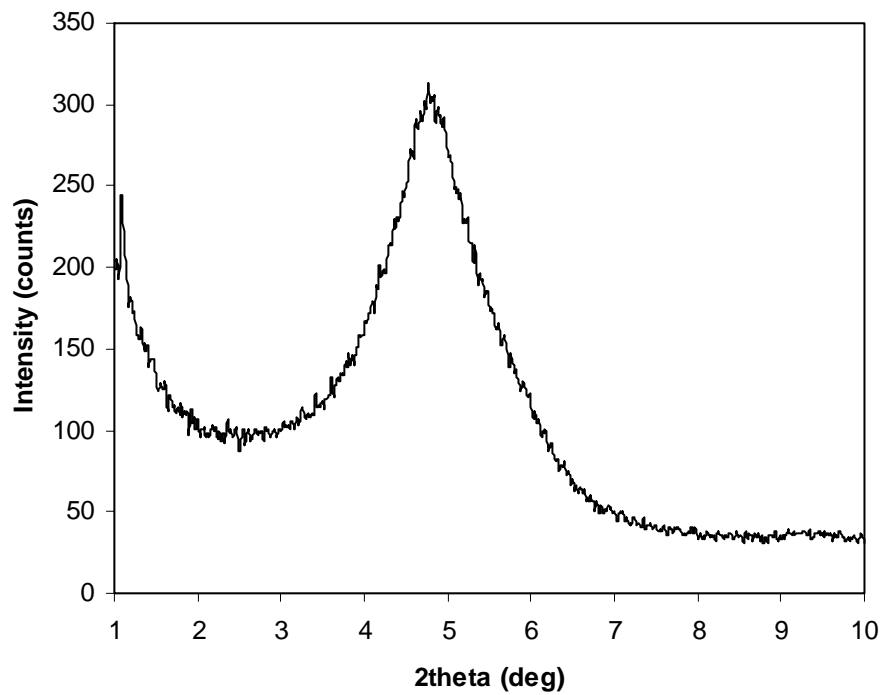


Figure B.12 X-ray diffraction pattern of Cloisite 30B.

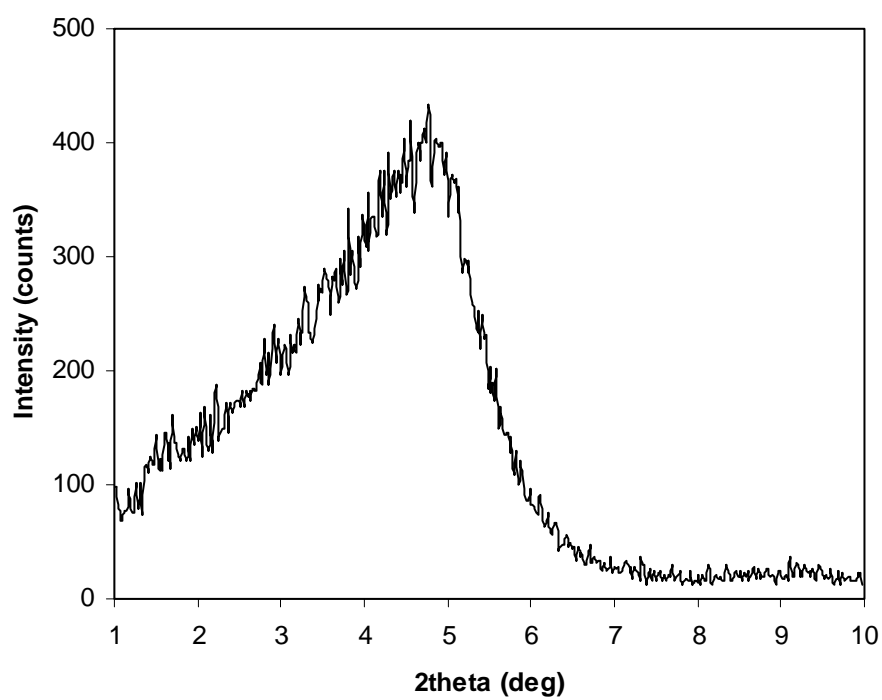


Figure B.13 X-ray diffraction pattern of Cloisite 25A.

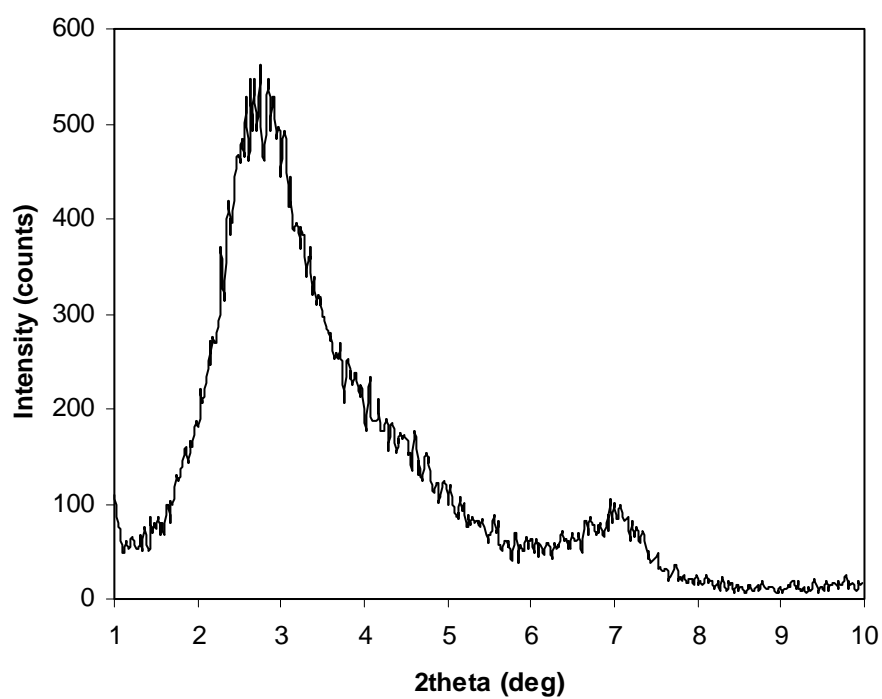


Figure B.14 X-ray diffraction pattern of Cloisite 15A.

APPENDIX C

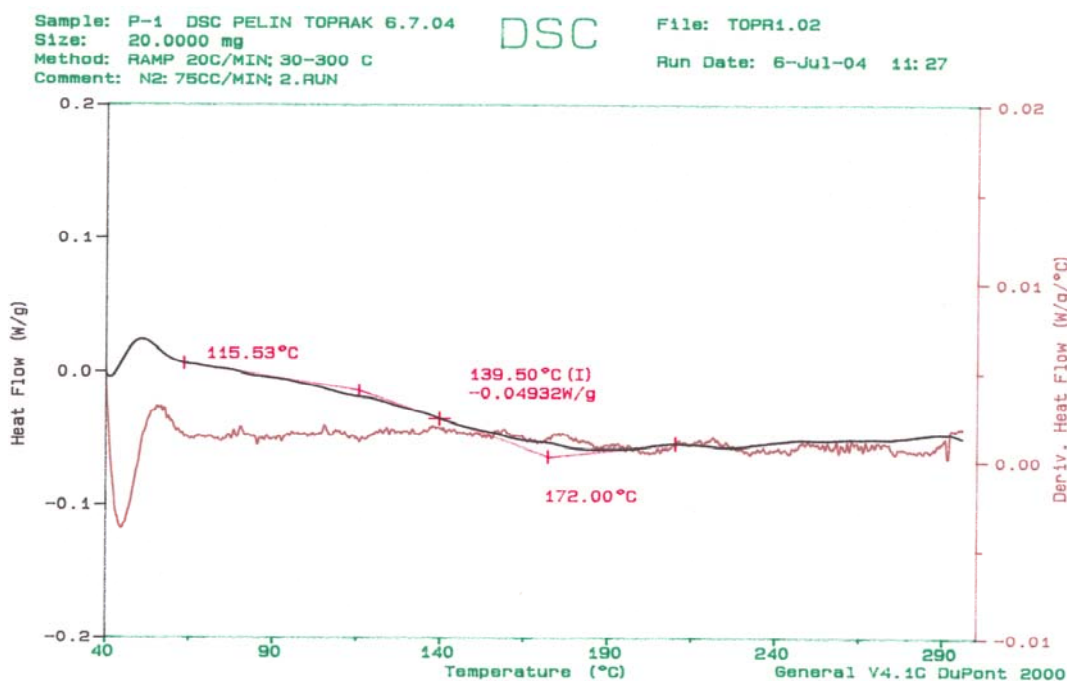


Figure C.1 DSC thermogram of pure unsaturated polyester (UP).

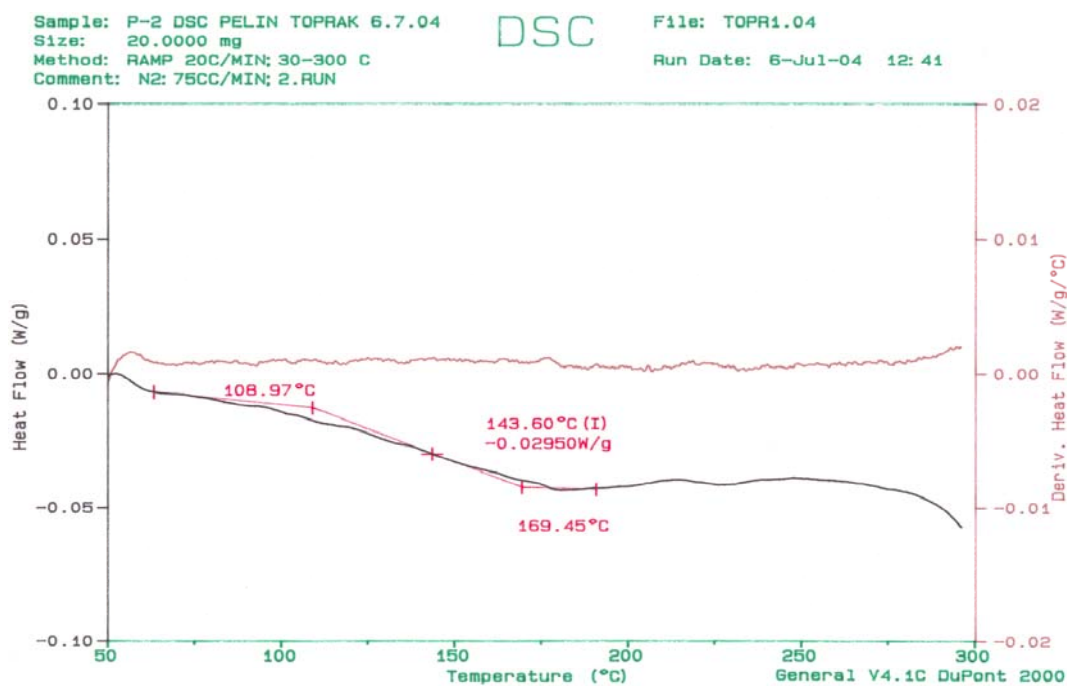


Figure C.2 DSC thermogram of UP nanocomposite synthesized by In-Situ Method containing 1 wt. % Cloisite 30B.

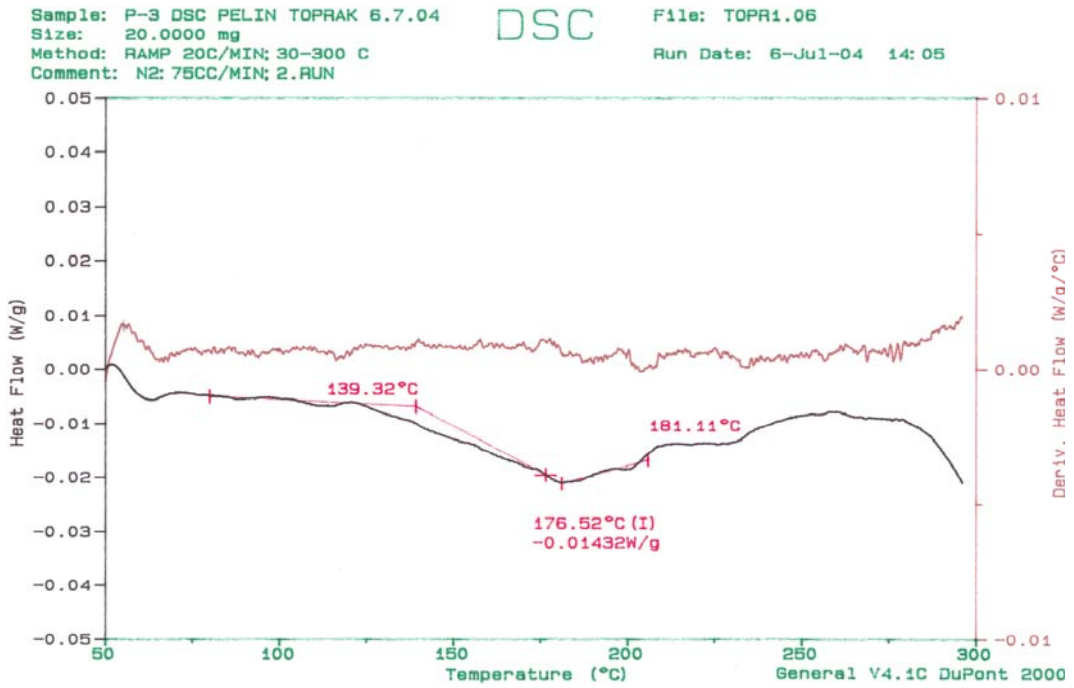


Figure C.3 DSC thermogram of UP nanocomposite synthesized by In-Situ Method containing 3 wt. % Cloisite 30B.

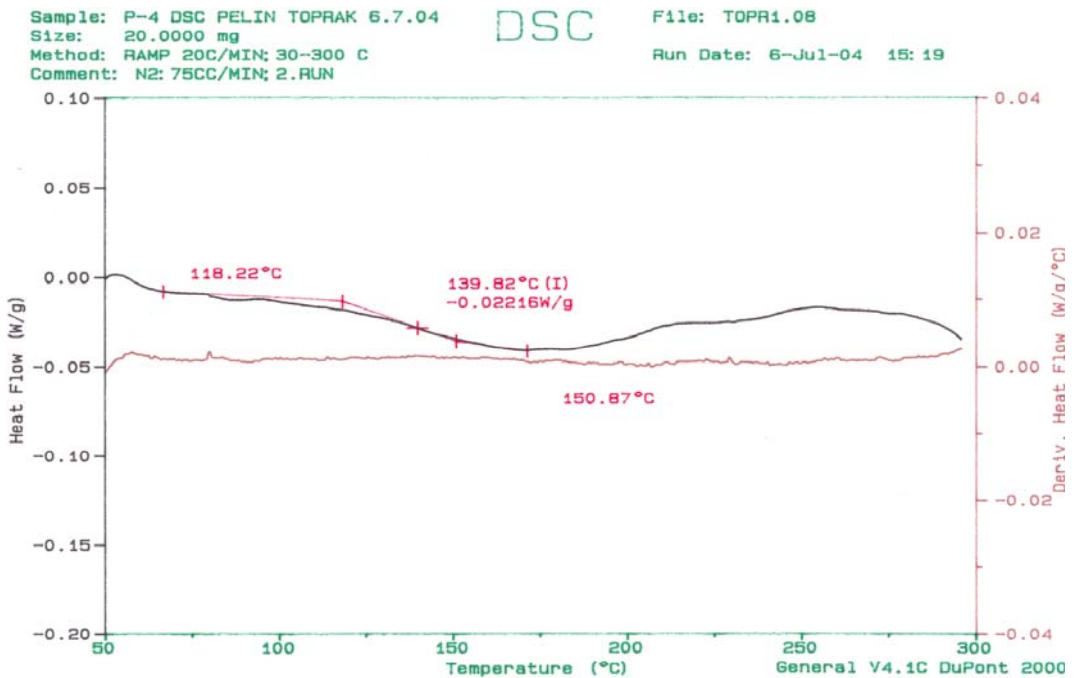


Figure C.4 DSC thermogram of UP nanocomposite synthesized by In-Situ Method containing 5 wt. % Cloisite 30B.

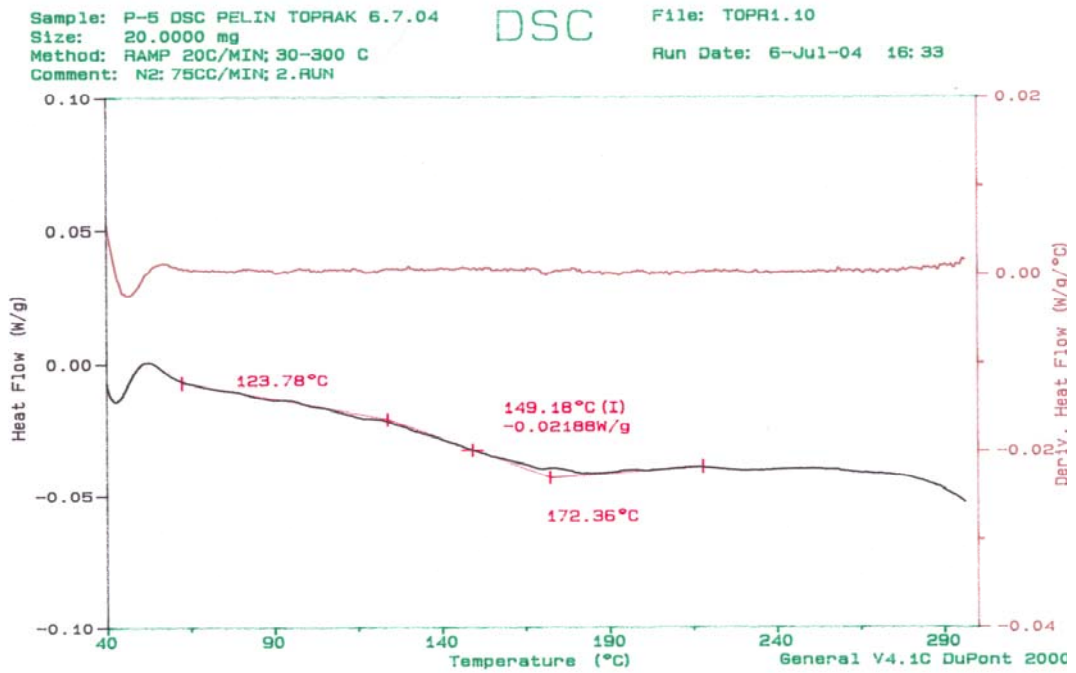


Figure C.5 DSC thermogram of UP nanocomposite synthesized by Prepolymerization Method containing 1 wt. % Cloisite 30B.

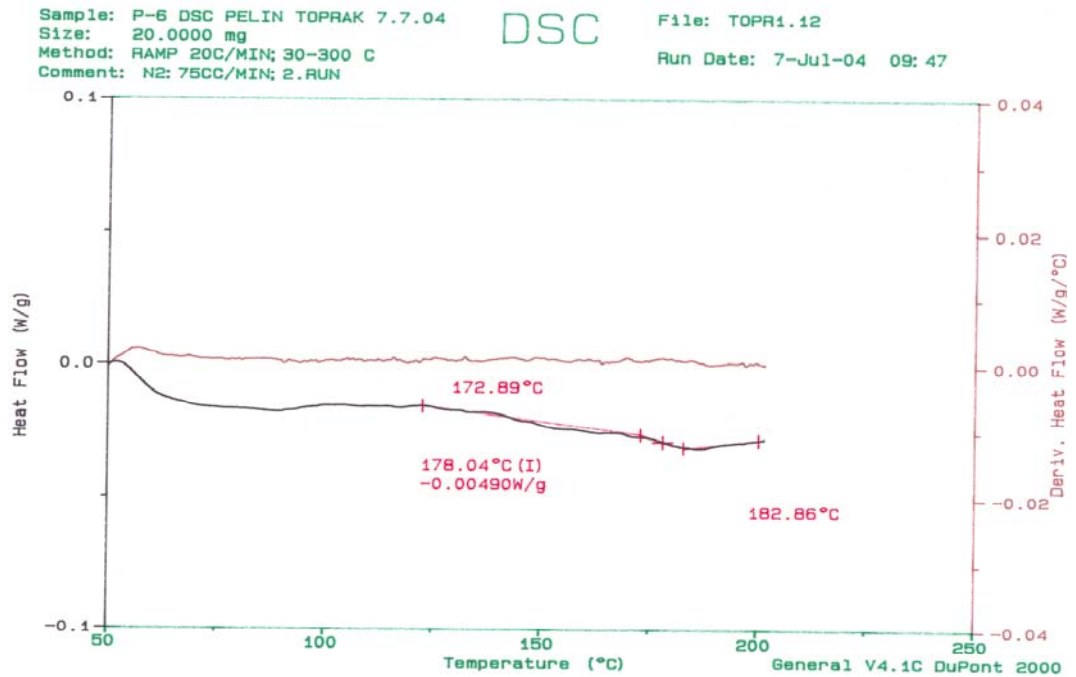


Figure C.6 DSC thermogram of UP nanocomposite synthesized by Prepolymerization Method containing 3 wt. % Cloisite 30B.

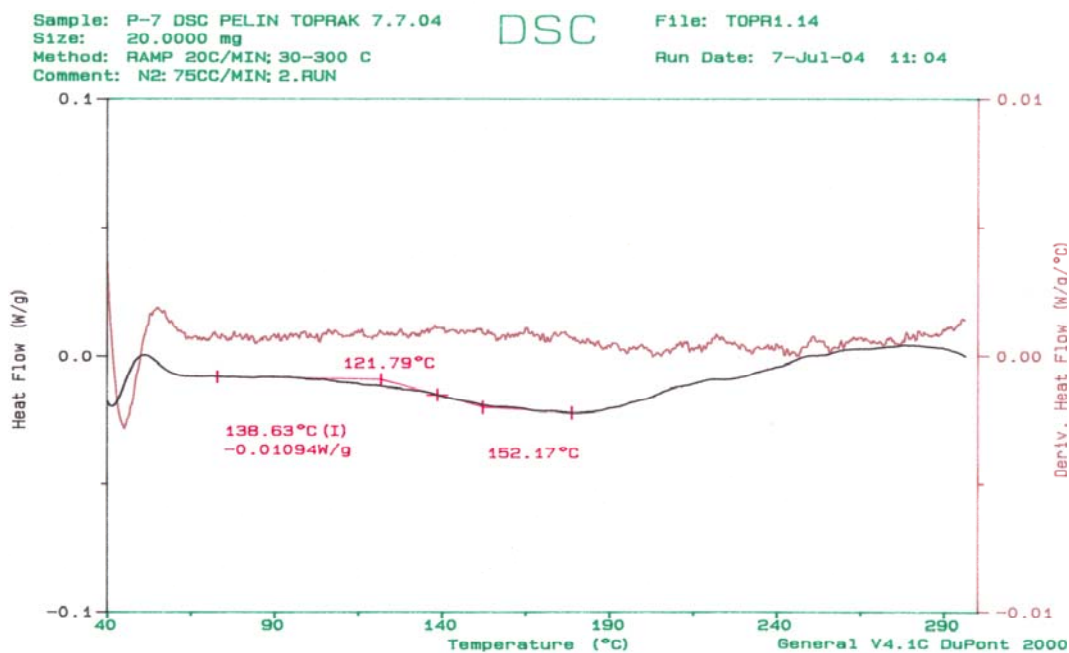


Figure C.7 DSC thermogram of UP nanocomposite synthesized by Prepolymerization Method containing 5 wt. % Cloisite 30B.

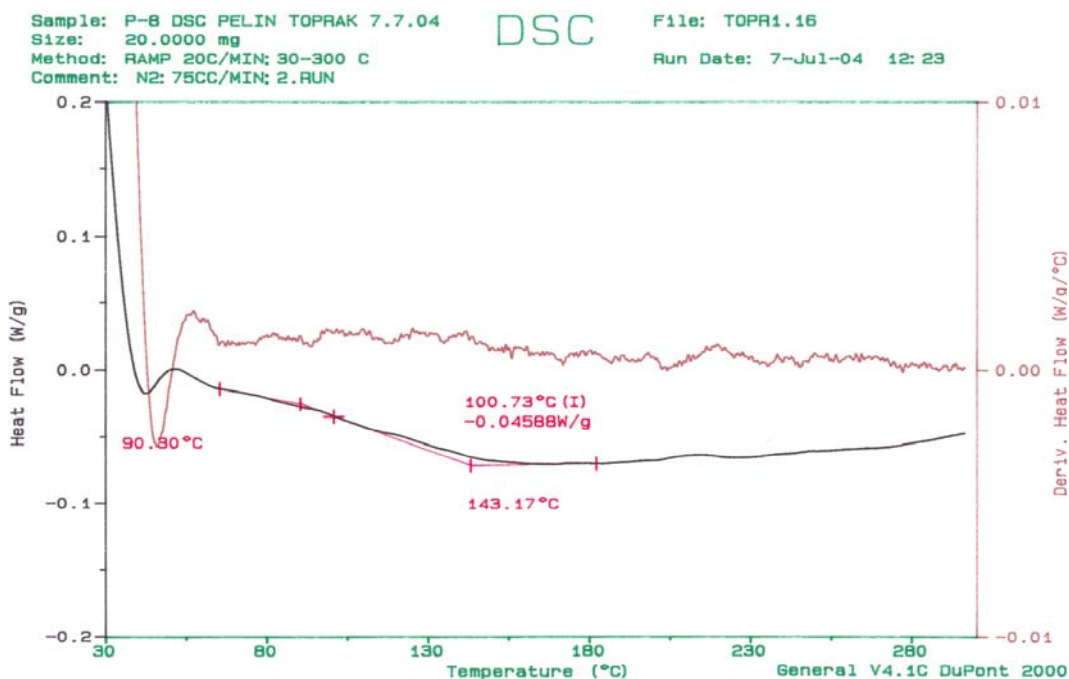


Figure C.8 DSC thermogram of UP nanocomposite synthesized by In-Situ Method containing 3 wt. % Cloisite 15A.

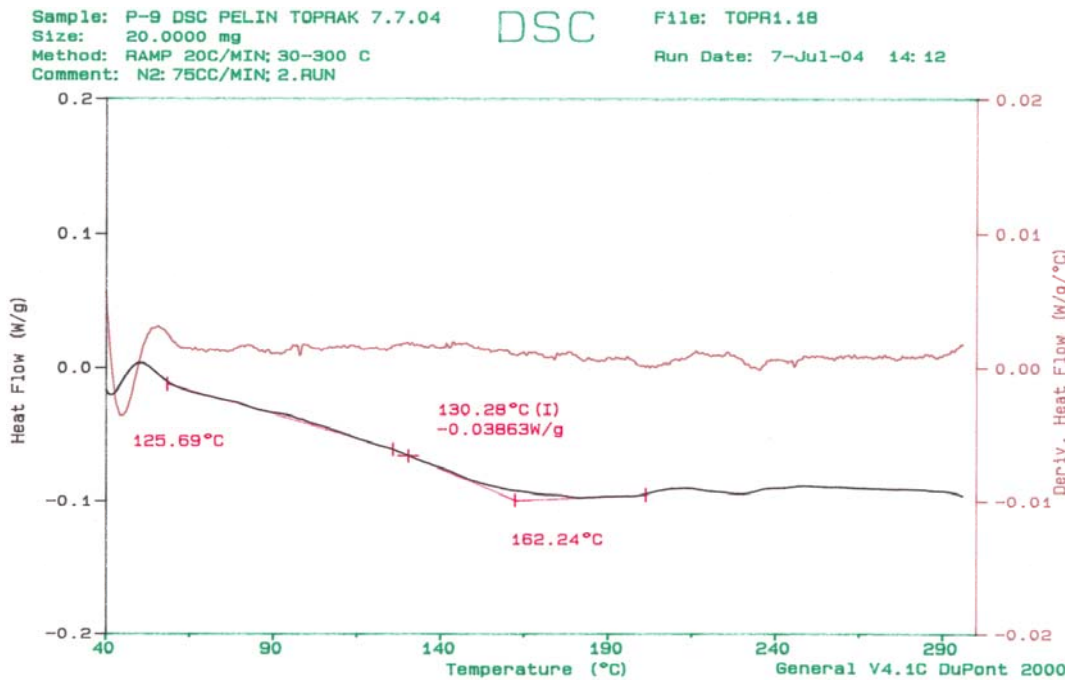


Figure C.9 DSC thermogram of UP nanocomposite synthesized by In-Situ Method containing 3 wt. % Cloisite 25A.

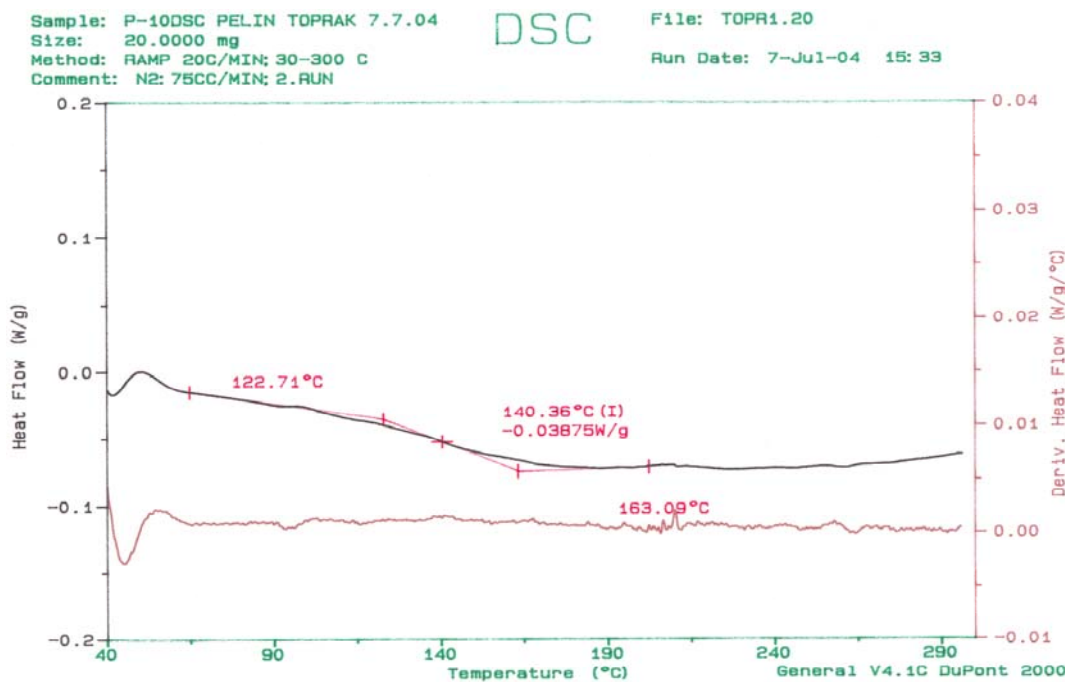


Figure C.10 DSC thermogram of UP nanocomposite synthesized by Prepolymerization Method containing 3 wt. % Cloisite 15A.

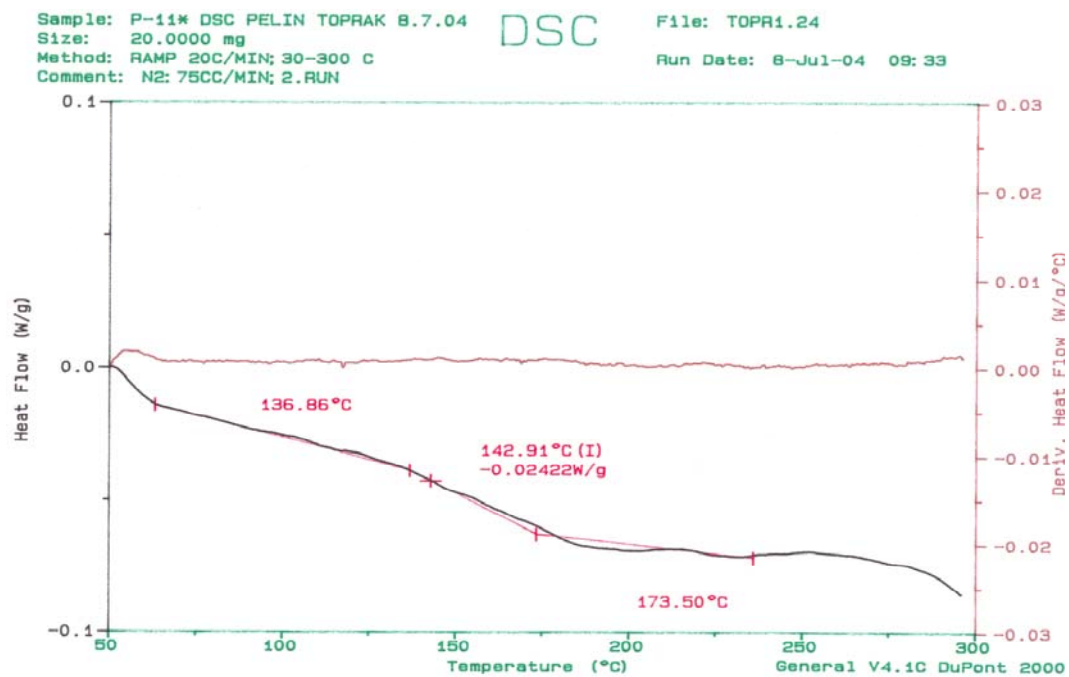


Figure C.11 DSC thermogram of UP nanocomposite synthesized by Prepolymerization Method containing 3 wt. % Cloisite 25A.